Universidad de la República
Facultad de Ciencias
Programa de Posgrado en Ciencias Ambientales

Evaluación satelital del estado trófico de reservorios de agua con fines productivos de la Cuenca del Río Santa Lucía: análisis de puntos calientes, riesgo de exportación de biomasa fitoplanctónica y variables ambientales asociadas

Autor
Bernardo Vicente Zabaleta López

Orientadores
Dr. Marcel Achkar y Dr. Luis Aubriot

Tribunal
Dr. Ismael Díaz, Dra. Sylvia Bonilla y Dra. Verónica Ciganda

Octubre de 2024

bzabaleta@fcien.edu.uy

Tabla de contenido

Agradecimientos

Agradezco a mis tutores, Dr. Marcel Achkar y Dr. Luis Aubriot por confiar en mí, su infinita paciencia, guía constante y aportes para enriquecer el trabajo y apoyarme a ir por más.

A los miembros del tribunal Dr. Ismael Díaz, Dra. Sylvia Bonilla y Dra. Verónica Ciganda por haber aceptado y por sus invaluables aportes científicos que enriquecieron tanto este documento como los artículos de forma independiente.

Mi familia, siempre presente para darme para adelante, incentivarme a concluir las metas propuestas, apoyar y bancar desde siempre mi curiosidad e interés por la ciencia.

Ana Clara, mi compañera de vida, que con su incondicional apoyo me ayudó a avanzar en todas las etapas del proyecto.

Todo el LDSGAT por estar ahí para lo que hizo falta y motivarme constantemente.

Los compas de limno, principalmente a Elena y Hernán por darme tremenda mano en las salidas de campo y en el laboratorio.

La investigación que da origen a los resultados presentados en el presente documento recibió fondos de la Agencia Nacional de Investigación e Innovación bajo el código POS_NAC_2020_1_163887.

Esta investigación fue financiada por la Comisión Sectorial de Investigación Científica de la Universidad de la República a través de los proyectos I+D 2018 y 2022.

Resumen

Las actividades agropecuarias intensivas aumentan la exportación de nutrientes desde tierras agrícolas a los cuerpos de agua, favoreciendo el desarrollo de fitoplancton. Este problema ambiental tiene impactos económicos y sanitarios negativos, en especial cuando las floraciones de cianobacterias alcanzan tomas para potabilización. La principal toma para potabilización del Uruguay, denominada Aguas Corrientes (AACC), se encuentra en la Cuenca del Río Santa Lucía (SLRB), donde se ubican numerosos reservorios de agua pequeños y medianos (0.25 - 30 ha) que son considerados fuentes de inóculo de cianobacterias. Sin embargo, aún no existe información sobre el estado trófico y la capacidad de producir floraciones de fitoplancton de dichos ambientes, lo que podría abordarse a través de un plan de monitoreo remoto de alta frecuencia. Esta tesis se propuso aportar herramientas que permitan evaluar por primera vez la calidad del agua de los reservorios ubicados en la SLRB, su distribución espacial y las condiciones que favorecen el desarrollo del fitoplancton mediante imágenes satelitales gratuitas. Para ello, se ajustaron indicadores ópticos para monitorear los reservorios, se identificaron zonas de la cuenca con mayor riesgo potencial de exportación de biomasa desde reservorios de agua hacia AACC, y se evaluó la dinámica espaciotemporal del estado trófico, su relación con variables meteorológicas, morfológicas de los cuerpos de agua y de usos del suelo. En términos generales, los reservorios con mayor concentración de clorofila-a (Chla) se agruparon en el sur y oeste, mientras que en el noreste y el centro de la cuenca se detectaron las concentraciones más bajas. Los principales factores reguladores de la Chla fueron el tamaño de los reservorios, la temperatura del aire y la intensidad de uso del suelo en el área de drenaje de los reservorios, sin embargo, se relacionaron de forma diferencial de acuerdo a su ubicación en la cuenca. Los resultados alcanzados evidencian la precisión de las herramientas de estimación satelital, lo cual aporta a las capacidades de monitoreo de los recursos hídricos del país. Asimismo, permiten realizar diagnósticos sinópticos rápidos y gratuitos de la calidad del agua, aportan insumos para la focalización de esfuerzos de monitoreo *in situ* y contribuyen a la mitigación de los procesos de eutrofización en ambientes con alto riesgo de transportar inóculos de cianobacterias hacia la principal toma para potabilización del país.

Abstract

Intensive agricultural activities increase the export of nutrients to water bodies, favoring phytoplankton growth, which represent a problem with negative economic and health impacts, especially when they reach water utilities. The main water utility in Uruguay (AACC) is located in the Santa Lucía River Basin (SLRB), where numerous small water reservoirs are considered sources of cyanobacteria inoculum. However, there is still no information on the trophic state and occurrence of phytoplankton blooms in these environments, which can be approached with a remote high-frequency monitoring plan. This thesis aimed to provide tools that allow evaluating for the first time the water quality of the reservoirs located in the SLRB, its spatial distribution, and the conditions that favor the development of phytoplankton blooms through free satellite images. To this end, optical indicators for monitoring reservoirs were adjusted, areas of the basin with a higher risk of export of cyanobacterial biomass were identified, and the spatiotemporal dynamics of the trophic state and its relationship with climatic, structural, and land use variables were evaluated. In general, the reservoirs with the highest chlorophyll-a concentration (Chla) were grouped in the southern and western areas, while the lowest concentrations were detected in the northeast and center of the basin. The main regulatory factors in Chla were the size of the reservoirs, the temperature, and the intensity of land use; however, they were differentially related according to their location in the basin. The results achieved increase the monitoring capacities of small continental water bodies in the country. They allow for rapid and free synoptic diagnoses of water quality, provide input for focusing on-site monitoring efforts, and contribute to mitigating eutrophication processes in environments with a high risk of transporting cyanobacteria inocula to the country's main drinking water utility.

1. Capítulo 1

1.1 Introducción general

La intensificación agraria ha generado un aumento progresivo en la exportación de nutrientes limitantes para la productividad primaria (nitrógeno y fosforo principalmente) en los cuerpos de agua continentales. Este fenómeno, favorece los procesos de eutrofización caracterizados por el aumento de la biomasa de productores primarios, en particular fitoplancton (cianobacterias y algas eucariotas), con respecto a un estado inicial (Carpenter et al., 2011; Schindler, 1977). Cuando el incremento de la biomasa es dominado por una o pocas especies, se denomina floración de fitoplancton (Smayda, 1997).

En las últimas décadas, la ocurrencia e intensidad de las floraciones de fitoplancton en diversos ecosistemas han aumentado a nivel mundial (Burford et al., 2020; O`Neil et al., 2012). Dicho fenómeno tiene numerosas consecuencias, impacta sobre la trama trófica, la biodiversidad y la calidad del agua, además estos organismos pueden producir toxinas (comúnmente microcistina) perjudiciales para la salud humana y animal (Chorus y Welker, 2021). Cuando las floraciones de fitoplancton ocurren en ecosistemas de uso recreativo, impactan sobre el sector turístico y pueden generar pérdidas económicas (Kruk et al., 2019). En los ambientes acuáticos que se utilizan con fines productivos, la elevada concentración de microcistina puede generar intoxicaciones graves tanto en el ganado como en la fauna autóctona (Brena et al. 2021; Svirčev et al., 2019; Carmichael, 1996). Cuando las floraciones de cianobacterias llegan a las tomas para potabilización, aumentan los costos derivados del proceso (Kouzminov et al., 2007). Asimismo, cuando no son detectadas a tiempo representan un riesgo sanitario significativo (Chorus y Welker, 2021), ya que pueden llegar a los hogares a través de la red de abastecimiento pública (Amorín y Larghero, 2017).

Los cuerpos de agua continentales ubicados en cuencas de uso agropecuario intensivo generalmente presentan elevadas concentraciones de nutrientes, que, en conjunto con el prolongado tiempo de residencia del agua, el aumento en la temperatura y el ingreso de la radiación solar generada por la sedimentación de materiales particulados, representan condiciones que potencian los procesos de eutrofización, generalmente dominados por cianobacterias (Bonilla et al., 2015; Burford y O'Donohue, 2006). Estos organismos poseen funciones fisiológicas que les confieren una gran adaptabilidad al ambiente, como

su capacidad de migrar en la columna de agua, el aprovechamiento de las fluctuaciones en la disponibilidad de nutrientes y su elevada plasticidad fenotípica (Aubriot y Bonilla, 2018; Aguilera et al., 2017).

Los reservorios de agua construidos con fines de explotación agropecuaria en general son pequeños, someros, reciben grandes cargas de nutrientes desde la cuenca y en muchos casos el ganado ingresa a abrevar (Olano, 2024). Sus características determinan que sean susceptibles a los procesos de eutrofización (Powers et al., 2015). Dichos ambientes, se destacan por su gran cantidad, ya que la mayoría de los establecimientos deben contar con fuentes de agua, esto genera que sean difíciles de regular y monitorear. Para avanzar en la elaboración de pautas de gestión de los reservorios, el primer paso es diagnosticar su estado de situación y el impacto de las actividades productivas sobre el desarrollo de floraciones de fitoplancton (Weber et al., 2020).

Para evaluar la incidencia de las actividades productivas, las variables meteorológicas y la dinámica del paisaje sobre la calidad del agua, se deben tomar a las cuencas hidrográficas como unidad espacial de análisis (Achkar, 2002), ya que los ambientes acuáticos lénticos reflejan los procesos que ocurren en las microcuencas y facilitan dicha evaluación (Weber et al., 2020). En este sentido, los sistemas de información geográfica son herramientas indispensables que permiten vincular variables mediante sus atributos espaciales y generar insumos fundamentales en la planificación y gestión ambiental (Moreno, 2007; Zhang y Jørgensen, 2005).

Los métodos tradicionales para evaluar el estado trófico y las floraciones de fitoplancton en cuerpos de agua continentales requieren de la obtención de muestras *in situ* y del análisis de laboratorio. Para ello, es necesaria la alta calificación de especialistas, y esfuerzos económicos y de tiempo (Lins et al., 2017; Navalgund et al., 2007). Dichas características imposibilitan el monitoreo de numerosos cuerpos de agua y limita la descripción de las dinámicas espacio temporales del estado trófico (Cook et al., 2023; Tamm et al., 2019). Esta situación se agrava durante los fenómenos de floración microalgal ya que los cambios en las comunidades suelen ser rápidos y pueden tener una alta variabilidad espacial de la clorofila-a (Chla), especialmente en el caso de las floraciones acumulativas (ej. *Microcystis*) (Chorus y Welker, 2021). Este tipo de floración puede formar estrechas agrupaciones de concentraciones elevadas y pasar desapercibida en muestreos espacialmente acotados (Bowling et al., 2015; Oliver et al., 2012). En este sentido es crítico el uso de métodos capaces de monitorear numerosos cuerpos de agua

de forma sinóptica y con alta frecuencia (Gallegos y Neale, 2015), entre los que se destacan las técnicas de teledetección aplicadas a partir de imágenes satelitales gratuitas (Bresciani et al., 2019; Clark et al., 2017).

1.1.2 Teledetección

La teledetección se basa en la interpretación de la reflectancia superficial censada de forma remota (Rrs) definida como la relación entre la radiación que emite la superficie y la radiación descendente (Chuvieco, 1995). En ecosistemas acuáticos, la Rrs es el resultado de la dirección del campo de luz y de las propiedades ópticas inherentes del medio, entre las que se encuentra el coeficiente de absorción y dispersión de los constituyentes ópticamente activos (COAs); los más reconocidos son: pigmentos de fitoplancton, sólidos en suspensión, y carbono orgánico disuelto coloreado (CDOM) (Ogashawara et al., 2017). Desde hace más de cuatro décadas que las imágenes satelitales se utilizan para inferir la concentración de los COAs a partir de los registros de Rrs; los estudios pioneros monitorearon océanos, estuarios y grandes lagos (Nechad et al., 2010; Vincent et al., 2004; Gons, 1999; Gitelson et al., 1986; Gordon et al., 1980; Strong, 1974). Con el avance tecnológico de los sensores remotos a bordo de satélites, se expandió el uso de la herramienta a cuerpos de agua continentales turbios y de menor tamaño (Cook et al., 2023; Ansper, 2018; Toming et al., 2016; Hansen et al., 2015). Las principales potencialidades de la teledetección son la disminución de los costos de monitoreo con respecto a las metodologías tradicionales, la disponibilidad de series de datos temporales, la posibilidad de monitorear grandes superficies y un gran número de cuerpos de agua con alta frecuencia (Page et al., 2018; Ritchie et al., 2003).

Para estimar satelitalmente la concentración de los COAs en cuerpos de agua continentales se utilizan indicadores de relación de bandas que deben ser ajustados para los ambientes objetivos del monitoreo (Yang et al., 2017). En este sentido, numerosos antecedentes bibliográficos han ajustado y validado indicadores de bandas espectrales para la cuantificación de la Chla. Entre los más utilizados se encuentra el Índice de Diferencia Normalizada de Clorofila (NDCI) (Mishra y Mishra, 2012); utiliza la relación normalizada de Rrs rojo (~ 665 nm) - Rrs *borde rojo* (~ 700 nm) y ha sido validado con éxito en aguas ópticamente complejas (Page et al., 2018; Beck et al., 2016; Augusto-Silva et al., 2014). Por otro lado, se destaca la alta precisión para estimar Chla mediante la

relación de Rrs entre rojo (~ 665 nm) y verde (~ 560 nm) (Ioannou et al., 2014), en ambientes con baja Chla (4.6 µg L^{-1}) (Ha et al., 2017) y alta Chla (65.1 µg Chla L^{-1}) (Oliveira et al., 2016).

La transparencia es determinada principalmente por la concentración de sólidos en suspensión, el carbono orgánico disuelto (CDOM) y la biomasa de fitoplancton; COAs que solapan su máxima absorción de la energía en ~ 500 nm y disminuyen progresivamente hacia los infrarrojos cercanos (Ogashawara et al., 2017). Dicha característica ha generado una amplia diversidad de enfoques para estimar satelitalmente la transparencia (Ouma et al., 2020; Topp et al., 2020), como ser la relación de bandas en la región visible (Zhang et al., 2021), de los infrarrojos cercanos (> 700 nm) (Le et al., 2009) y otras combinaciones de bandas (Ouma et al., 2020). Además de estimar la transparencia, se han evaluado mediante indicadores de relación de bandas las concentraciones de CDOM (Kutser et al., 2017), sólidos en suspensión de origen inorgánico y orgánico (Giardino et al., 2017; Pierson y Strömbeck, 2001).

Los indicadores de bandas son ampliamente utilizados y permiten aproximarse a los COAs, sin embargo, la complejidad óptica de las aguas continentales introduce interferencias en su estimación e impide la aplicación de indicadores de forma global (Nechad et al., 2015). Para abordar esta limitante, una metodología posible es clasificar previamente los cuerpos de agua según su respuesta espectral, para ello, se utiliza la magnitud y forma de los espectros Rrs (firmas espectrales), y se aplican técnicas de agrupamiento (Spyrakos et al., 2018; Eleved et al., 2017; Shi et al., 2013). Una vez identificadas las principales características ópticas del agua y generadas las agrupaciones de ambientes con estado trófico similar (Neil et al., 2019), se aplican indicadores de bandas ajustados con información *in situ* (Werther et al., 2021).

Las imágenes satelitales ofrecen la posibilidad de obtener regularmente información georreferenciada del estado trófico de numerosos cuerpos de agua. La recopilación de esta información permite elaborar grandes bases de datos que pueden ser utilizadas para conocer la dinámica espacio-temporal del estado trófico y/o de floraciones de fitoplancton (Torbick et al., 2013). Además, hace posible cartografiar cambios del estado trófico en series de tiempo (Hu et al., 2021), detectar patrones en su distribución espacial (Coffer et al., 2021), identificar tendencias (Tate, 2019), evaluar la incidencia de variables ambientales, usos del suelo y superficie del cuerpo de agua, sobre el estado trófico (Weber et al., 2020), entre otros. Los análisis mencionados se pueden utilizar como insumos que

aportan al diseño y manejo de los cuerpos de agua, a la focalización de los esfuerzos de monitoreo *in situ* (Yunus et al., 2015) y la prevención del contacto de bañistas con floraciones de fitoplancton tóxicas (Aubriot et al., 2020; Copado et al., 2020).

En la actualidad, numerosos programas satelitales brindan imágenes multiespectrales de forma libre, entre ellos, se destaca el sensor Multi Spectral Instrument (MSI) a bordo del satélite Sentinel-2 (2015) de la Agencia Espacial Europea (ESA). Uno de los principales objetivos de Sentinel-2 es aportar a la monitorización de zonas costeras y continentales proporcionando imágenes con una frecuencia de 5 días, y una resolución espectral de 13 bandas con una centrada en 705 nm que permite estimar la concentración de Chla (Dörnhöfer et al., 2018; Liu et al., 2017; Soria et al., 2017; Kutser et al., 2016). Asimismo, su resolución espacial (10, 20 y 60 m) permite evaluar concentraciones de COAs con precisión, lo cual resulta especialmente útil en reservorios de agua pequeños (Toming et al., 2016).

1.1.3 Reservorios de agua

Las actividades agropecuarias y agroindustriales requieren fuentes de agua; en las cuencas con producción intensiva, se construyen numerosos reservorios artificiales o tajamares de distintos tamaños con diferentes diseños de construcción, que varían según las necesidades del establecimiento productivo y de la geomorfología del emplazamiento (García et al., 2008). La mayor parte de los tajamares del Uruguay son construidos a partir de la unión de dos laderas mediante una cortina de tierra (taipa) que funciona como una barrera de contención del escurrimiento superficial y forma una laguna (Ghiggia, 1976). Para la construcción de tajamares es imprescindible una topografía ondulada, tierra disponible para construir la taipa y contar con un escurrimiento superficial suficiente para ser interceptado o la presencia de un curso fluvial intermitente (cañada) (García et al., 2008). En algunos casos se complementa con la profundización del terreno mediante la extracción de materiales con maquinaria, asimismo se pueden requerir obras de mantenimiento para extraer materiales originados por la pérdida de suelo y que reducen la capacidad de almacenamiento del reservorio (Koolhaas, 2003). En menor medida, algunos establecimientos optan por realizar excavaciones y generar pozos que capturan agua de lluvia y de las napas freáticas, si bien su construcción es más costosa que los tajamares, se inunda menos terreno para alcanzar el mismo volumen de agua, por lo tanto,

esta práctica es más frecuente en establecimientos ubicados en zonas con mayor valor de la tierra.

Los sistemas fluviales pueden presentar elevada concentración de nutrientes sin manifestar crecimiento fitoplanctónico (Aubriot et al., 2017; Bonilla et al., 2015). Sin embargo, cuando son represados disminuye la velocidad de flujo, aumenta el tiempo de residencia del agua, la sedimentación, el ingreso de luz a la columna de agua y el consecuente aumento en la temperatura, dichas condiciones son ideales para el desarrollo del fitoplancton (Beaver et al., 2014; Schindler, 1977), especialmente las cianobacterias (Huisman et al., 2018; Burford y O'Donohue, 2006).

En los reservorios artificiales se pueden desarrollar floraciones de cianobacterias, que son transportadas aguas abajo de forma constante en pequeñas cantidades (Grill et al., 2019; Remmal et al., 2017). Por otro lado, en eventos puntuales de precipitaciones elevadas se pueden transportar grandes cantidades de biomasa, debido a la apertura de vertederos en el caso de las represas y a desbordes en los reservorios más pequeños (Grabowska y Mazur-Marzec, 2011). El origen de este fenómeno de transporte de cianobacterias aguas abajo puede ser identificado cuando se trata de grandes cuerpos de agua (Aubriot et al., 2020), sin embargo, otros casos son particularmente complejos como en las cuencas con múltiples embalses eutróficos de pequeño tamaño que drenan a un curso fluvial.

1.1.4 Eutrofización en ecosistemas acuáticos de Uruguay

En las últimas décadas se identificaron tendencias crecientes de la agricultura intensiva, la cual se expandió y consolidó en todo el territorio nacional en suelos con alto y bajo potencial productivo (Gazzano et al., 2019). Esta tendencia es acompañada y fomentada por políticas que promueven el aumento en la producción de granos (soja, maíz, arroz), como las modificaciones (2017) a la Ley 16.858 de Riego con Destino Agrario que favorece la construcción de embalses con fines de riego, por lo tanto, se espera que aumenten su cantidad en los próximos años.

En Uruguay, se reportan síntomas de eutrofización desde hace décadas en diversos ecosistemas (Bonilla et al., 2015), entre los que se destacan las lagunas costeras (Crisci et al., 2017), lagos urbanos (Zabaleta et al., 2021; Martigani, 2017), represas de producción hidroeléctrica (Kruk et al., 2019; Bordet et al., 2017), playas del Río de la

Plata (Zabaleta et al., 2023b; Aubriot et al., 2020; Kruk et al., 2019), ríos y arroyos (Aubriot et al., 2017; Goyenola et al., 2015). Se destaca que las floraciones de cianobacterias son una de las principales problemáticas en la potabilización del agua superficial que generan aumentos en los costos de potabilización principalmente por el mayor uso de carbono activado (Santos et al., 2021) y riesgos para la salud humana (Somma et al., 2022; Gonzalez-Madina et al., 2021; Aubriot et al., 2017). En los últimos años se ha evidenciado el riesgo sanitario y económico de los reservorios artificiales ubicados en cuencas de uso agropecuario intensivo; por ejemplo, en el verano de 2019 una extensa floración de cianobacterias proveniente de los grandes embalses del Río Negro alcanzó las playas uruguayas del Río de la Plata y se instaló durante más de noventa días, lo cual generó grandes impactos sobre la actividad turística (Aubriot et al., 2020, Kruk et al., 2019).

Numerosas investigaciones realizadas en el país sugieren que la principal causa de la eutrofización de los cuerpos de agua continentales es el incremento en la intensidad en los usos del suelo, seguida por los usos del suelo urbano y agroindustrial (Mazzeo et al., 2024; Chalar et al., 2011; Ernst y Siri-Prieto, 2011; Bonilla et al., 2006). La exportación de nutrientes a los cuerpos de agua es explicada por numerosos factores, la variabilidad climática intra-anual en conjunto con variables estructurales (topografía, suelos, características morfométricas) de la cuenca condicionan el uso del territorio y generan "pulsos" de nutrientes (Goyenola et al., 2015). Asimismo, en cuencas de uso agrícola intensivo el manejo de las unidades productivas podría determinar en mayor medida dicha exportación (Aubriot et al., 2017; Díaz, 2013). La aplicación de fertilizantes en conjunto con el reemplazo de la cobertura vegetal en zonas riparias, donde podrían retenerse nutrientes en la vegetación y disminuir la concentración de nutrientes en el agua de escorrentía superficial (Calvo et al., 2024; Aguiar et al., 2015), favorecen la llegada de nutrientes a los cuerpos de agua continentales. Por otro lado, los monocultivos cerealeros remueven por completo la cobertura vegetal durante el período post cosecha y durante la siembra, lo cual promueve procesos erosivos que determinan el transporte de materiales particulados y sustancias disueltas ricas en nutrientes orgánicos e inorgánicos (García et al., 2018).

En los próximos años se prevén aumentos en la temperatura y en los fenómenos extremos de lluvias intensas y sequías extremas (IPCC, 2023); tendencias climáticas que promueven el aporte de nutrientes hacia los cuerpos de agua continentales (Paerl, 2017;

Sinha et al., 2017). Estos factores en conjunto con las alteraciones hidrológicas que aumentan los tiempos de residencia del agua (O'Neil et al., 2012), constituyen las principales variables que favorecen las floraciones de fitoplancton en intensidad, extensión, frecuencia y duración (Zabaleta et al., 2023b; Burford et al., 2020; Ho et al., 2019).

En los últimos años se propiciaron algunos avances en el monitoreo de los ecosistemas acuáticos del país. Se destaca la colocación de boyas en el Río Negro, las que brindan información en tiempo real, disponible en https://www.ambiente.gub.uy/oan/irn/, y el monitoreo satelital generado a partir del entrenamiento de modelos mediante detección visual de floraciones de fitoplancton https://observatorioan.users.earthengine.app/view/visualizador-floraciones-dinacea.
También se destaca la información de banderas sanitarias generada por los servicios departamentales de guardavidas, que, durante la temporada cálida registran de forma diaria la colocación o no de banderas sanitarias a partir de técnicas de detección visual de floraciones de fitoplancton. A pesar de la gran cantidad de reservorios de agua con fines productivos (1363 registrados hasta 2015; MVOTMA 2017), aún no se han desarrollado programas de monitoreo continuo de ecosistemas acuáticos pequeños, lo cual limita el conocimiento sobre la calidad del agua y la prevención de eventos de floraciones en tomas para potabilización.

Los sistemas de alerta temprana de floraciones de cianobacterias en aguas para potabilización se componen de niveles de alerta que focalizan los esfuerzos de monitoreo y desencadenan acciones de gestión de los ambientes afectados (Chorus y Welker, 2021). Para el desarrollo de estos sistemas se debe contar con un indicador de biomasa fitoplanctónica validado, que pueda ser monitoreado con alta frecuencia y que permita obtener niveles de riesgo potencial de presencia de cianobacterias. En este sentido, el monitoreo remoto posibilita el diagnóstico en simultáneo de numerosos cuerpos de agua distribuidos en grandes extensiones territoriales de forma simultánea y con alta frecuencia (Matthews y Bernard, 2015), lo cual representa un insumo clave para el desarrollo de un sistema de alerta temprana y que contribuye a su predicción mediante la identificación de las variables que condicionan el desarrollo de las floraciones (Weber et al., 2020).

1.1.5 Agua para potabilización en el Río Santa Lucía

La Cuenca del Río Santa Lucía (SLRB) es la principal fuente de abastecimiento de agua potable del país que alcanza a cubrir la demanda del 60% de la población nacional y que se encuentra en una situación crítica de deterioro en la calidad de sus aguas (Aubriot et al., 2017). En 2013, una floración de cianobacterias pasó inadvertida en la principal toma para potabilización del Uruguay en el Río Santa Lucía, Aguas Corrientes (AACC), cuyas consecuencias de mal sabor, olor del agua, y posible presencia de metabolitos tóxicos, alcanzó a más del 60% de la población (Amorin y Larghero, 2017). Un estudio posterior determinó que los períodos de mayor caudal en el Río, luego de importantes precipitaciones, conllevaba el transporte de grandes biomasas de cianobacterias típicamente dominantes en cuerpos de agua represados (lénticos); por lo tanto, su origen apuntó a los reservorios de agua en predios productivos de la cuenca de drenaje (Somma et al., 2022).

Con el objetivo de formular y ejecutar acciones para controlar, detener y revertir el proceso de deterioro de la calidad del agua en la SLRB, así como para asegurar su calidad y cantidad para el uso sustentable como abastecimiento de agua potable, el gobierno nacional presentó el "Plan de acción para la protección del agua en la cuenca del Santa Lucía" (https://www.gub.uy/ministerio-ambiente/comunicacion/publicaciones/plan-accion-para-proteccion-del-agua-cuenca-del-santa-lucia-junio-2015). Este documento parte de la premisa que la calidad del agua bruta para potabilizar depende de la calidad ambiental de la cuenca. En primer lugar, se identificaron las principales fuentes de contaminación, que se dividieron en fuentes puntuales de efluentes urbanos y agroindustriales, y fuentes difusas relacionadas a las actividades agropecuarias. De los análisis realizados surge la necesidad de implementar medidas que permitan mitigar las causas del deterioro en la calidad del agua. Para ello, se definieron 11 medidas de control de la degradación ambiental de la SLRB entre las que se destaca: suspender la instalación de nuevos emprendimientos de engorde de ganado a corral en cielo abierto, y la ampliación de los existentes; restringir el acceso directo del ganado a abrevar en los cursos de la cuenca de AACC; instaurar una zona de amortiguación o buffer en la cuenca hidrográfica declarada sin laboreo de la tierra y uso de agroquímicos (para la conservación y restitución del monte ribereño como forma de restablecer la condición hidromorfológica del Río). Se destaca que ninguna medida apunta a gestionar los reservorios pequeños de uso productivo con la finalidad de mitigar y prevenir los procesos de eutrofización y de

floraciones de fitoplancton, los que implican un riesgo para la potabilización del agua debido al potencial transporte de las floraciones hacía AACC.

Debido a que las floraciones de cianobacterias en AACC restringen el uso de potabilización se requieren herramientas que aumenten las capacidades de detección de floraciones a nivel temporal y de extensión territorial, para aportar al sistema de gestión y aumentar la capacidad de respuesta del país. En este sentido, las herramientas de teledetección resultan innovadoras ya que permiten monitorear numerosos ambientes de difícil acceso desplegados en grandes extensiones del territorio de forma simultánea, lo que facilita focalizar esfuerzos de gestión y mitigación de los procesos de eutrofización.

1.2 Objetivo General

Contribuir a la gestión de los reservorios de agua de uso productivo de la Cuenca del Río Santa Lucía a través del desarrollo e implementación de técnicas de teledetección que permitan conocer su distribución espacial, su estado trófico, y los factores que favorecen el desarrollo de floraciones de fitoplancton

1.3 Objetivos específicos

Ajustar indicadores ópticos para la estimación satelital de la Chl-a y transparencia en los reservorios ubicados en la Cuenca del Río Santa Lucía (Cap. 2)

Evaluar la dinámica espacial y temporal de indicadores de biomasa fitoplanctónica e identificar los reservorios con mayor riesgo potencial de exportación de cianobacterias hacia la planta potabilizadora de Aguas Corrientes (Cap. 3)

Evaluar la dinámica espacial y temporal del estado trófico de los reservorios ubicados en la Cuenca del Río Santa Lucía en el período 2016-2022 (Cap. 4)

Establecer la relación entre las precipitaciones, variables morfológicas de los cuerpos de agua y de usos del suelo con el comportamiento óptico de los reservorios (Cap. 4)

1.4 Estrategia general de investigación

En Uruguay, la implementación de técnicas de teledetección para conocer y evaluar procesos de eutrofización de cuerpos de agua continentales es reciente. El primer paso fue ajustar indicadores de relación de bandas en cuerpos de agua específicos como lagos urbanos (Zabaleta et al., 2021), embalses hidroeléctricos (Drodz et al., 2019), laguna del Sauce (Caussi, 2017). Sin embargo, en Uruguay hay miles de cuerpos de agua lénticos pequeños utilizados con fines productivos de los que se desconoce su cantidad y calidad del agua. El aporte de la tesis es aproximarse al estado trófico de esos ambientes caracterizados por su importancia estratégica tanto para el sistema productivo como para el agua destinada a potabilización. Para ello, se ajustaron modelos de estimación satelital del estado trófico mediante información in situ de catorce reservorios; nutrientes totales, sólidos en suspensión, Chla y Chla de cianobacterias. Los modelos más exitosos fueron utilizados posteriormente para monitorear estacionalmente 325 reservorios distribuidos en la SLRB (6355 Km^2) en el período 2016-2022.

Los resultados alcanzados en la tesis fueron estructurados para presentarse en tres capítulos, cada uno corresponde a un artículo publicado o en revisión en una revista internacional arbitrada. El segundo capítulo tuvo como objetivo ajustar un indicador de bandas que permita estimar la Chla y la Transparencia mediante imágenes satelitales Sentinel-2 y explorar su aplicación en fechas puntuales. Para ello, se realizaron muestreos in situ en simultáneo con el pasaje del satélite (-/+ 3 h), se ajustaron modelos lineales y se aplicaron en 486 embalses. En el tercer capítulo, con la finalidad de aproximarse a identificar las fuentes de inóculo de cianobacterias que llegan a AACC, se elaboraron productos cartográficos que ilustran el riesgo potencial de exportación de biomasa en los días previos a los eventos de concentración elevada de cianobacterias. Para ello, se integró la información de Chla de los reservorios estimada mediante el indicador ajustado en el primer capítulo, con la de precipitaciones acumuladas y con la distancia recorrida a través de la red hidrográfica entre los ambientes y AACC, en esta sección se redujo el área de estudio a la cuenca que drena directamente hacia AACC y por lo tanto disminuyó la cantidad de reservorios a monitorear, con un total de 325. En el cuarto capítulo se realizó el monitoreo satelital de los reservorios entre los años 2016 y 2022, se evaluaron patrones de distribución espacial de su estado trófico y de sus relaciones con las condiciones ambientales; por otro lado, se exploraron las principales variables relacionadas con el comportamiento óptico de los cuerpos de agua (Fig. 1.1).

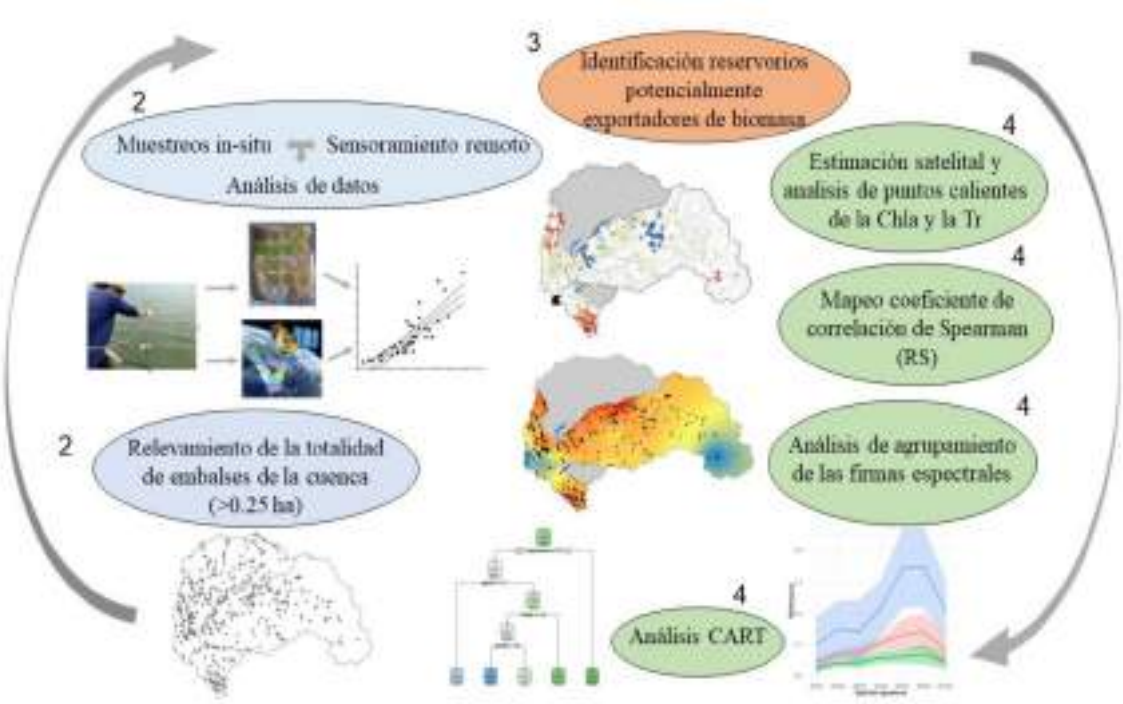

Fig. 1.1 Estructura de la tesis. Por color y número se diferencian las actividades por capítulo.

2. Capítulo 2

Satellite assessment of eutrophication hot spots and algal blooms in small and medium-sized productive reservoirs in Uruguay's main drinking water basin

Bernardo Zabaleta [a, b, *], Luis Aubriot [b], Hernán Olano [b], Marcel Achkar [a]

[a] Laboratorio de Desarrollo Sustentable y Gestión Ambiental del Territorio, Instituto de Ecología y Ciencias Ambientales, Facultad de Ciencias, Universidad de la República, Montevideo, Uruguay

[b] Grupo de Ecología y Fisiología de Fitoplancton, Sección Limnología, Instituto de Ecología y Ciencias Ambientales, Facultad de Ciencias, Universidad de la República, Montevideo, Uruguay

*Corresponding author. Facultad de Ciencias, Universidad de la República, Iguá 4225, CP11400, Montevideo, Uruguay. E-mail address: bzabaleta@fcien.edu.uy (B. Zabaleta)

Environmental Science and Pollution Research (2023), 30(15), 43604-43618

https://doi.org/10.1007/s11356-023-25334-9

2.1 **Abstract**

Intensive agricultural activities favor eutrophication and harmful phytoplankton blooms due to the high export of nutrients and damming of rivers. Productive watersheds used for water purification can have multiple reservoirs with phytoplankton blooms, which constitutes a high health risk. In general, water quality monitoring does not cover small and medium-sized reservoirs (0.25-100 ha) of productive use due to their large number and location in private properties. In this work, the in-situ trophic state of fourteen reservoirs was simultaneously assessed using Sentinel-2 images in the Santa Lucía River Basin, the main drinking water basin in Uruguay. These reservoirs are hypereutrophic (0.18-5.22 mg total P L^{-1}) with high phytoplankton biomasses (2.8-4439 µg chlorophyll-a L^{-1}), mainly cyanobacteria. Based on data generated in-situ and Sentinel-2 imagery, models were fitted to estimate satellite Chl-a and transparency in all the basin reservoirs (n=486). The best fits were obtained with the green-to-red band ratio (560 and 665 nm, R^2=0.84) to estimate chlorophyll-a and reflectance at 833 nm (R^2=0.73) to determine transparency. The spatial distribution of the trophic state was explored by spatial autocorrelation and hotspot analysis, and the variation in spatial patterns could be determined prior and subsequent to a maximum cyanobacteria value in water treatment plant intakes. Therefore, reservoirs with greater potential for phytoplankton biomass export were identified. This work provides the first fitted tool for satellite monitoring of numerous reservoirs, and strengthens the country's ability to respond to harmful phytoplankton blooms in its main drinking water basin.

Keywords: Drinking water, remote sensing, phytoplankton bloom, hotspot, cyanobacteria, space pattern, Sentinel-2.

2.2 **Introduction**

Eutrophication is one of the most widespread environmental problems affecting surface waters worldwide (Michalak et al., 2013; Burford et al., 2020), since it affects the trophic web, biodiversity, and water quality (Carpenter et al., 1998; Chapin et al., 2011). This

excessive nutrient enrichment process has a detrimental effect not only on ecosystem conservation and recreation but also on water supply for animal and human drinking, to name a few. Indeed, this gives rise to particular concern in terms of human health and economic costs (Conley et al., 2009; Dodds et al., 2009).

Increased nutrient concentration, high water residence time, increased temperature, and low turbidity create suitable conditions for phytoplankton growth (Reynolds, 2006). In lentic aquatic systems, excessive growth of phytoplankton biomass is often dominated by cyanobacteria (Burford and O'Donohue, 2006). These can produce toxins detrimental to aquatic and terrestrial biota, among which the most common is microcystin (Chorus and Welker, 2021), represented by several genera, most notably Microcystis (Carmichael, 2001; Leflaive and Ten-Hage, 2007; Pearson et al., 2016). In recent decades, the occurrence of cyanobacterial blooms has been exacerbated on a global scale in terms of frequency, magnitude, and duration (Huisman et al., 2018; Burford et al., 2020).

Traditional monitoring methods require obtaining samples from numerous water bodies and subsequent laboratory analysis, thus entailing high economic, time, and skilled efforts (Navalgund et al., 2007; Lins et al., 2017). As an alternative, numerous indicators have been developed to quantify phytoplankton pigments and water transparency based on remote sensing reflectance (Rrs) and information collected in-situ (Ha et al., 2017; Watanabe et al., 2018; Giardino et al., 2019). Regarding inland waters, there is no consensus on the use of specific indicators for estimating chlorophyll-a (Chl-a) concentrations (Nechad et al., 2015). In general terms, approaches to successfully estimate Chl-a use reflectance near the red edge (~700 nm), where Chl-a exhibits its lowest absorption coefficient (maximum Rrs), and in the red (~665 nm) edge where it exhibits the highest absorption coefficient (minimum Rrs) (Gitelson et al., 1992). The Normalized Difference Chlorophyll Index (NDCI), which is based on the difference between Rrs ~700 nm and Rrs ~665 nm (Mishra and Mishra, 2012), is worth noticing. Also, some research studies have shown high accuracy for estimating Chl-a based on the red (~665 nm) to green (~560 nm) reflectance ratio (Ioannou et al., 2014), both in environments with low (4.6 µg L^{-1}) (Ha et al., 2017) and high (65.1 µg L^{-1}) Chl-a concentrations (Oliveira et al., 2016). It should be underlined that these indicators should be adjusted with in-situ information gathered from the environments to be monitored (Yang et al., 2017).

The concentration of suspended solids, Chl-a, and dissolved organic carbon determine the transparency of inland waters, which has historically been measured in-situ with the Secchi disk. Likewise, several research studies have estimated transparency from surface reflectance in the visible region (Zhang et al., 2021), near-infrared region, and by band combination (Ouma et al., 2020). This diversity of approaches is based on the fact that suspended solids and Chl-a increase water brightness, and, therefore, reflectance throughout the visible/NIR spectrum (Topp et al., 2020).

Uruguay has been facing issues related to eutrophication and phytoplankton blooms in several ecosystems for decades (Bonilla et al., 2015). They are mainly associated with excess nutrient inputs from agribusiness expansion, urban, and agroindustrial initiatives, as well as reservoir construction (Conde et al., 2002; Bonilla et al., 2006; Chalar et al., 2011; Ernst and Siri-Prieto, 2011; Aubriot et al., 2017). Even though great efforts have been undertaken to assess eutrophication in various water bodies distributed throughout the national territory (Bonilla et al., 2015; Haakonsson et al., 2017), the lack of information on the trophic state of small and medium-sized reservoirs for productive purposes (irrigation, agro-industrial, animal consumption) raises our concern.

In general, agricultural reservoirs receive significant nutrient inputs for being located in watersheds where intensive agriculture is practiced. This, along with the high residence time of water, creates favorable conditions for the development of cyanobacterial blooms (Bowling et al., 2013; Beaver et al., 2014). These environments frequently suffer overtopping due to excess rainfall, flushing the bloom downstream and leading to their potential transport to the water treatment plant intakes. This scenario was evaluated in the Santa Lucia River Basin (SLRB), where high flows (and rainfall) were associated with the presence of harmful phytoplankton in the river, typically found in lentic and eutrophic environments, with the potential to affect water purification in the main treatment plant in the country (Aguas Corrientes) (Somma et al., 2022).

A large number of reservoirs have been registered in Uruguay as of 2015 (1,363 reservoirs that supply domestic, commercial, industrial, irrigation, and other agricultural uses; MVOTMA 2017). The number of reservoirs amounts to approximately 7,800 if small- and medium- (0.25- 10 ha) sized unregistered reservoirs are included (Achkar et al., 2016). Reservoirs are expected to increase in number in this country due to the enforcement of policies that promote their construction (Act 16.858/1997 modified in

2017). Given their large number and the fact that they are located in private properties in most cases, conducting an in-situ evaluation of water quality is not always feasible.

SLRB is the main source of drinking water in Uruguay, accounting for 60% of the national supply. Considering that harmful phytoplankton blooms restrict water treatment, tools are required to enhance monitoring practices at a temporal and spatial level in order to improve the current management interventions and strengthen the country's response capacity (Aubriot et al., 2020). In this context, the present work aims at fitting optical indicators for satellite estimation of Chl-a concentration and transparency in order to monitor all the agricultural reservoirs in SLRB before and after high cyanobacterial concentrations in the Planta Potabilizadora de Aguas Corrientes (PPAC) (National Administration of State Sanitary Works, OSE). This work seeks to develop continuous monitoring tools for reservoirs and generate a rapid water quality diagnosis to improve the identification of eutrophication hot spots, as well as to strengthen the country's ability to respond to harmful phytoplankton blooms in its main drinking water basin.

2.3 **Methodology**

The methodological strategy is divided into four sections. The first one deals with the survey of all the reservoirs (0.25-100 ha) in the SLRB upstream PPAC, reservoir selection, and obtaining the authorizations needed to carry out in-situ sampling. The second delves into the acquisition of in-situ information, for which three sampling campaigns were carried out in fourteen agricultural reservoirs. Physicochemical parameters, total nitrogen and phosphorus (TN and TP, respectively), phytoplankton pigments, transparency, and suspended solids were measured. Surface level Rrs was also calculated using Sentinel-2 images obtained +/- 4 hours apart from in-situ sampling. In the third stage, spectral signatures were analyzed and linear models were developed to monitor satellite Chl-a concentration and transparency on two specific dates. Finally, the spatial distribution patterns of these variables were explored (Fig. S2.1).

2.3.1 Study area

The study area includes the basin that drains to the water treatment plant intakes in the PPAC, as well as the basins of the Santa Lucía and Santa Lucía Chico rivers and La

Virgen and Canelón Grande streams (Fig. 2.1), covering a total area of 9131 km2. Various productive activities are carried out in this area. In the southern region, horticulture, fruit growing, wine production, pig and poultry farming prevail, while in the central region, dairy farming stands out. In the east, livestock, forestry crops, and mining dominate (Achkar et al., 2012) (Fig. 2.1). Increasing trends in land-use intensity have been identified in the basin from 2000-2017, mainly linked to the cultivation of cereals in monoculture, mostly soybean, but also corn, and sorghum (Gazzano et al., 2019).

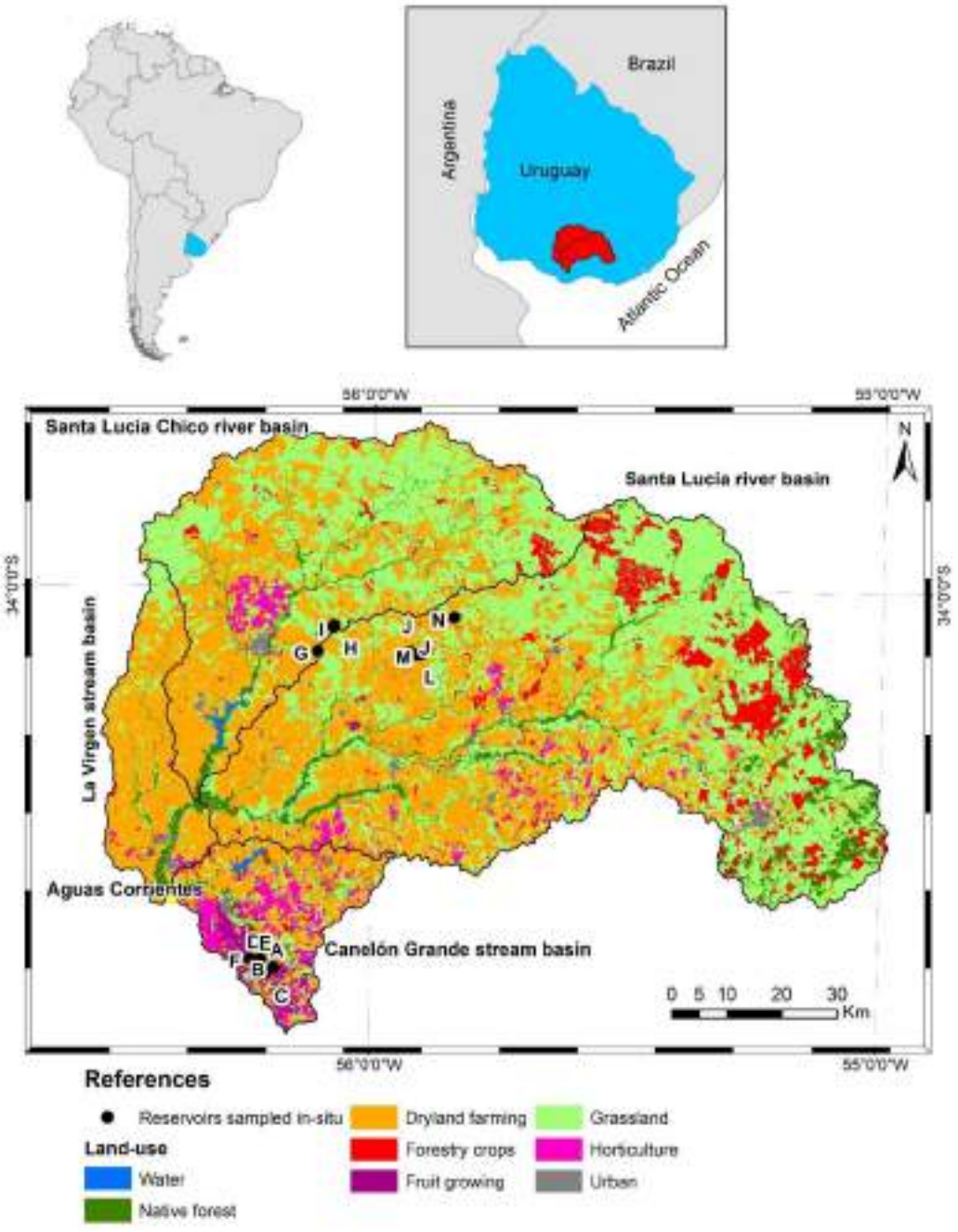

Fig. 2.1 Study area, location of the fourteen reservoirs sampled in-situ and land use as of 2015 according to information provided by the Environmental Protection Ministry

2.3.2 Sampling

To select the reservoirs to be sampled in-situ, in the first place, potential reservoirs were chosen using surrounding land use as a criterion, according to the aerial imagery provided by the Spatial Data Infrastructure Agency of Uruguay (IDEUY). The first field trip was carried out in July 2019 in order to obtain access permits to establishments under different land-use types, such as pastures, planted grasslands, fruit trees, dairy farms, and dryland farming. Fourteen reservoirs were finally chosen according to accessibility (Fig. 2.1).

Three in-situ samplings were performed in fourteen reservoirs on 07/11/2019, 02/12/2019, and 16/11/2020), and a total n of 42 samplings were obtained, made up of three replicates per reservoir (126 samples). In each reservoir, physicochemical parameters (temperature, pH, conductivity, dissolved oxygen, turbidity) were measured using Horiba U-52G probe, and transparency with Secchi disk. Three replicates of 1 L were taken for the analysis of phosphorus and nitrogen (total), chlorophyll-a, total solids, organic and inorganic suspended solids. Cyanobacterial Chl-a (Chl-a Cy) was determined in each replicate by in-vivo fluorometry (Aquafluor Turner Designs) according to Cremella et al., (2018).

2.3.3 Laboratory analysis

Each water replicate was filtered with two filters (MGF, Munktell): one previously burned at 450ºC and weighed for suspended solids analysis, and the other for Chl-a extraction. Total phosphorus (TP) and total nitrogen (TN) were measured in the unfiltered sample volume (Valderrama, 1981; APHA, 1985). In parallel, the concentration of suspended solids and suspended organic matter was determined by the gravimetric/calcination method (APHA, 1985). The Chl-a concentration was carried out using the hot ethanol extraction method (Nusch, 1980).

2.3.4 Satellite imagery processing

The images captured with the MSI on-board Sentinel-2 were downloaded from https://scihub.copernicus.eu/dhus/, which provides free and open access to MSI/S-2 L1C imagery. Level-1C processing includes radiometric and geometric corrections including ortho-rectification of reflectance at the top-of-the atmosphere and spatial registration on

a global reference system (Fletcher et al., 2012). Prior to the acquisition of spectral information, L1C images were converted to surface reflectance estimates using ACOLITE software (v20181210.0), which performs Rayleigh scattering and aerosol correction (Ansper, 2018).

Reflectance values coincident with in-situ sampling were obtained from grids of 3 x 3 pixels (90 m2) with a minimum distance to shore of 10 m. This procedure was performed since data may not be accurate for a single pixel (Clark et al., 2017). The average surface reflectance of each grid was extracted for all bands from the MSI/S-2 images. Image processing and extraction of spectral information were carried out in the Sentinel Application Platform (SNAP) of the European Space Agency.

2.3.5 Data analysis

Basic exploratory data analyses were conducted. Linear regression (log-log) analyses with total Chl-a and Chl-a Cy were used as the response variable. Differences between reservoirs were evaluated for physicochemical and pigment variables using Kruskal-Wallis.

In order to estimate satellite Chl-a and transparency, band indicators and band ratios were fitted using Linear Models (LM). Subsequently, the residuals generated were evaluated using Shapiro-Wilk normality test and Breusch-Pagan homoscedasticity test. First, the spectral signatures of the reservoirs sampled in-situ were obtained and the surface reflectance of each Sentinel-2 band was correlated with the variables in-situ. From this analysis, the most appropriate band for estimating transparency was chosen. Chl-a estimation models used the reflectance ratio red (665 nm) to red edge (705 nm) bands and green (560 nm) to red (665 nm) edge bands as predictor variables. Chl-a concentration and transparency logarithms were considered (Kayastha et al., 2022) as response variables.

2.3.6 Satellite monitoring

To monitor the study basin, in the first place, all the reservoirs with a surface area > 0.25 ha were identified, using the information on cutwaters and water bodies provided by the Spatial Data Infrastructure Agency of Uruguay. Since this coverage includes the entire

floodable area as reservoir surface and vectorization was used to extract spectral information from the water bodies, the polygons were manually adjusted to cover only the surface area corresponding to water.

In order to diagnose the trophic state of the reservoirs at two contrasting times according to precipitation metrics and evaluate biomass transport downstream to PPAC water intakes, Sentinel-2 MSI images were analyzed on a date before and after a high precipitation event (>20 mm daily). Once the dates were identified and the images downloaded, the accumulated precipitation for the thirty days prior to each image was calculated using data from Las Brujas weather station, National Institute of Agricultural Research, located 17 km south of Aguas Corrientes (Fig. 2.1). The records of cyanobacterial concentration in the Santa Lucía River taken at PPAC were also assessed (Fig. S2.2).

The images were acquired at L1C level, and the surface Rrs was calculated using ACOLITE software. The reservoir vectors previously elaborated were then used to calculate the median Rrs values for each band. Based on said information, the equation resulting from the Chl-a and transparency estimation models was applied. Once Chl-a was estimated, the reservoirs were classified according to their trophic state (Cunha et al., 2013).

In order to assess Chl-a spatial distribution and transparency in all the reservoirs under study, Spatial Auto-correlation (SA) was used. This tool refers to the degree to which one object is similar to other nearby objects. Moran's I, a measure of spatial autocorrelation, was applied. It is a Pearson's correlation coefficient with a spatial location weighting matrix (Moran, 1948).

To detect patterns of Chl-a distribution and transparency among reservoirs, hot spot analyses were performed with information from satellite monitoring (Torbick et al., 2013; Coffer et al., 2021). Said analyses identify statistically significant clusters called hot or cold spots. In this study, the Getis-Ord Gi* (Getis and Ord, 2010) statistic was used to determine hot spot incidence. For a feature to be recognized as a statistically significant hot spot, it must have a high value and must also be surrounded by other high-value features. The opposite applies to cold spots.

SNAP software was used to extract Rrs information, and ArcMap software version 10.4.1 for the spatial autocorrelation and hot spot analyses.

2.4 **Results**

All the reservoirs in the basin with a surface area of 0.25-100 ha were identified and vectorized to select the reservoirs where in-situ sampling was carried out. A total of 486 reservoirs were recorded, ranging in size from 0.25 to 60 ha (median 0.93 ha), with the first to third quartiles located at 0.6, 0.9, and 1.8 ha respectively. In order to simplify the subsequent analyses, the size was categorized in increasing order between 1 and 4 according to the aforementioned quartiles. Fourteen reservoirs were then selected according to land-use type and the corresponding access permits were obtained (Fig. 2.1). The reservoirs sampled in-situ presented sizes ranging from 0.4-54 ha (Table 2.1).

In the three samplings, rainfall varied substantially depending on the accumulated precipitation in the previous thirty days; 02/12/19 was the driest day with 25 mm, followed by 16/11/20 when 81 mm were computed, and 07/11/19 with 204 mm of accumulated precipitation.

2.4.1 Physicochemical analysis and trophic state of reservoirs

Except for temperature (range: 21.1-28.1°C), dissolved oxygen (4.7-19.5 mg L^{-1}), turbidity (11.8- >1000 NTU), pH (6.0-10.7), conductivity (0.06-1.203 mS cm-1), total suspended solids (8.9-691.8 mg L^{-1}), and suspended organic matter (16-92 %) showed wide value ranges (Fig. 2.2). The K-W analysis indicated that reservoirs H to N (northern portion of the basin) differed mainly in elevated pH, conductivity, suspended solids, and suspended organic matter.

Total phosphorus (TP) was in all cases within the category range of hypereutrophic reservoirs (≥0.078 mg TP L^{-1}, Cunha et al., 2013) (range: 0.18-5.22 mg TP L^{-1}, reservoir G and I, respectively), with extremely high cases such as reservoirs I and J (Fig. 2.2). These two reservoirs also accounted for high total nitrogen (TN) values. TN ranged from 0.70 to 23.56 mg TN L- 1 (F and I, respectively). Reservoirs Chl-a also presented a wide range of concentrations (2.8-4439 µg L^{-1}, B and I, respectively) (Fig. 2.2). The trophic state index of Cunha et al., (2013) for chlorophyll-a exhibited a gradient from mesotrophic (4 cases) to hypereutrophic (8 cases). The percentage of Chl-a corresponding to cyanobacteria yielded high values in reservoirs categorized as mesotrophic (B, C, E, and G), eutrophic (A), and hypereutrophic (D, F, H, I, J, K, M, and N).

Table 2.1 Characteristics of the sampled reservoirs: size, surrounding productive activity, and water use

Reservoir	Coordinates		Size (ha)	Activity	Usage
A	34°37'15"S	56°11'25"W	3.2	Forage	Irrigation
B	34°37'17"S	56°11'18"W	1.6	Forage	Irrigation
C	34°37'54"S	56°12'18"W	4.0	Forage	Irrigation
D	34°36'30"S	56°12'59"W	3.6	Pig farming	Animal consumption
E	34°36'48"S	56°13'17"W	12.9	Forage	Irrigation
F	34°36'28"S	56°14'06"W	4.2	Fruit growing	Irrigation
G	34°06'17"S	56°06'27"W	2.2	Cattle raising	Animal consumption
H	34°03'58"S	56°04'34"W	1.6	Milk production	Agribusiness, irrigation
I	34°03'49"S	56°04'30"W	0.5	Milk production	Agribusiness, irrigation
J	34°06'20"S	55°55'30"W	0.4	Crop, cattle raising	Animal consumption
K	34°06'26"S	55°55'50"W	3.2	Crop, cattle raising	Animal consumption
L	34°06'36"S	55°55'02"W	1.0	Crop, cattle raising	Animal consumption
M	34°06'36"S	55°54'21"W	2.0	Crop, cattle raising	Animal consumption
N	34°02'55"S	55°50'20"W	53.9	Milk production	Agribusiness, irrigation

Significant correlations were obtained between most of the variables evaluated in-situ (Table 2.2). Those with the highest magnitude were identified between turbidity and total suspended solids (TSS), transparency and suspended organic matter (SOM) (Rs= 0.93, -0.87, and 0.81, respectively). SOM was positively associated with Chl-a, TSS, and TN (Rs= 0.89, 0.84, and 0.81, respectively). Likewise, Cyanobacterial Chl-a (Chl-a Cy) was strongly correlated with total Chl-a and SOM (Rs= 0.91, 0.84, respectively). On the other hand, size was associated with all evaluated variables. The highest magnitude of correlation was detected in SOM followed by transparency (Rs=-0.60, 0.59, respectively) (Table 2.2). Even though Chl-a was significantly associated with TP, the correlation showed a high dispersion mainly in the reservoirs with higher turbidity (A, B, C, and G).

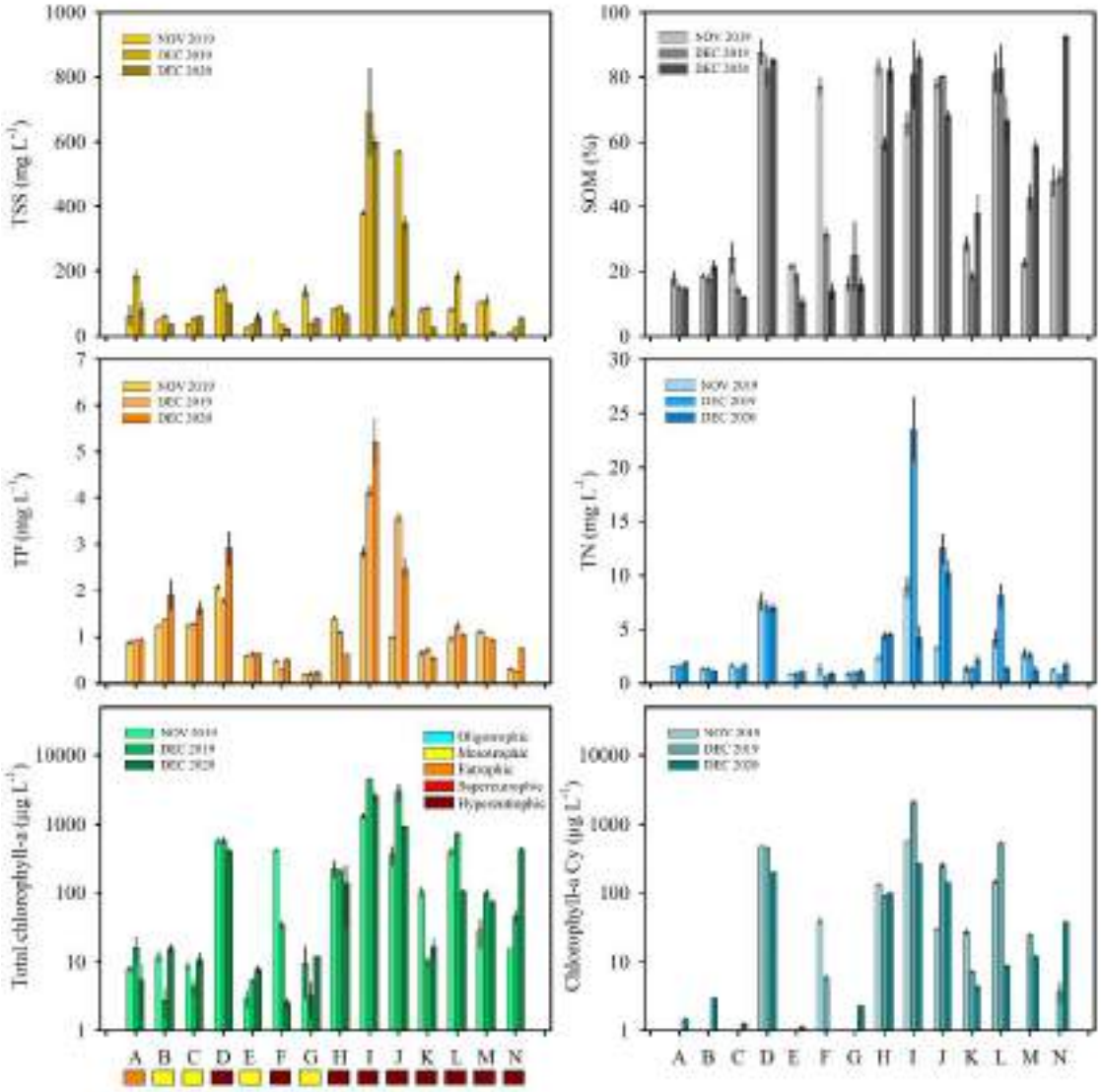

Fig. 2.2 Concentration of total suspended solids (TSS), percentage of suspended organic matter (SOM), total phosphorus (TP), total nitrogen (TN), total chlorophyll-a and cyanobacterial chlorophyll-a (Cy) (log scale) measured in situ for the fourteen reservoirs (A-N). Bars represent the mean of each sampling (3 replicates) and standard deviation for each sampling campaign (November and December 2019, December 2020). The colors on the x-axis of the chlorophyll-a plot indicate the trophic state for each reservoir according to Cunha et al., (2013). The trophic state according to TP was hypereutrophic in all cases

Table 2.2 Spearman correlation coefficients between physicochemical and pigment variables, significance level (p-value < 0.05) in bold, correlations of higher magnitude (Rs> 0.7) are highlighted (*). T: temperature (°C), K: conductivity (mS L^{-1}), Turb: turbidity (NTU), DO: dissolved oxygen (mg L^{-1}), Secchi: transparency (cm), ISS: inorganic suspended solids (mg L^{-1}), SOM: suspended organic matter (mg L^{-1}), TSS: total suspended solids (mg L^{-1}), Chl-a: chlorophyll-a (µg L^{-1}), Chl-a Cy: cyanobacterial Chl-a, TP: total phosphorus (mg P L^{-1}), Size (ha), TN: total nitrogen (mg N L^{-1})

	T	pH	K	Turb.	OD	Secchi	ISS	SOM	TSS	Chl-a	Chl-a Cy	TP	Size
pH	***0.72**												
K	0.16	**0.31**											
Turb.	0.29	**0.31**	**0.46**										
OD	-0.07	0.09	**0.48**	**0.47**									
Secchi	-0.26	-0.18	**-0.39**	***-0.87**	**-0.35**								
ISS	0.11	-0.22	0.24	**0.53**	0.08	**-0.65**							
SOM	**0.42**	**0.53**	**0.46**	***0.81**	**0.57**	**-0.64**	0.19						
TSS	**0.32**	0.28	**0.44**	***0.93**	**0.44**	***-0.84**	**0.63**	***0.84**					
Chl-a	**0.44**	**0.66**	**0.45**	**0.60**	**0.50**	**-0.42**	-0.01	***0.89**	**0.64**				
Chl-a Cy	**0.40**	**0.64**	**0.41**	**0.59**	**0.51**	**-0.42**	-0.05	***0.84**	**0.60**	**0.91**			
TP	0.03	0.17	**0.49**	**0.56**	**0.58**	**-0.48**	**0.30**	**0.55**	**0.57**	**0.53**	**0.51**		
Size	**-0.44**	**-0.40**	**-0.30**	**-0.62**	**-0.50**	**0.59**	**-0.34**	**-0.60**	**-0.56**	**-0.50**	**-0.47**	**-0.53**	
TN	**0.24**	**0.44**	**0.42**	**0.74**	**0.60**	**-0.61**	0.22	***0.81**	**0.75**	***0.75**	***0.73**	***0.74**	**-0.61**

2.4.2 Spectral signatures

In the signatures with concentrations above 20 µg Chl-a L^{-1}, a valley in the blue region (492 nm), a peak in the green one (560 nm), followed by a valley in the red region (665 nm) can be observed, with its lowest Rrs values in the cases with the highest Chl-a concentration. After this valley, a sharp increase can be noticed (Fig. 2.3). In general terms, the spectral signatures with higher magnitude in the near-infrared region (>704 nm) were those with higher Chl-a concentrations. Conversely, spectral signatures corresponding to reservoirs with concentrations below 20 µg Chl-a L^{-1} presented a progressive increase from 443 nm to 665 nm (Fig. 2.3).

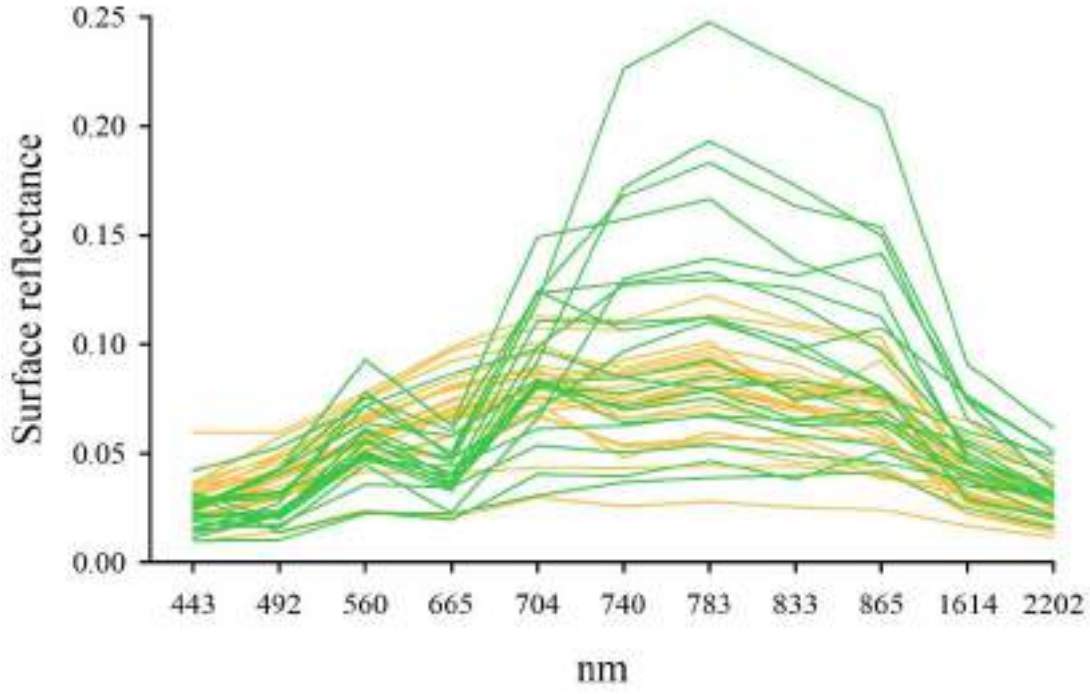

Fig. 2.3 Spectral signatures of reservoirs sampled *in-situ.* In orange: reservoirs with chlorophyll-a values below 20 µg L^{-1}, in green: reservoirs with chlorophyll-a values above 20 µg L^{-1}

At wavelengths >740 nm, Rrs was associated with all trophic state variables determined in-situ, among which, the 833 nm band displayed the highest correlation intensity with transparency (Rs=-0.88), TSS (Rs=0.76), and ISS (Rs=0.60) which were also positively related to all bands. It should be noted that all the associations detected for transparency were negative. On the other hand, SOM was positively correlated with Rs in the 704-2202 nm range, while in the 443-665 nm range it was only associated with the 492 nm and 665 nm bands, and negatively. TSS was related to Rrs at all wavelengths >740 nm, while between 443-665 nm it was only related to the 560 nm band. In the 492-665 nm range the higher concentrations of Chl-a and Chl-a Cy the lower the Rrs. The correlations obtained in the 665 nm band stand out, where the correlation magnitude was the highest with Rs=-0.69 followed by Rs=-0.57, also in the 492 nm band, where maxima was identified with a magnitude of Rs=-0.53 and Rs=-0.44 for Chl-a and Chl-a Cy respectively (Table 2.3).

Table 2.3 Spearman correlation magnitude between reflectance (Rrs) of Sentinel-2 bands and trophic state variables determined *in-situ*. ISS: inorganic suspended solids (mg L^{-1}), SOM: suspended organic matter (mg L^{-1}), TSS: total suspended solids (mg L^{-1}), Chl-a: chlorophyll-a (µg L^{-1}), in bold: cases where a significant correlation was identified according to the p-value<0.05

Rrs (nm)	ISS (mg L^{-1})	SOM (mg L^{-1})	TSS (mg L^{-1})	Chl-a (µg L^{-1})	Secchi (cm)	Chl-a Cy (µg L^{-1})
443	**0.41**	-0.21	0.06	**-0.32**	-0.17	**-0.30**
492	**0.36**	**-0.38**	-0.05	**-0.53**	-0.09	**-0.44**
560	**0.36**	0.08	**0.33**	-0.09	**-0.39**	0.06
665	**0.41**	**-0.51**	-0.12	**-0.69**	-0.07	**-0.57**
704	**0.44**	**0.36**	**0.59**	0.18	**-0.61**	**0.34**
740	**0.57**	**0.54**	**0.73**	**0.32**	**-0.82**	**0.39**
783	**0.55**	**0.55**	**0.73**	**0.33**	**-0.81**	**0.38**
833	**0.60**	**0.57**	**0.76**	**0.36**	**-0.88**	**0.41**
865	**0.53**	**0.59**	**0.73**	**0.36**	**-0.79**	**0.39**
1614	**0.45**	**0.54**	**0.61**	**0.38**	**-0.59**	**0.38**
2202	**0.39**	**0.46**	**0.53**	**0.31**	**-0.52**	**0.32**

2.4.3 Linear models

Two linear models were developed for satellite estimation of Chl-a concentration based on the Chl-a logarithm observed in-situ as the response variable. The normalized differences of the red edge-red Rrs (NDCI) and the green-red Rrs (VR) were used as explanatory variables. For model fitting, the maximum value of Chl-a in-situ (4500 µg L^{-1}) was excluded as an outlier. Therefore, a total of n=41 cases were used.

The linear model based on the NDCI indicator (adjusted R^2=0.81) showed no evidence of lack of normality in the distribution of the Shapiro-Wilk test results of the residuals (p=0.44), nor was there evidence of non-homocedasticity according to the Breusch-Pagan test (p=0.22). Therefore, it is an acceptable model for Chl-a estimation (Fig. 2.4).

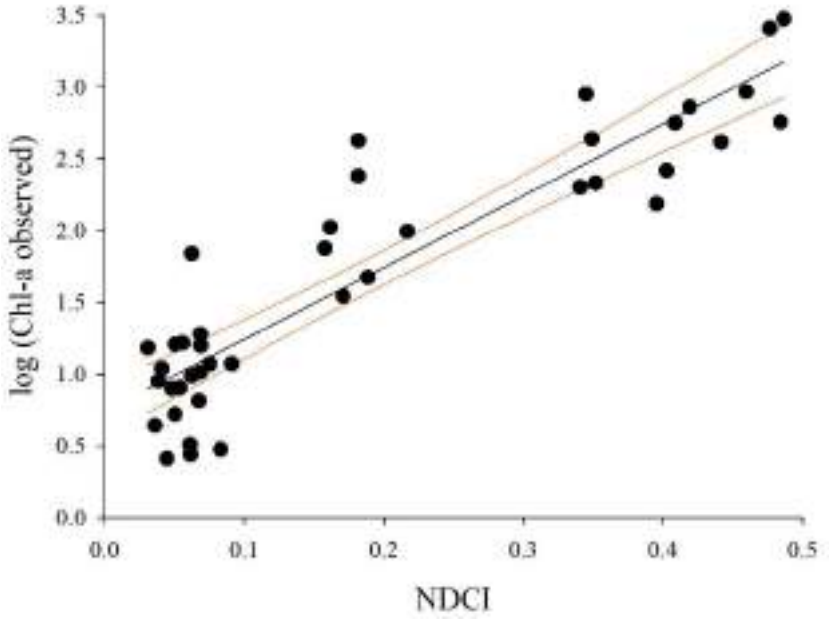

Fig. 2.4 Dispersion of the chlorophyll-a (Chl-a) estimation model in µg L^{-1} fitted based on NDCI indicator: (Rrs 705 nm - Rrs 665 nm) / (Rrs 705 nm + Rrs 665 nm), where Rrs: surface reflectance

The linear model based on the VR indicator (adjusted R^2 =0.84; Shapiro-Wilk p=0.25; Breusch-Pagan p=0.59) is also an acceptable model for estimating Chl-a (Fig. 2.5). VR indicator was more fitted than NDCI, therefore, the equation resulting from the former was used to monitor total reservoirs: Chl-a (µg L^{-1}) = 10 ∧ (1.6218 + 6.0575 * VR).

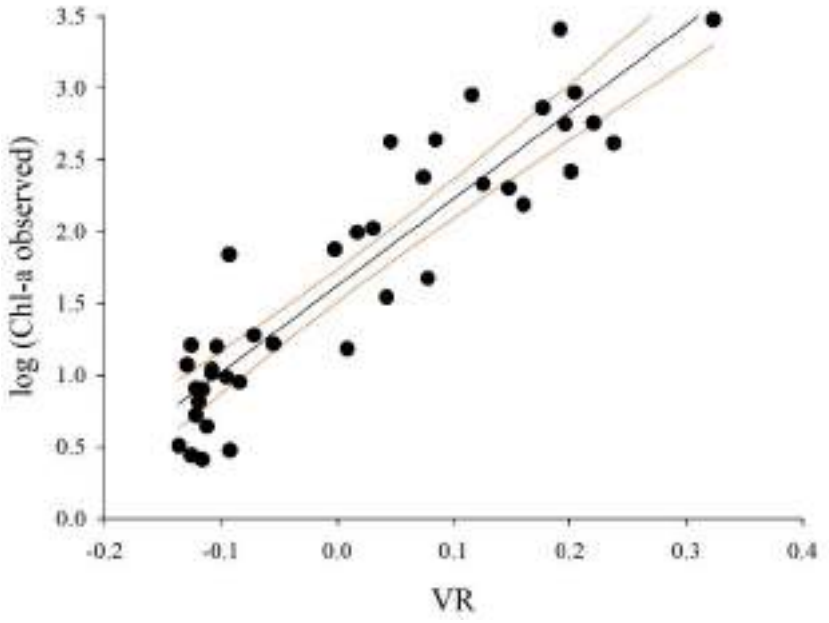

Fig. 2.5 Dispersion of the chlorophyll-a (Chl-a) estimation model in µg L^{-1} fitted based on VR indicator: (Rrs 560 nm - Rrs 665 nm) / (Rrs 560 nm + Rrs 665 nm), where Rrs: surface reflectance

To estimate reservoir transparency, a linear model was fitted based on the transparency logarithm observed in-situ and the surface reflectance at 833 nm (Table 2.3). This particular band was chosen as it presented the highest correlation intensity with transparency (adjusted R^2 =0.73; Shapiro-Wilk p=0.16; Breusch-Pagan p=0.77) (Fig. 2.6). Therefore, the model was accepted for transparency estimation. The resulting model equation is: Transparency (cm) = 10 ^ (1.68706 - 6.03732 * Rrs (833 nm)).

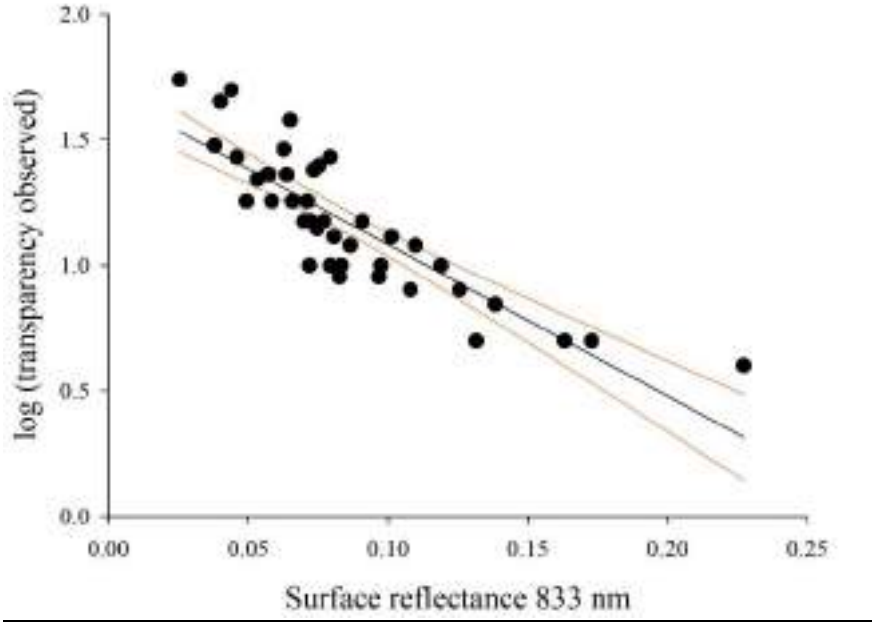

Fig. 2.6 Dispersion of the transparency estimation model fitted based on the surface reflectance of the band centered at 833 nm

2.4.4 Satellite monitoring

Two Sentinel-2 MSI images were obtained with contrasting precipitation values. The first one corresponds to 12/12/16 with 50 mm of accumulated precipitation on the previous thirty days, while the second was captured on 11/01/17 with 264 mm of accumulated precipitation on the previous thirty days. Among the dates with images available, a maximum value of cyanobacterial abundance (3581 cells. ml^{-1}) was detected on 01/01/17 in PPAC (Fig. S2.2).

Monitoring using the VR indicator fitted model revealed that most of the reservoirs are hypereutrophic. On 12/12/16, 225 reservoirs were classified as hypereutrophic, 86 as eutrophic and 133 as mesotrophic. In addition, the area with Chl-a > 20 µg L^{-1} according to each reservoir median values reached 861 ha. On 11/01/17, a larger number of hypereutrophic environments (335) and a decrease in eutrophic and mesotrophic ones were detected, 64 and 65, respectively, (Fig. 2.7). Also, the area covered by Chl-a concentrations > 20 µg L^{-1} was 1044 ha.

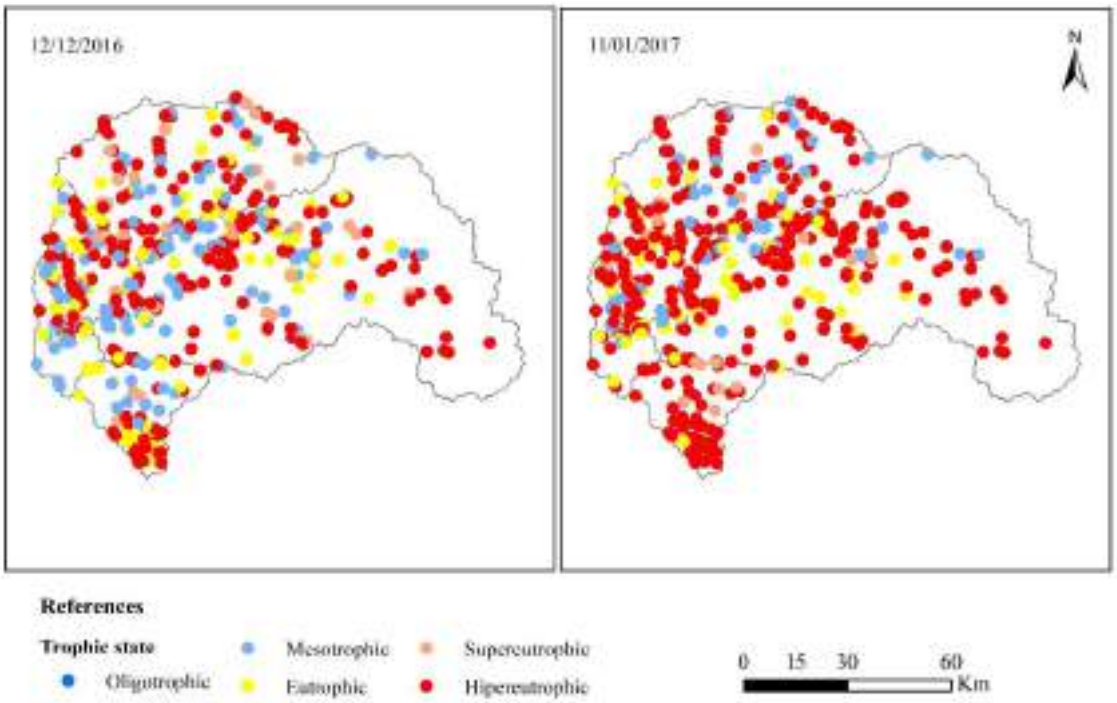

Fig. 2.7 Trophic state of monitored reservoirs according to the trophic state index of Cunha *et al.* (2013) estimated from chlorophyll-a concentration

On 12/12/16, the median Chl-a value for all reservoir sizes categorized them as super-eutrophic, with the exception of those of 0.6-0.9 ha (quartile 2), which yielded the highest Chl-a concentrations and were categorized as hypereutrophic. It is worth mentioning that the smallest reservoirs (quartile 1) presented the lowest Chl-a concentrations. On the other hand, on 11/01/17, the median Chl-a value for all reservoir sizes categorized them as hypereutrophic regardless of their size, the smallest reservoirs also presented the lowest median values while those from quartile 2 accounted for the highest (Fig. 2.8). On the two dates evaluated, the standard deviation of Chl-a was higher in the smallest reservoirs, followed by the reservoirs from quartile 2 on 12/12/16 and the largest ones on 11/01/17.

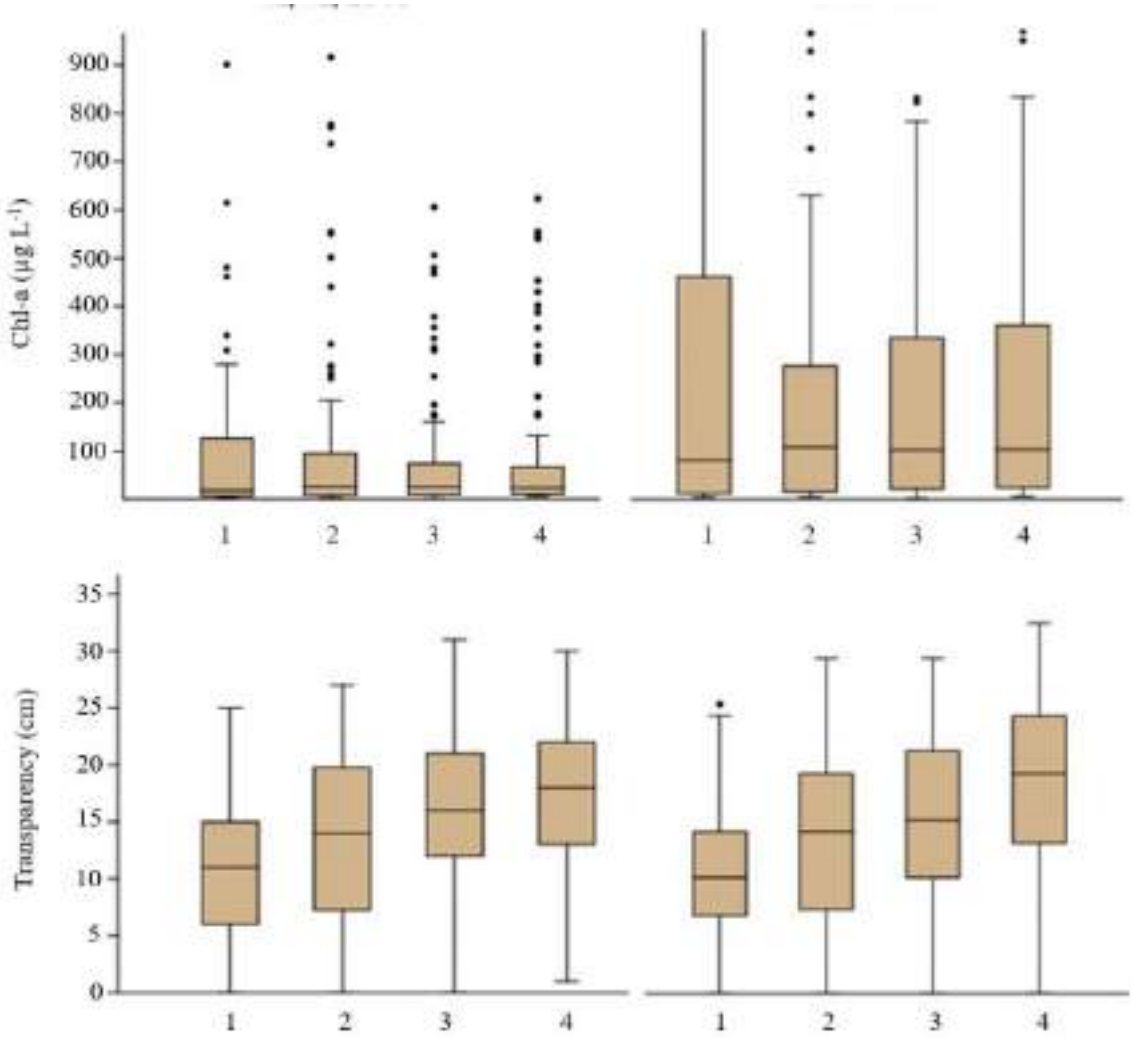

Fig. 2.8 Satellite-estimated chlorophyll-a concentration and transparency for 12/12/16 and 11/01/17 clustered by reservoir size quartile

On the two dates monitored, transparency was similar and tended to increase with size (Rs= 0.38 and Rs= 0.40, 12/12/16 and 11/01/17, respectively). The minimum values were recorded in the smallest size reservoirs (quartile 1), while the largest sized (quartile 4) accounted for the maximum values according to the median (Fig. 2.8). Chl-a was not significantly associated with size (Spearman test), although it was positively associated with transparency both in December ($p<0.05$; Rs=0.28) and January ($p<0.05$; Rs=0.25).

2.4.5 Hotspot analysis

Spatial clustering patterns were identified in the distribution of Chl-a and transparency of the monitored reservoirs. According to Moran's I test, the highest autocorrelation intensity

(Z) was detected for transparency with values of Z=5.83 in December and Z=4.88 in January. Likewise, Chl-a was distributed in clusters with higher intensity in December (Z=2.06) than in January (Z=1.86).

On 12/12/16, Chl-a formed clusters of high values. The highest intensity clustering occurred in the southern region, followed by the clusters in the eastern, northern, and western areas. The central area was characterized by a large cluster of reservoirs with low Chl-a concentrations. In contrast, on 01/11/17, Chl-a was distributed forming a cluster of reservoirs with low concentrations in the southern area, while the central and western areas did not present a specific clustering pattern. On the other hand, the high-value cluster in the northern area was maintained over time as was the low-value cluster in the center of the basin (Fig. 2.9).

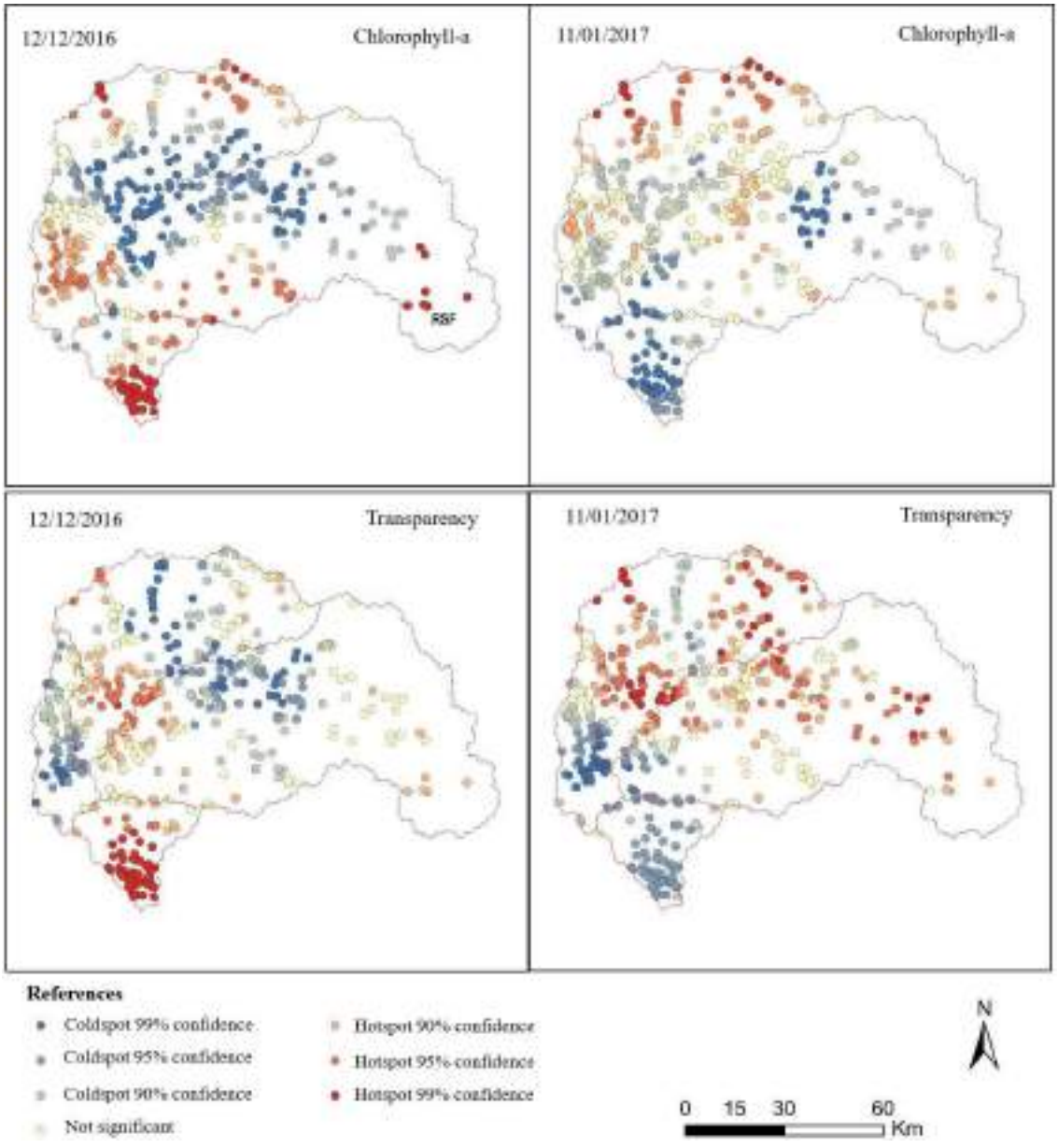

Fig. 2.9 Estimated chlorophyll-a and transparency hotspots in the 486 satellite-monitored medium- and small-sized reservoirs according to the Getis-Ord hotspot analysis

In December, transparency was distributed forming a cluster with the clearest reservoirs in the southern area and another in the central-eastern area. On the other hand, the most turbid reservoirs close to each other were found mainly in the central, northern, and western areas. In contrast, in January, the southern area presented the largest cluster of turbid reservoirs, while clusters of clear reservoirs were detected in the rest of the basin (Fig. 2.9).

2.5 **Discussion**

Linear models for satellite estimation of Chl-a and transparency based on in-situ information allowed to monitor all the reservoirs in the Santa Lucía River Basin for the first time in Uruguay. These results represent the first approximation to the trophic state of 486 small- and medium-sized (0.25-100 ha) agricultural reservoirs located in the basin that supplies drinking water to 60% of the population of this country. Despite the fact that large basin databases on water quality monitoring systems have been developed in Uruguay, they only cover the main river courses and the two largest reservoirs (Aubriot et al., 2017; Somma et al., 2022). Therefore, prior to this work, little was known about the trophic state of more than a hundred productive reservoirs in the basin. This study allowed us to determine that most of these water bodies are in a hypereutrophic state, and present high levels of phytoplankton biomass, mostly composed of cyanobacteria, and with a high potential for downstream transport of this biomass. Therefore, either due to their overtopping and release resulting from high rainfall or the possible artificial opening of dams during low-water flow, this large number of reservoirs with a detected high biomass of potentially toxic phytoplankton undoubtedly represents a health threat.

The great impact of agricultural activities on the export of nutrients and organic matter in SLRB is manifested in the high degree of eutrophication of productive reservoirs. The percentage of the area covered by crops in the drainage basin has a direct impact on the eutrophication of reservoirs, particularly when they are shallow and have a larger basin size relative to the surface area of their water body (Knoll et al., 2015). In our study, the

smallest-sized reservoirs presented the highest concentrations of Chl-a, TP and TN in the three in-situ sampling sites. These results are in agreement with Brainwood et al., (2004) who suggested that smaller agricultural reservoirs have higher nutrient and Chl-a concentrations than larger ones. The reservoirs with the highest TP and Chl-a concentrations in our study were located in dairy farms, crop farms, and pig farms. Likewise, the maximum TN values were obtained from sites located on livestock farms (Fig. 2.2 and Table 2.1). These results are in line with Chalar et al., (2011), who postulated that dairy and pig farms are one of the main sources of nutrient pollutants in the Santa Lucía River Basin. Modeling of nitrogen and phosphorus in SLRB watercourses, with projections of productive intensification, predicts a scenario of increased eutrophication under current agricultural practices (Díaz et al., 2021). In this sense, the satellite indices applied in this work are an input for the diagnosis of eutrophication evolution in SLRB.

In the sites sampled in-situ, phytoplankton development was found to fit better to TN concentration variability, while a lower TP correlation was observed (Table 2.2). This behavior agrees with the findings obtained by O' Farrell et al., (2021) who monitored Pampean shallow lakes monthly for three years and found that as the trophic state increases, the growth of cyanobacteria can be limited by N. High TP concentrations in SLRB are generally ascribed to high concentrations of soluble reactive phosphorus (> 88%), mainly associated with surface runoff and soil phosphorus saturation in the basin (Goyenola et al., 2015; Aubriot et al., 2017; Barreto et al., 2017).

Most suspended solids corresponded to suspended organic matter, which is strongly associated with phytoplankton biomass (Table 2.2). Nonetheless, some reservoirs, despite being hypereutrophic according to TP and TN levels, and having suspended solids mainly made up of inorganic origin, did not show high phytoplankton development. This is consistent with some postulations that suggest that inorganic solids limit phytoplankton growth due to the decrease in radiation penetrating the water column (Reynolds, 2006; Dzialowski et al., 2011). It is worth noting that most sites with this behavior are located in the southern portion of the basin (Fig. 2.1), where clay soils predominate (MGAP, 1976) which could increase inorganic suspended solids.

The results obtained in-situ show a close proportionality of total Chl-a to cyanobacterial Chl-a (Fig. 2.2; Table 2.2). This finding raises the level of health risk in the watershed due to cyanobacterial blooms toxicity (Chorus and Welker, 2021). Moreover, they support the statement by Somma et al., (2022) who inferred that the small and medium-

sized reservoirs in SLRB are environments conducive to the development of cyanobacterial blooms, and that they can be transported downstream as evidenced by the increased cyanobacterial biomass recorded during high flow periods in the main channel. The evaluation of hot spots of high phytoplankton biomasses in the basin, and their spatial and temporal evolution contributes to eutrophication management and to anticipate high-risk scenarios of biomass transport to the water treatment plant.

2.5.1 Satellite estimation models

In this study, two indicators for satellite estimation of Chl-a were compared. The best results were obtained from the VR indicator that measures the surface reflectance ratio between the green (560 nm) and red (665 nm) bands with an R^2 =0.85 in the range 3-2992 µg L^{-1} (Fig. 2.5). This result is in line with Ha et al., (2017) who used the green-to-red ratio to monitor Chl-a from Sentinel-2 images, and obtained successful results even at minimum concentrations < 6 µg Chl-a L^{-1}, as did Avdan et al., (2019). Likewise, Oliveira et al., (2016) tested said ratio to monitor coastal waters and obtained fits up to R^2 =0.71 over a wide range from 1 to 974 µg Chl-a L^{-1}. According to the information obtained in situ in this study, the only case with > 20 µg Chl-a L^{-1} and no green reflectance peak was the K reservoir in the first sampling. As a consequence, this is an exceptional case worthy of further validation of the fitted model. Likewise, a validation with in-situ information of the transparency model is required, mainly due to the inconsistency found in the satellite monitoring where high concentrations of Chl-a and high transparency are found (Fig. 2.9). This discrepancy could be due to the underestimation of organic solids, which could be related to the high spectral response in the infrared that both organic and inorganic solids in the reservoirs (Neil et al., 2019).

The spectral signatures of the reservoirs sampled in-situ presented characteristics of productive inland waters as reported by Spyrakos et al., (2018), and were differentiated into two major groups according to Chl-a concentration. Those reservoirs in which concentrations >20 µg L^{-1} were recorded, presented a green reflectance peak between the minimum values recorded in the blue (~ 492 nm) and red (~ 665 nm) bands (Fig. 2.3). This behavior is expected since, according to Gitelson et al., (1992), the energy absorption maxima of Chl-a is close to the blue and red bands, while the minimum is close to the green (~ 560 nm) band.

The NDCI indicator yielded good results as expected according to Neil et al., (2019) who achieved high NDCI fits in several water bodies. Likewise, Uudeberg et al., (2020) reported fits for NDCI of up to R^2= 0.89 specifically using Sentinel-2 MSI imagery in very organic and inorganic turbid waters. However, in some of the in-situ sampling sites with concentrations <20 µg Chl-a L^{-1}, positive slopes between the red and red-edge bands (705 nm) were detected that could lead to Chl-a overestimation. In these cases, reflectance increases progressively from the blue (~ 490 nm) to the infrared (> 705 nm) bands. According to the review by Giardino et al., (2019), such behavior could be explained by the high content of inorganic suspended solids as they are characterized by maximum absorption in the blue and exponential decrease towards the infrared. Therefore, it could be affirmed that in the sampling sites reflectance in the blue and red-edge bands was influenced by the optical behavior of both Chl-a and suspended solids, while the reflectance in the red band was mainly dominated by Chl-a.

2.5.2 Satellite monitoring

In this study, all the reservoirs in SLRB were monitored by fitting the linear models with in-situ information. Even though this is the first experience in the country, monitoring plans for agricultural reservoirs integrating satellite estimation tools in a complementary manner have already been developed worldwide. In this sense, Papenfus et al., (2020) and McCullough et al., (2012) found advantages in their application such as spatial scope, high sampling frequency, and the savings in monitoring costs.

In this sense, Papenfus et al., (2020) and McCullough et al., (2012) found advantages in its application such as spatial scope, high sampling frequency, and savings in monitoring costs.

In spite of the fact that less hypereutrophic environments and less surface area covered by high concentrations of Chl-a were detected prior to rainfall (12/12/16) than after rainfall (11/01/17; austral summer), PPAC displayed a post-rainfall maximum of cyanobacteria, which is consistent with the results reported by Somma et al., (2022) who associated cyanobacterial abundance in the PPAC with high rainfall. Several investigations suggest that the effect of precipitation can act both as an exacerbating factor of cyanobacterial blooms, through the transport of nutrients from the watershed, and as a temporal disrupting factor through washing and dilution of biomass in precipitation

events (Reichwaldt and Ghadouani, 2012; Haakonsson et al., 2017; Sinha et al., 2017). The overall increase in biomass recorded in most reservoirs would indicate a growth-stimulating effect due to nutrient input by rainfall and the early summer temperature effect. However, the maximum bloom of cyanobacteria observed in the river channel (PPAC) post-rainfall would not be linked to an effect of the overall biomass flushing, but to possible specific contributions from certain groups of reservoirs. Further research should be conducted to elucidate which reservoirs release significant toxic cyanobacterial biomass to PPAC.

As in the study by Coffer et al., (2021), we identified sets of elevated Chl-a values that transcended watershed and eco-region boundaries, representing essential information for targeting management efforts and risk forecasting. Trophic state mapping reveals the increase in hypereutrophic reservoirs in early summer (Fig. 2.7). While the changes detected in Chl-a distribution patterns before and after heavy rainfall reveal contrasting situations that could be linked to cyanobacteria transport to PPAC. Prior to rainfall, the main hotspots of Chl-a are reported in the southern and eastern areas of the basin. After rainfall, the distribution is reversed and these reservoirs become coldspots (Fig. 2.9). Therefore, the reservoirs located in the southern and eastern areas of the basin could be the main contributors to the cyanobacterial maximum recorded in PPAC.

2.6 **Conclusions**

All the reservoirs in the SLRB were remotely monitored for the first time in Uruguay. Most of these water bodies were classified in a hypereutrophic state, with high levels of phytoplankton biomass, mostly composed of cyanobacteria. The linear models fitted for satellite estimation of Chl-a and transparency achieved high fits compared to those reported in the literature for turbid and small environments. This is the first experience at a national level in which chlorophyll-a concentration and transparency were monitored in all the reservoirs of SLRB, after fitting a linear model with information obtained in-situ. The relevance of advancing the research agenda on the validation of the fitted models based on new information should be emphasized.

The results obtained in-situ allowed us to identify two sets of environments. On the one hand, one with high concentrations of Chl-a, phosphorus, and total nitrogen, and on the other, one that, despite having high concentrations of nutrients, does not develop

phytoplankton biomass, and turbid conditions caused mainly by inorganic solids in suspension prevail.

The reservoir cluster located in the southern and eastern areas of SLRB presented the highest risk of high cyanobacterial biomass contribution according to Chl-a distribution before and after rainfall, which would have led to biomass transport to the water treatment plant intakes. The geo-statistical analyses allowed to evaluate all the reservoirs on a synoptic basis, and thus identify behaviors and differentiate areas at risk of phytoplankton biomass export. An in-depth study of biomass transport to the drinking water treatment plant should be conducted, based on the analysis of the Sentinel-2 series (2016-present) available for SLRB and the joint analysis of the water quality dataset recorded in PPAC.

2.7 **Supplementary material**

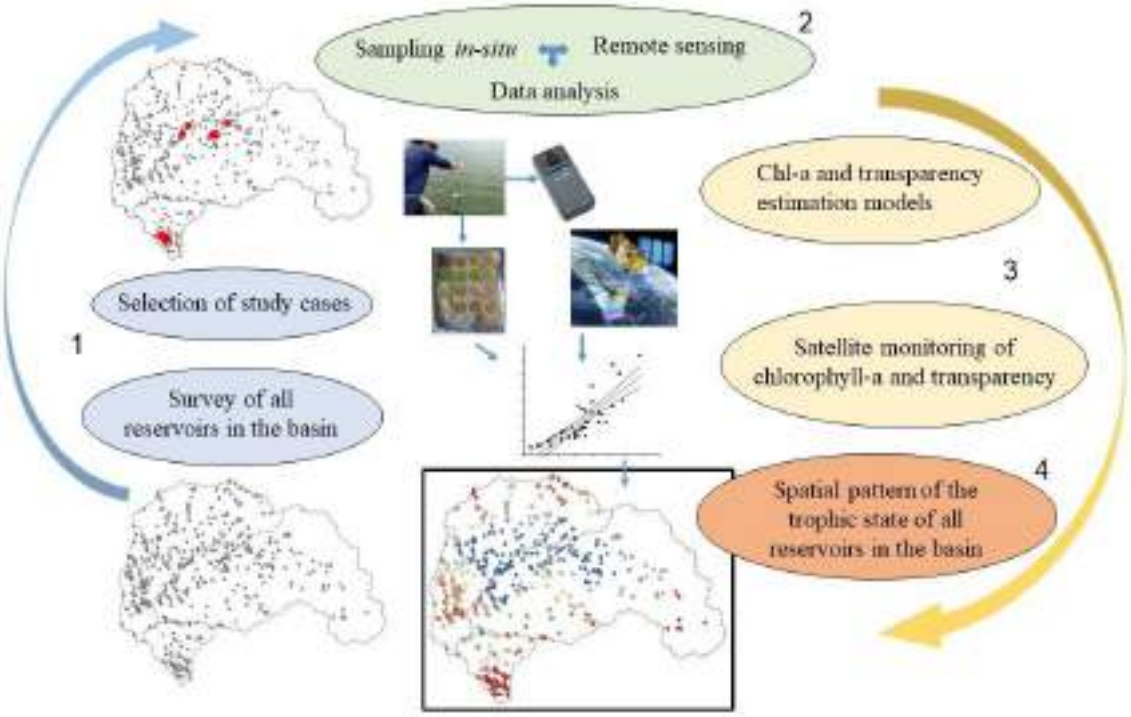

Fig. S2.1 Methodological strategy. The study stages are differentiated in colors and numbers. The outline corresponds to the study area in the Santa Lucía river basin

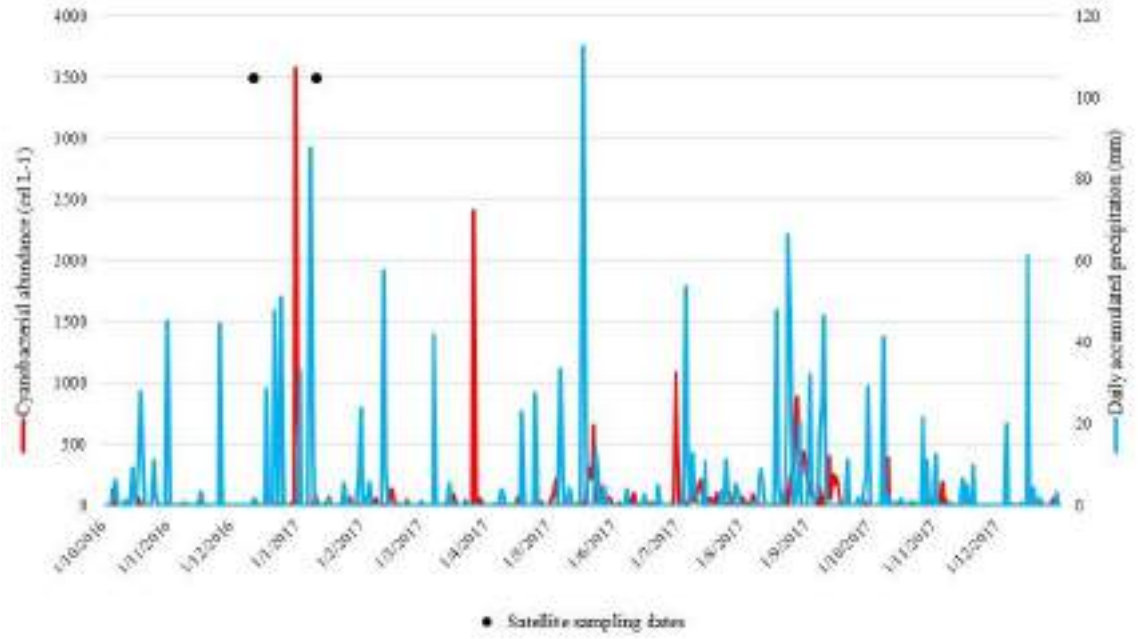

Fig. S2.2 Cyanobacterial abundance (cel ml^{-1}) at the Aguas Corrientes water treatment plant (data provided by OSE), daily accumulated precipitation recorded at INIA las Brujas, and satellite sampling dates.

3. Capítulo 3

Zoning the risk of transporting cyanobacterial blooms to the main water utility in Uruguay

3.1 **Abstract**

Cyanobacterial blooms pose potential health and economic risks, particularly when reaching drinking water intakes. In basins with intensive agricultural production, there are numerous small and medium-sized (0.25-30 ha) productive freshwater reservoirs. These reservoirs create favorable conditions for excessive growth of phytoplankton, which can be transported downstream after heavy rainfall events that are projected to worsen under future climate variability scenarios. These environments have been identified as potential sources of cyanobacterial biomass in Uruguay's main drinking water intake, located in the Santa Lucía River Basin. To pinpoint areas with the highest risk of export of cyanobacterial biomass, this study integrated chlorophyll-a concentration monitoring in 325 reservoirs using Sentinel-2 satellite images, along with meteorological and structural information from the reservoirs. Spatial distribution patterns explored through geostatistical and multivariate analyzes showed that the southern and western

zones, characterized by intensive agricultural land uses such as dairy farming and horticulture, suggest a high risk of biomass export. On the contrary, the northeastern zone exhibited the lowest risk, aligning with extensive cattle ranching practices associated with low nutrient export to aquatic systems. This study marks the first effort to assess the risk of transporting cyanobacterial biomass from numerous reservoirs to Uruguay's primary drinking water intake. We propose the basis for the development of a biomass export indicator as a fundamental input for an early warning system of cyanobacteria bloom events in drinking water plants located downstream.

Keywords: Remote sensing, water purification, space pattern, chlorophyll-a.

3.2 **Introduction**

Cyanobacterial blooms have emerged as a significant global water quality challenge (Burford et al., 2020; Michalak et al., 2013). During the past few decades, this phenomenon has shown an increase in frequency, scale, and duration (Huisman et al., 2018). Cyanobacteria have the capacity to produce harmful toxins in aquatic and terrestrial ecosystems (Pearson et al., 2016; Leflaive & Ten-Hage, 2007; Carmichael, 2001), leading to adverse health and economic impacts, particularly related to increased costs associated with drinking water treatment (Dunlap et al., 2015).

Typically, basins characterized by intensive agricultural activities host numerous artificial freshwater reservoirs. These reservoirs alter the flow of the river system, extend the residence time of the water, attain elevated temperatures due to their shallow depth, and, in conjunction with nutrient-rich runoff from intensive agricultural areas, create conditions conducive to excessive proliferation of phytoplankton (Zabaleta et al., 2023; Beaver et al., 2014). Frequently, these conditions result in cyanobacteria dominating the phytoplankton community (Huisman et al., 2018; Burford & O'Donohue, 2006).

Headwater reservoirs with intensive agricultural activity represent health (Aubriot et al., 2020; Kruk et al., 2019) and economic risks, due to the potential transport of cyanobacteria that, when unexpected, increases purification costs and threats to human and animal health (Dunlap et al., 2015). This phenomenon occurs because artificial reservoirs can accumulate substantial amounts of cyanobacterial biomass, which poses a constant risk of downstream transport of these organisms (Grill et al., 2019; Remmal et al., 2017). Furthermore, these reservoirs can experience overflows during heavy rainfall,

leading to the transport of large amounts of biomass downstream (Aubriot et al., 2020; Grabowska & Mazur-Marzec, 2011).

The distance along the lotic systems traveled by the cyanobacterial blooms is a determining factor for their survival. In some cases, cyanobacteria originating in headwater reservoirs survive hundreds of kilometers in their downstream transport (Bowling et al., 2013; Baldwin et al., 2010), while in other cases their biomass decreases rapidly (Grabowska & Mazur-Marzec, 2011). Williamson et al. (2018) evaluated the survival of cyanobacteria in turbulent transport and suggested that the geomorphological characteristics of the river bed, flow velocity, and depth could determine the survival of cyanobacteria. Generally, cyanobacterial blooms detected in lotic systems correspond to allochthonous blooms generated in headwater reservoirs (Somma et al., 2022), which can generate negative consequences on the quality of the water to be treated (Shin et al., 2022).

Conventional monitoring approaches require significant financial resources, time, and specialized expertise (Lins et al., 2017; Navalgund et al., 2007). Remote sensing emerges as an alternative tool that facilitates the quantification of phytoplankton pigments using remotely sensed surface reflectance and in situ data. Chlorophyll-a (Chl-a) stands out as the pigment most commonly used in remote sensing, serving as an indicator of total phytoplankton biomass (Giardino et al., 2019; Watanabe et al., 2017). In particular, the Sentinel-2 satellite's Multi-Spectral Instrument sensor, with its frequent revisit interval (5 days) and 10-meter pixel resolution, has proven effective in monitoring Chl-a concentration, even in small and turbid reservoirs (Zabaleta et al., 2023; Ansper, 2018).

Numerous studies have used satellite monitoring to assess the trophic status of water reservoirs with a high probability of cyanobacterial blooms (Bresciani et al., 2019; Clark et al., 2017). Satellite imagery facilitates the collection of Chl-a information for multiple water bodies concurrently over time, enabling the construction of extensive databases. Geostatistical analyzes can then be applied to identify spatial distribution patterns, hotspots, and trends (Coffer et al., 2021; Torbick et al., 2013). However, the development of warning systems predicting cyanobacterial bloom occurrences (Almuhtaram et al., 2021), assessing biomass transport to drinking water intakes (Somma et al., 2022) and pinpointing their specific origin remains a challenge.

The downstream transport of cyanobacterial blooms is even more critical in the global context of climate change because temperature increases and extreme precipitation events are expected in the coming years (IPCC 2023). The consequent increase in runoff and nutrients inputs to continental water bodies will promote eutrophication processes (Paerl, 2017; Sinha et al., 2017), and concomitantly with hydrological alterations that increase water residence times (O'Neil et al., 2012), constitute the main variables that favor phytoplankton blooms (Burford et al., 2020; Ho et al., 2019). In this sense, to focus on mitigation efforts and increase the effectiveness of management measures, it is essential to identify the origin of phytoplanktonic bloom proliferations. Although various episodes of biomass transport from large headwater reservoirs have been studied (Shin et al., 2022), there is a lack of research evaluating the potential risk of bloom transport from hundreds of reservoirs used for agricultural purposes.

In Uruguay, the recurrent occurrence of cyanobacterial blooms poses a significant challenge in surface water purification (Somma et al., 2022; Gonzalez-Madina et al., 2021; Aubriot et al., 2017). Health and economic risks associated with drinking water intake for drinking water treatment are increased when cyanobacteria blooms are not effectively prevented (Kouzminov et al., 2007). Addressing this concern, Zabaleta et al. (2023) developed a model for the satellite estimation of Chl-a in small and medium-sized reservoirs within the Santa Luca River Basin (SLRB), the main source of drinking water in Uruguay. However, the specific origin of the blooms that reach the intake after high rainfall has not yet been thoroughly analyzed.

The SLRB serves as the main source of drinking water supply in the country, catering to 60% of the demand of the national population. Somma et al. (2022) identified small and medium reservoirs for productive use in the SLRB as potential sources of cyanobacterial inoculum, based on water quality data in the drinking water intake of the SLRB in Aguas Corrientes (AACC). The authors stress the need for studies to identify and evaluate these potential sources to mitigate the contribution of harmful phytoplankton. These reservoirs are abundant and their numbers are expected to increase due to policies that favor their construction (Act 16.858). In this context, this study aims to explore the potential sources of cyanobacterial inoculum in reservoirs with the risk of being exported to the water utility in AACC. We analyzed the spatial distribution patterns of Chl-a and precipitation, together with reservoir size, the distance of the water network to AACC, the river level dynamics, and high-frequency cyanobacteria monitoring data in the water utility. This

study aims to provide baseline information for the development of early warning systems for health risks in water purification.

3.3 **Methodology**

The methodological strategy comprises four stages, each with a different purpose. The initial stage aims to approach the interaction between rainfall in the SLRB and river level in AACC. To do so, time series from the State Water Administrator (OSE) were accessed, from meteorological stations located within or close (< 10 km) to the study area, and cross-correlation analyzes were performed. The next stage sought to identify events with high concentrations of cyanobacteria in AACC and to evaluate the conditions that can promote the transport of biomass from reservoirs. To do so, water reservoirs (0.25 to 30 ha) dispersed in the study basin were identified and the cumulative rainfall and Chl-a concentration in the days before these events were mapped by processing satellite images. The third stage aimed to approach the conditions linked to the non-occurrence of cyanobacteria in AACC. To do this, dates with minimum concentration of cyanobacteria and with precipitation ranges similar to when high cyanobacteria events were identified. Finally, the fourth stage sought to identify the reservoirs that could have determined the transport of biomass to AACC. To do this, clustering analyzes were performed with precipitation data, Chl-a, the size of the reservoirs and their distance from AACC (Fig. 3.1).

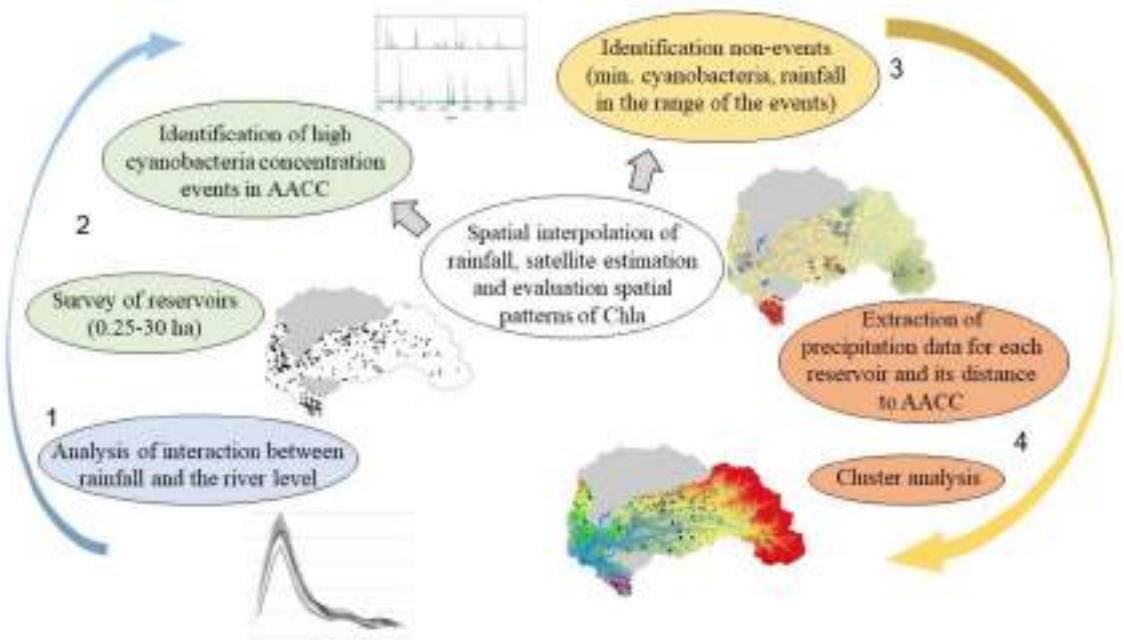

Fig. 3.1 Methodological strategy. The four main stages of the study are differentiated by colors and numbers. The outline corresponds to the Santa Lucía River basin

3.3.1 Study Area

The study area encompasses the SLRB, which drains to AACC, excluding the subbasins of the Paso Severino and Canelón Grande dams due to their indirect drainage to drinking water intake in AACC and the absence of substantial cyanobacterial blooms (Somma et al., 2022). The basin covers a total area of 6355 km^2, predominantly comprising the subbasins of the Santa Lucía River (81.4%), La Virgen stream (10.5%), Canelón Grande stream (6.9%), and the Santa Lucía Chico River (1.2%) (Fig. 3.2).

SLRB is marked by various productive activities: horticulture, fruit, wine, pig and poultry farming dominate the south; dairy farming and rainfed crops dominate the central and western areas; livestock farming prevails in the eastern region, along with forestry crops and mining (Achkar et al., 2012) (Fig. 3.2). In recent decades, there has been an intensification of land use in high- and low-productivity soils, driven by rainfed monocultures, particularly soybeans, and also corn and sorghum (Gazzano et al., 2019).

In the basin that drains directly into the AACC, a total of 325 water reservoirs were identified (Fig. 3.2), ranging in size from 0.25 to 30 ha (median, 0.3 ha), according to the adjustment in Google Earth of the polygons downloaded from the Spatial Data Infrastructure of Uruguay (https://visualizador.ide.uy/ideuy/core/load_public_project/ideuy/). Two primary types of construction were distinguished according to their method, namely those formed by excavations (46 ponds) located exclusively in the southern zone and the remaining 279 formed by dammed gullies (taipas). The distance between reservoirs and AACC was calculated (median 74 km, range 3-191 km) along the hydrographic network, path developed from processing the ALOS PALSAR digital elevation model (12.5 m resolution) downloaded from https://search.asf.alaska.edu/#/. This model was also used to delimit the microbasins of each reservoir.

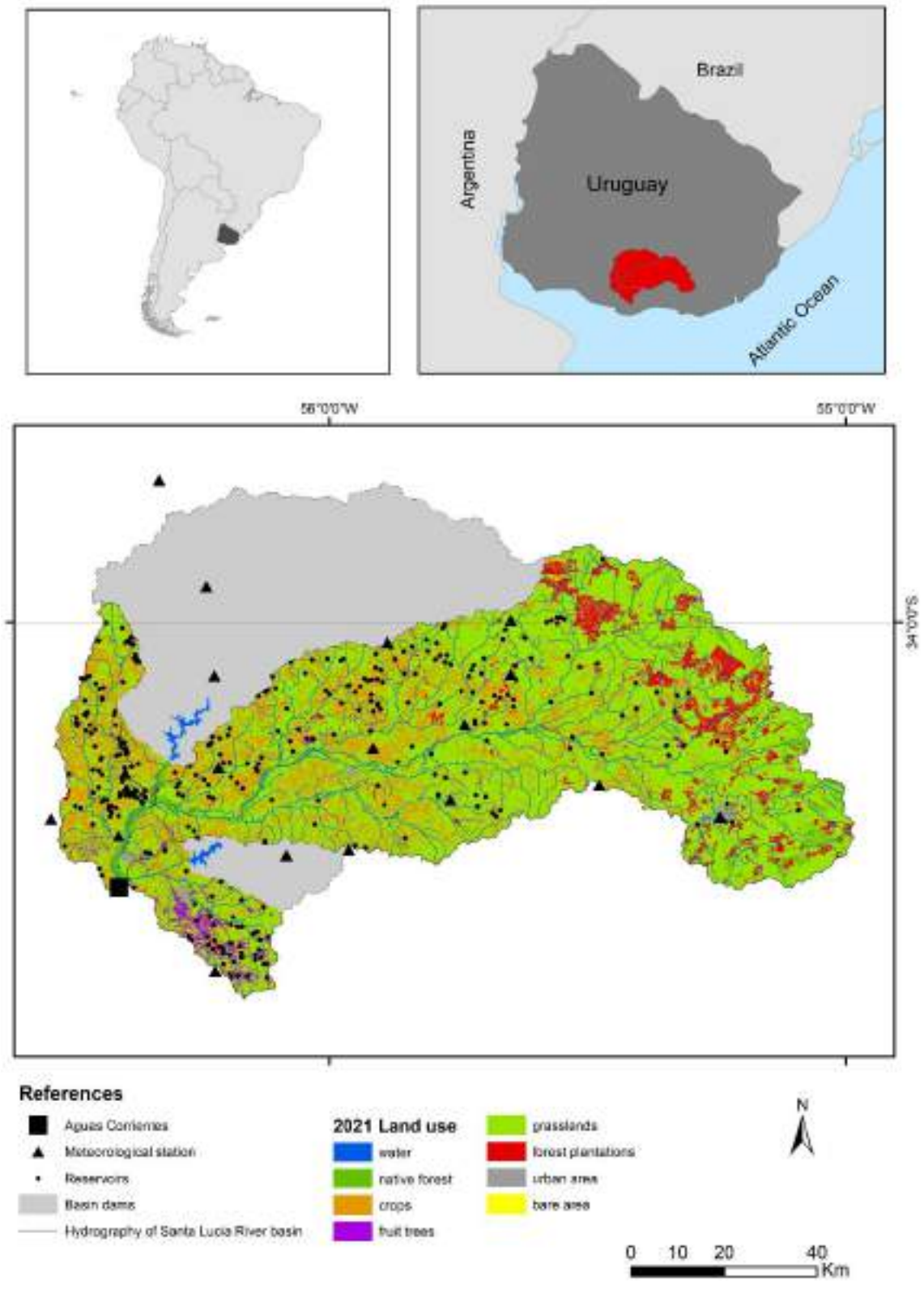

Fig. 3.2 Study area. Land uses in the Santa Lucía River basin reported for 2021 by the National Directorate of Territorial Planning. Meteorological stations within and near the basin (<10 km) are indicated. The basins of the Paso Severino and Canelón Grande reservoirs, excluded from the study, are delineated in gray

3.3.2 Data Acquisition and Analysis

Cyanobacteria biomass transport events from the reservoirs to AACC require the overflow of the dams due to high rainfall. Therefore, the time span of influence of precipitations on SRLB and the effect on river level in AACC were analyzed. Information corresponding to the daily flows and levels of the Santa Lucía River in AACC and the daily concentrations of phytoplankton and cyanobacteria recorded in the water for drinking treatment in AACC were requested from public water purification company (*Obras Sanitarias del Estado*, OSE) (period 2016-2022). Daily accumulated rainfall data were obtained from the National Institute of Meteorology (INUMET) for meteorological stations within or near (<10 km) the study area during the period 2016-2022 (Fig. 3.2). To approach the relationships between rainfall and river level in AACC, cross-correlation analyzes were performed, which estimates a significance value (p), the magnitude (M), and its variation with a time delay (lag) (Schön et al., 2022; Berbery and Barros, 2002).

To evaluate the potential transport events of cyanobacterial biomass from the productive reservoirs located in the SLRB to the intake of drinking water from AACC, phytoplankton data recorded by microscopy at AACC (OSE) were analyzed. The phytoplankton data is provided as cells/mL of total phytoplankton and cyanobacteria, without quantifying their biovolume. Possible correlations between these variables were then evaluated using Spearman's nonparametric test, and dates were explored when the concentration of cyanobacteria exceed 1000 cells/mL, half of the Alert 1 level (Vidal & Britos, 2012). After performing cross-correlation for identifying periods with a significant increase in river level after precipitations, a time window was taken to estimate the accumulated precipitation in that period. Then the availability of Sentinel-2 images captured before high cyanobacterial concentration events was explored. Once the events were identified, the previously detected time window was used to calculate the accumulated precipitation using spatial interpolations using the inverse distance weight (IDW) method. On the other hand, specific dates were identified when the concentration of cyanobacteria was below the detection limit (~ 0 cells/ml) and the precipitation was similar in range to the events, for which the precipitation that occurred in the time window was also calculated (as now called non-events).

To obtain the Chl-a information of the reservoirs in the days prior to the events and non-events, we explored the availability of cloud-free (<5%) Sentinel-2 MSI images at the SLRB and downloaded them from the site https://dataspace.copernicus.eu/. After

downloading the images, the surface reflectance (Rrs) was calculated using the atmospheric correction module of the ACOLITE software (v20231023.0), a widely used tool for remote detection of water quality. This correction method includes the Rayleigh correction for molecular scattering and aerosol correction (Ansper, 2018).

To estimate the concentration of Chl-a in water reservoirs, the study initially identified reservoirs (0.25-30 ha) within the basin, classifying them according to their type of construction. Subsequently, the average surface reflectance of each reservoir was extracted using polygons placed over the water surface. Using this information, Chl-a concentration was estimated using the satellite estimation model calibrated by Zabaleta et al. (2023) specifically for the SLRB reservoirs using information collected in situ. Zabaleta et al. (2023) compared Chl-a estimation models, and the most successful one uses the Rrs ratio between the green (~560 nm) and red (~665 nm) bands. The estimation equation employed was Chl-a (µg L^{-1}) = 10 ^ (1.6218 + 6.0575 * VR), where VR = (Rrs 560 nm - Rrs 665 nm) / (Rrs 560 nm + Rrs 665 nm). The entire process of image processing and spectral information extraction was carried out within the Sentinel Application Platform (SNAP) provided by the European Space Agency.

To evaluate the size of the total surface of the biomass that could potentially be transported downstream, on each monitored date, reservoirs with Chl-a> 20 µg L^{-1} were selected and their size was added. This threshold was used by Zabaleta et al. (2023) as the limit at which phytoplankton dominates the spectral response of the reservoirs located in the SLRB and corresponds to the lower Chl-a range of a bloom. Other research also used this threshold to determine high concentrations (Aubriot et al., 2020).

To explore spatial patterns in the distribution of Chl-a, spatial autocorrelations were performed according to Moran's I. This test consists of a Pearson scoring coefficient with a spatial location weighting matrix, for each data set, it provides a p-value and the magnitude of autocorrelation (Z) (Moran 1948). Once the analysis was carried out for all study dates (events and non-events), hot spots were mapped using the Getis–Ord Gi* statistic (Getis & Ord, 2010). This methodology is widely used with water quality information obtained through satellite monitoring and allows the summarization of large amounts of spatial data (Coffer et al., 2021; Torbick et al., 2013). For spatial autocorrelation and hot spot analyzes, ArcMap version 10.4.1 software was used. This analysis allowed Chl-a to be associated with the main productive activities in different

regions, using the land use classification of the National Directorate of Territorial Planning for the year 2021 (Fig. 3.2).

To identify groups of reservoirs that could have contributed biomass for the elevated cyanobacteria events in AACC, a cluster analysis was performed using accumulated precipitation (mm) data and estimated Chl-a (μg L^{-1}) for the events together with the size (ha) of the reservoir and the inverse of the distance to AACC (km). In the case of precipitation, the microbasins of each reservoir were used to extract the average and to include the spatial heterogeneity in the cluster analysis. The optimal number of clusters is processed by the "elbow" analysis, which guides the subsequent application of the k-means analysis. The main characteristics of the resulting cluster were evaluated by calculating the median of the variables used for each cluster of reservoirs. Statistical analyzes were performed in the R environment (R Core Team, 2020).

3.4 **Results**

The daily flow rates of the Santa Lucia River in Aguas Corrientes from January 2016 to July 2022 exhibited a median of 1.61 hm^3/day within a range of 0.12-475.51 hm^3/day. The level of the river was positively correlated with daily accumulated precipitation at 16 of the 18 meteorological stations evaluated. Always presenting correlation magnitudes M < 0.5, in all cases, M increased progressively from the first day to the fourth, where it reached its maximum at all stations, then the magnitude decreased continuously with values of $p < 0.05$ up to a maximum of 21 days. In some cases, the p-value returned to < 0.05 a few days later, although it follows the trend with which it had been, the magnitudes are weak (M < 0.1) (Fig. S3.1).

Total phytoplankton recorded in AACC ranged from 1-132,129 cells/mL, with a median of 94 cells/mL. The phytoplankton concentration was low and negatively correlated with river flow (Spearman test, Rs=-0.04; $p<0.05$). The cyanobacterial concentration showed a range of 0-4,371 cells/mL, with a median of 0 cells/mL (below the detection limit), positively correlated with flow (Rs=0.21; $p<0.001$).

During the study period, the cyanobacteria exceeded 1,000 cells/mL on 15 dates, mainly occurring in 2019 (seven days) and 2016 (five days). Some elevated concentrations of cyanobacteria occurred on consecutive days, treated as the same event. Cross-correlation

analysis showed that the maximum time window in which rainfall is continuously correlated with river levels in AACC is 21 days. Therefore, the availability of cloud-free MSI/S-2 images was explored for the 21 days prior to elevated cyanobacteria events. A total of six images were obtained and analyzed (Table 3.1 and Fig. 3.3). In the six images, possible biases due to isolated cloudiness or shadow were visually determined and were only detected on the images 05/01/2019 and 05/16/2019, which led to 3 and 1 reservoirs being discarded from subsequent analyzes, respectively.

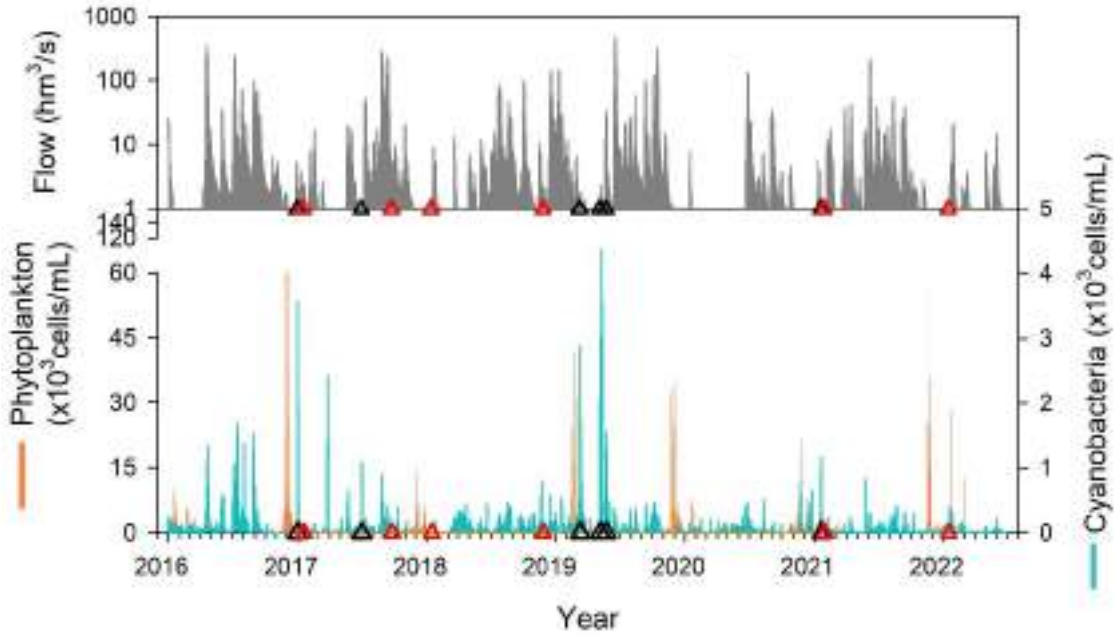

Fig. 3.3 Top: Flow of the Santa Lucia River. Bottom: Concentration of phytoplankton and cyanobacteria cells in the Aguas Corrientes (OSE) water potabilization plant. Black triangles indicate dates that exceed 1000 cells/mL of cyanobacteria selected for Sentinel-2 image analysis. The red triangles indicate dates where the cyanobacteria were below the detection limit (~ 0 cells/mL), rainfall over the previous 21 days was in the range (48-141 mm) and the Sentinel-2 imagery is available for the previous 21 days

Table 3.1 Study events**.** Dates with cyanobacteria concentrations greater than 1000 cells/mL in Aguas Corrientes with Sentinel-2 images from the previous 21 days. Chlorophyll-a concentration was estimated for all reservoirs (325), with reported median values and standard deviations in parentheses

Event	Duration (days)	Cyanobacteria (cel./mL)	S-2 image	River flow AACC (hm^3/day)	Chlorophyll-a (µg L^{-1})
01/01/2017	1	3581	12/12/2016	2.09	24 (263)
07/01/2017	1	1089	06/10/2017	0.84	10 (189)

03/10/2019	2	2038 (1195 - 2880)	02/20/2019	1.57	116 (1039)
05/07/2019	5	2823 (1182-4371)	05/01/2019	1.57	49 (312)
05/24/2019	1	1553	05/16/2019	28.60	44 (414)
01/21/2021	1	1163	01/10/2021	1.34	40 (489)

In the Sentinel-2 images captured in the days prior to the six events, Chl-a of the 325 reservoirs exhibited a median of 36 µg L^{-1}. The highest concentrations were recorded on event 03/10/2019 (median 116 µg L^{-1}; ranged from 4 to >2000 µg L^{-1}), while the lowest concentrations were recorded on 07/01/2017 (10 µg L^{-1}; 2-1049 µg L^{-1}), followed by 01/01/2017 (24 µg L^{-1}; 4 to >2000 µg L^{-1}) (Fig. 3.4).

Clustering patterns were detected with Chl-a data on all dates prior to the events according to Moran's autocorrelation analysis, except for the event dated 01/01/2017 with a p-value> 0.05 suggesting a random distribution. The highest magnitude of autocorrelation was obtained for the event 07/01/2017 (Z = 8.54), followed by 01/21/2021 (Z = 3.82), 03/10/2019 (Z = 3.80), 05/24/2019 (Z = 2.22) and 05/07/2019 (Z = 1.87). The clustering of reservoirs with the highest recurrent Chl-a concentrations was located in the southern zone, followed by the south-central and eastern parts of the basin. However, reservoirs with lower Chl-a concentrations were grouped in the center and west of the basin according to the Getis-Ord statistics (Fig. 3.4).

Accumulated precipitation was obtained during the 21 days prior (P21) to the events. The highest P21 records occurred before the events on 05/24/2019, 01/01/2017, and 1/21/2021, with median accumulations for all stations of 141 mm, 101 mm, and 94 mm, respectively. The lowest records occurred before 07/01/2017, with a median of 2 mm, therefore, it could not be considered as a cyanobacterial transport event and will be discarded for subsequent analyses (Fig. 3.4). In this sense, the precipitation range before the events was between 48 and 141 mm. It should be noted that on some dates the rainfall coincided with the high Chl-a sets, mainly in the southern zone in the events 03/10/2019, 05/07/2019, and 01/21/2021, as well as in the central-south zone in the events 05/24/2019 and 01/21/2021.

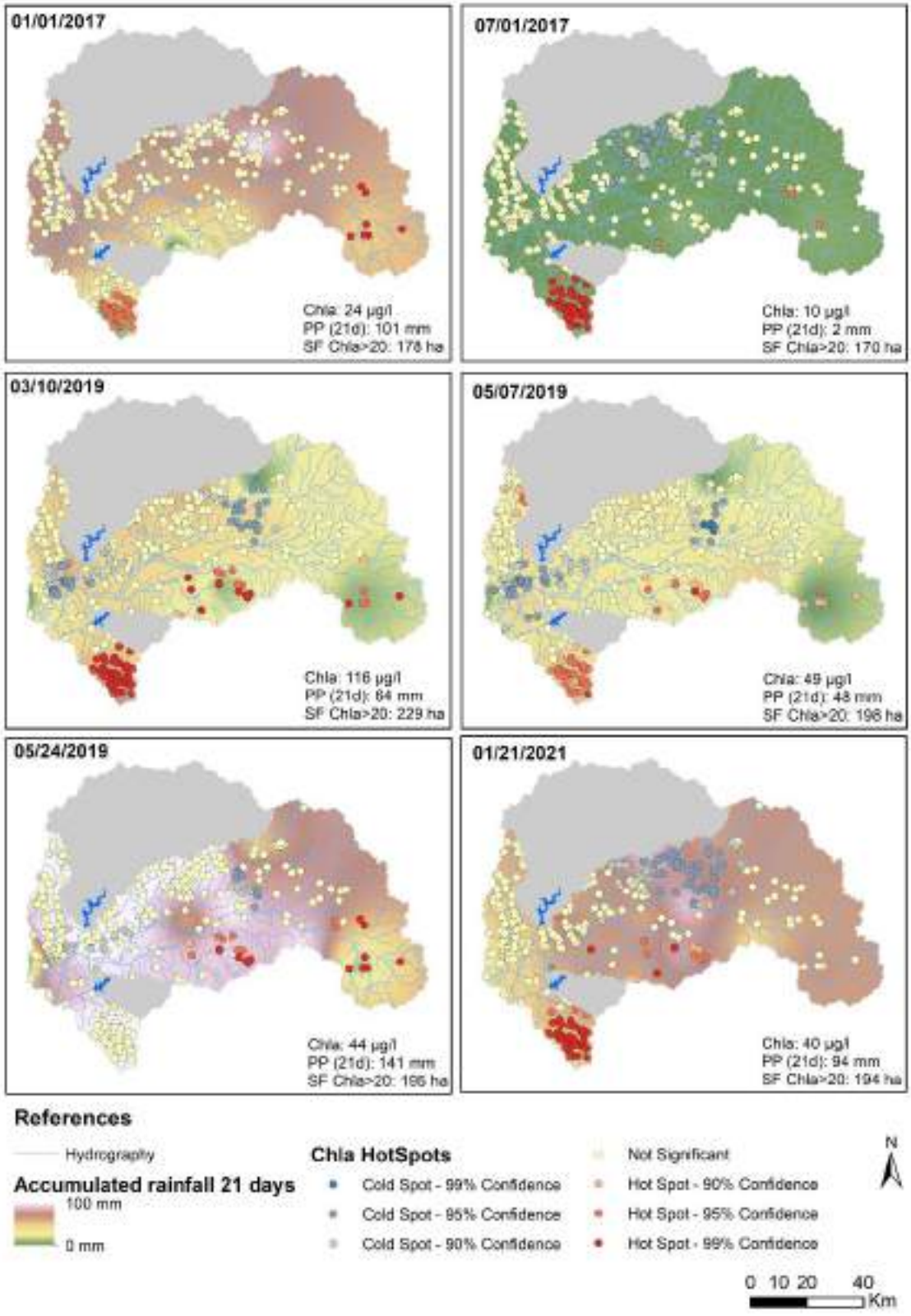

Fig. 3.4 The dates presented correspond to dates exceeding 1000 cells/mL of cyanobacteria in the potabilization plant. Satellite-estimated Chl-a hot spot analysis for a maximum of 21 days prior to each date, as a background, spatial interpolation of accumulated rainfall for the 21 days prior to each date. In addition, the following data are presented; Chl-a: median of Chl-a in the 325 monitored reservoirs, PP (21d):

average accumulated rainfall 21 days prior to each date. SF Chl-a > 20 µg/L: sum of the surface of reservoirs with a Chl-a concentration > 20 µg/L.

Six dates (non-events) where cyanobacteria records are below the detection limit (~ 0 cells/ml) in AACC were identified and rainfall is within the range (P21: 60 - 134 mm) reported for biomass transport events. Non-events showed a wide gradient in terms of satellite-monitored Chl-a. The non-event of 09/25/2017 is characterized by the low Chl-a concentration (median 9 µg L^{-1}; ranging from 3 to >2000 µg L^{-1}), the lowest Chl-a surface >20 µg L^{-1} (80 ha) and the highest rainfall of the selected dates (134 mm). At the other extreme, 01/18/2017 had the highest Chl-a concentration (median 93 µg L^{-1}; ranged from 3 to >2000 µg L^{-1}), the lowest rainfall (60 mm), and the largest Chl-a surface >20 µg L^{-1} (232 ha) (Fig. 3.5).

As in the events, in the non-events, Chl-a clustering patterns were detected for all the dates evaluated, except for 11/27/2018 where p-value> 0.05 suggests a random distribution. The autocorrelation magnitudes showed less variation among themselves than in the events evaluated. The highest magnitude was obtained for the non-event 01/15/2018 (Z = 4.71), followed by 01/16/2022 (Z = 4.67), 01/30/2021 (Z = 4.25), 01/18/2017 (Z = 4.06) and 09/25/2017 (Z = 3.04).

The most recurrent clusters of high Chl-a concentration reservoirs were also located in the southern zone, followed by the eastern and central-southern zones in a fluctuating manner between the dates, while in the non-event 01/18/2017 two clusters were formed particularly in the west and central-west of the basin. On the other hand, clusters of reservoirs with low Chl-a concentrations were located in the center of the basin. Unlike the events, intense rainfall occurred mainly over reservoirs identified as cold spots or nonsignificant according to the Getis-Ord statistic. Except for the non-event 01/30/2021 with high rainfall that coincided with the Chl-a hotspot located in the central-southern area of the basin (Fig. 3.5).

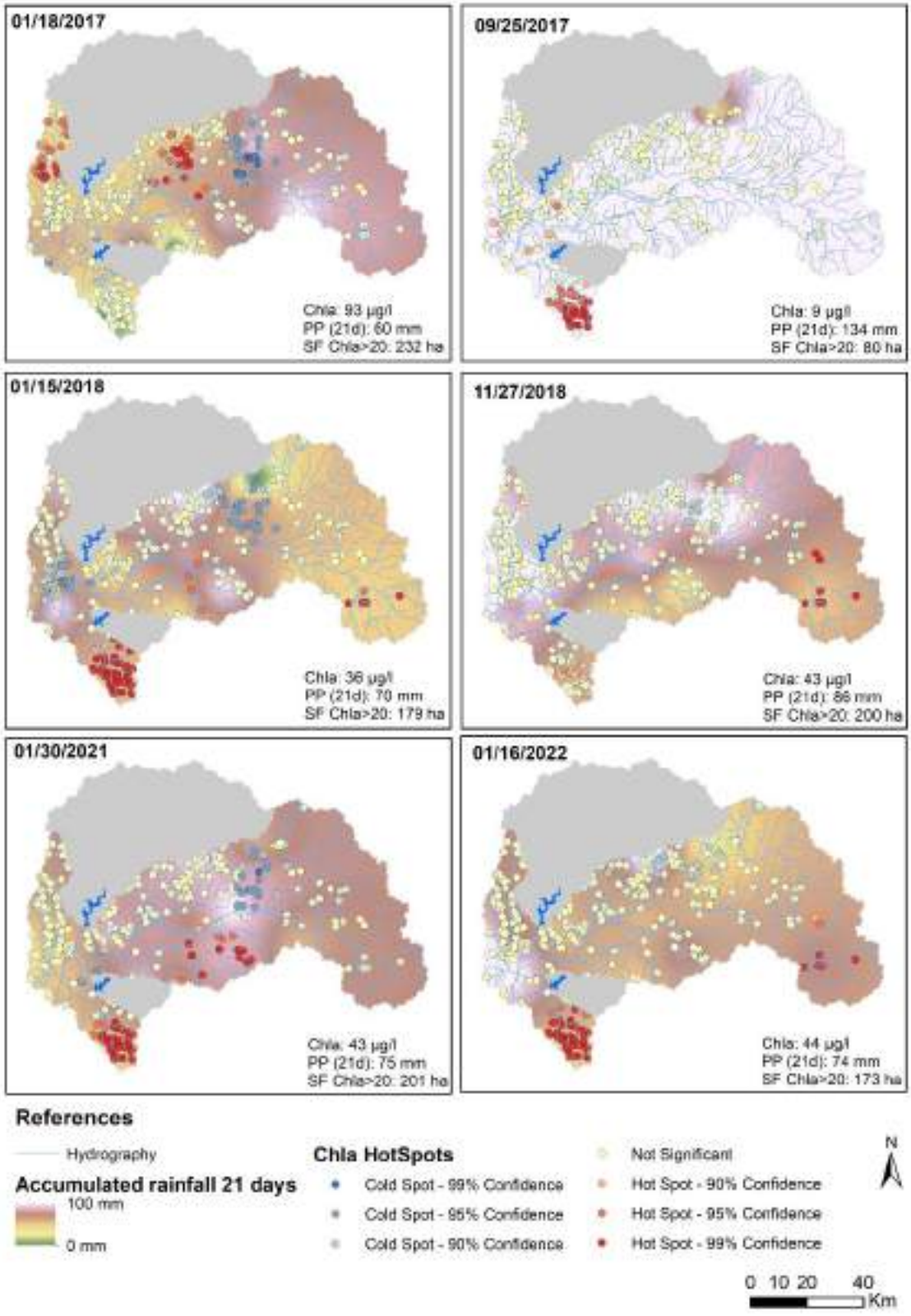

Fig. 3.5 The dates presented correspond to cyanobacteria being below the detection limit (~ 0 cells/mL) in the potabilization plant, the rainfall over the previous 21 days was in the range (48-141 mm), and Sentinel-2 imagery is available for the previous 21 days**.** Satellite-estimated Chl-a hot spot analysis for a maximum of 21 days prior to each date, as a background, spatial interpolation of accumulated rainfall for the 21 days prior to each date. Furthermore, the following data are presented; Chl-a: median of Chl-a in

the 325 monitored reservoirs, PP (21d): average accumulated rainfall 21 days before each date. SF Chl-a > 20 µg/L: sum of the surface of reservoirs with a Chl-a concentration > 20 µg/L

According to the potential risk of biomass export in the events evaluated with the data of reservoir size, fluvial distance to AACC, Chl-a concentration and average rainfall occurred in the microbasins, the optimal number of clusters was 5. Group 1 stands out, which comprises 19 reservoirs spread throughout the basin that present the highest concentrations of Chl-a (853 µg L^{-1}). The second set with a high concentration of Chl-a (94 µg L^{-1}) corresponds to cluster 3; it is composed of 38 water bodies located in the south of the basin close to AACC (44 km). The third group with a high potential risk of biomass export is group 4, with reservoirs close to AACC (47 km) located west of the basin and with a median Chl-a (49 µg L^{-1}). Group 5 has the same Chl-a median as group 4, composed of more distant sites (151 km) mainly located in the east and south-central part of the basin. Group 2 includes 84 reservoirs located in the center of the basin and presents the lowest potential risk of biomass export, as it records the lowest concentrations of Chl-a (15 µg L^{-1}) and is located far from AACC (82 km) (Table 3.2 and Fig. 3.6).

Table 3.2 Characteristics of the identified clusters based on the total average of biomass, including the median and range in parentheses of the variables. The size of the reservoirs was defined using information from the Spatial Data Infrastructure of Uruguay and was subsequently adjusted in Google Earth. The distance between the reservoirs and the potabilization plant was estimated using the water network

Cluster	Size (ha)	Distance (km)	Chlorophyll-a (µg/L)	Rainfall (P21)	Reservoirs
1	0.3 (0.1-25.4)	82 (74-176)	853 (6-6915)	79 (2-172)	19
2	0.5 (0.1-9.1)	106 (32-162)	15 (3-5772)	103 (13-201)	84
3	0.3 (0.1-2.4)	44 (3-74)	94 (4-4813)	79 (3-200)	38
4	0.3 (0.1-3.4)	47 (6-180)	49 (3-3621)	82 (1-188)	142
5	0.3 (0.1-1.8)	151 (27-191)	49 (5-4303)	74 (1-134)	42

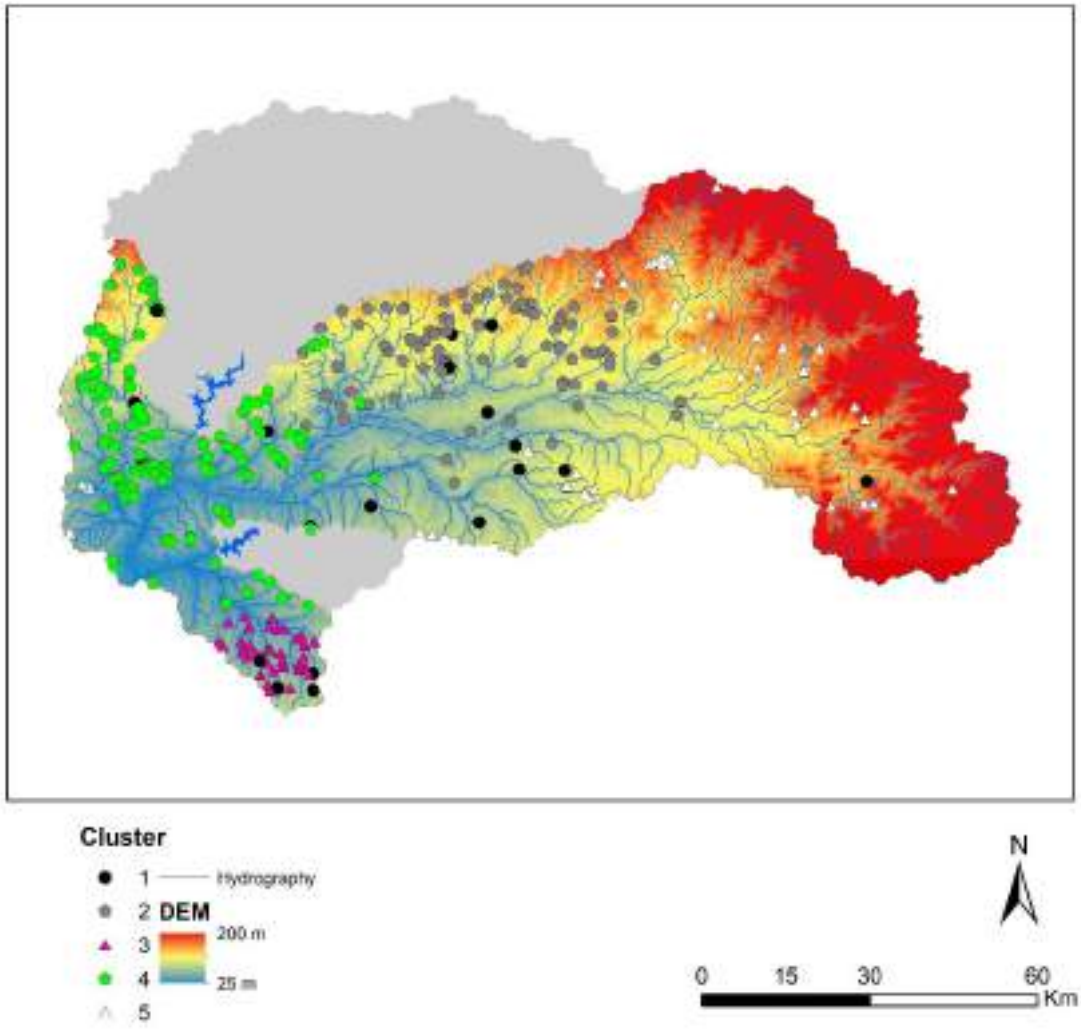

Fig. 3.6 Cluster analysis performed from the data for each reservoir: size (ha), distance to the water treatment plant (km), Chl-a concentration (µg/L), and accumulated rainfall in the events evaluated (mm). DEM: Digital Elevation Model according to the product Alos Palsar (12.5 m)

3.5 **Discussion**

This study achieved the first evaluation of the risk of phytoplankton biomass export events from multiple reservoirs to the main water potabilization plant in the country. Cartographic products were generated that allow us to identify the areas with the highest risk of biomass export in the SLRB and identify the reservoirs with the greatest potential impact. This work contributes to the mitigation of eutrophication by focusing efforts on particular water bodies with the highest risk of phytoplankton export in the basin. Our results constitute the basis for the development of a biomass transport indicator that

allows improving the effectiveness of eutrophication management measures and anticipating the transport of blooms to AACC.

The correlations observed between the flow of the Santa Lucía River and the concentration of phytoplankton and cyanobacteria are in line with the findings of Somma et al. (2022). The authors indicate that eukaryotic phytoplankton increases during periods of low flows, while cyanobacterial biomass increases with high flows. This provides evidence for the transport of biomass through the river from upstream eutrophicated lentic eutrophic systems, consistent with regional (Aubriot et al., 2020; Kruk et al., 2019) and international research (Grabowska & Mazur-Marzec, 2011). Furthermore, eutrophication is expected to be enhanced by the increase in extreme precipitation in some regions (Sinha et al., 2017; Donat et al., 2016). The presented approach is applicable to basins with similar characteristics, where intensive productive activities overlap with water purification, leading to eutrophication of reservoirs and high risk of downstream cyanobacterial transport.

During the study period, fifteen days with cyanobacteria concentrations exceeding 1000 cells/mL (half of Alert 1; Vidal & Britos, 2012) were identified. Unnoticed events of this nature can significantly impact the quality of drinking water. This issue leads to increases in purification costs and, subsequently, rates (Dunlap et al., 2015). Over the years, the public water purification company (OSE), has significantly increased its investment in activated carbon, from US$ 90,196 in 2008 to a peak of US$ 2,683,240 in 2015 (Santos et al., 2021). Coffer et al. (2021) reported numerous cases of elevated levels of cyanotoxins in drinking water in the United States, where local governments issued warnings, resulting in the loss of access to water for hundreds of thousands of people. In particular, the 2013 event at AACC in Uruguay caused water to be supplied with unpleasant odor and taste to 60% of the population (Amorín & Larghero, 2017). Taking into account future scenarios with increased precipitation and a higher frequency of extreme events in the region (IPCC, 2023), the potential risk of transporting harmful cyanobacterial blooms is likely to increase without effective eutrophication mitigation measures.

Our study identified areas in the basin where the reservoirs are grouped according to the concentration of Chl-a. The southern zone, reservoirs composed mainly by group 3 exhibited high Chl-a values on five dates and is located in the lowest lands of the basin and close to AACC (see Fig. 6). These characteristics determine that it is the zone with

the highest potential risk of biomass export. The high Chl-a may be attributed to the extended residence time of water characteristic of dug ponds, which is prevalent in this zone. Distinguishing reservoirs according to their construction method revealed that southern reservoirs are predominantly ponds, while others are *taipas*. This difference may be influenced by soil cost disparities, as the southern region has soils of higher value due to increased productivity and infrastructure. One of the key distinctions between these types of reservoir lies in their water sources. The ponds receive water from precipitation and groundwater, while the *taipas* are replenished by surface runoff. Consequently, *taipas* receive larger water volumes, making them more prone to overflow. The southern region of the SLRB is characterized by a higher intensity of land use associated with horticulture, fruit growing, and viticulture. In this area, numerous farms could contribute substantial nutrient loads to ponds and reservoirs (Darré et al., 2019), through continuous irrigation systems (Liu et al., 2019). The combination of intensified agricultural activities, the morphological characteristics of the water reservoirs in the southern SLRB, and the short distance to AACC contribute to the distinct classification of these reservoirs.

The reservoirs in cluster 4 are the most numerous and are located in the western zone of the basin. These are lowland reservoirs, which exhibited high Chl-a values and are characterized by proximity to AACC. These characteristics can increase the probability of bloom survival (Williamson et al., 2018); however, Chl-a hotspots were not detected. The western region of the SLRB is distinguished by having the highest concentration of dairy cattle, as reported by the Division of Livestock Control (https://web.snig.gub.uy/arcgisprtal/apps/opsdashboard/index.html#/f977f4c49b29466a a0ef13d09beb3fc6). Additionally, this area is characterized by extensive rainfed crop cultivation (see Fig. 2). Combined, these land uses have been identified as the main diffuse sources of nutrients entering inland water bodies after periods of heavy rainfall (Aubriot et al., 2017; Chalar et al., 2017; Goyenola et al., 2015).

The mapping and cluster analysis identified isolated cases with high Chl-a (cluster 1), mainly due to their large size and high Chl-a records. These cases represent special instances that warrant specific evaluation. The reservoirs in this group are candidates for in situ monitoring to obtain information on their physicochemistry, nutrient load, dominant phytoplankton type, and potential toxicity. Furthermore, the identification of such reservoirs allows the application of good practices, such as declaring the management of spillway outflows and eventual drainage that the Ministry of Environment

and OSE need to know in advance. In future studies, recategorization of reservoirs is expected to occur due to the improvement of its water quality or, on the contrary, by including more reservoirs in group 1. Following the proposed approach, in situ evaluations can be implemented for each reservoir to define specific measures to mitigate eutrophication and control harmful phytoplankton growth.

Additionally, areas with low risk of biomass export were detected, located mainly in the northeast region of the basin (see Fig. 6), characterized by lower soil productivity and extensive livestock use. This region, according to Chalar et al., (2017), exhibits the lowest nutrient exports for the Santa Lucía Chico River basin. Specifically, the northeast area, including the Casupá stream basin, showed a low Chl-a, making it an appropriate site for the environmental protection of the stream basin with the priority of water quality conservation for purification. Therefore, based on our findings, it would be a suitable location for this purpose due to its low risk of exporting the cyanobacterial inoculum. As suggested by Kibuye et al. (2021), water utilities involved in watershed management programs tend to implement fewer controls on drinking water. Furthermore, zoning the risk of contact or importation of cyanobacterial blooms enables the issuance of alerts and facilitates prompt decision making (García et al., 2019). In this context, satellite imagery has significant potential, offering near-real-time monitoring capabilities. The use of Chl-a and its spatial analysis also enables the identification of priority conservation areas with relatively good water quality. This information can contribute to its sustainable management through measures such as regulating specific agricultural practices and establishing buffer zones and protected watersheds.

The spatial analysis of Chl-a with the precipitation patterns between events and non-events revealed that the location of high precipitation areas was consistent with the events of increased cyanobacterial concentration in AACC. In general terms, the Chl-a was similar between both sets of dates; however, precipitation patterns together with distance and ground relief conditions of the basin can be the main factors determining the transport of biomass to AACC. In non-events, the most intense precipitations occurred over sets of reservoirs detected as coldspots, while in cyanobacterial events heavy rainfall occurred over hotspots. However, in three non-events (01/15/2018, 11/27/2018 and 01/16/2022) intense or moderate precipitations occurred over Chl-a hotspots located in the east of the basin, and likewise, cyanobacteria did not reach AACC. This phenomenon could be due to the fact that the greater the distance, the turbulence generated in the river bed in the

basin area with greater ground relief could determine a lower survival of cyanobacteria (Williamson et al., 2018). On the other hand, the analysis of non-events allowed us to identify a case (09/25/2017) in which high flows (see Fig. 3), due to long-lasting heavy rainfall washed out the cyanobacterial biomass.

3.6 **Conclusions**

The most relevant variables for the occurrence of cyanobacterial bloom events in AACC are Chl-a, the distance between the reservoirs and AACC, and the location and intensity of the rainfall. The relief from the ground could be considered as an important variable for the development of a future indicator of the potential risk of biomass transport, however, in the case of the SLRB the relief and the distance from the AACC increase proportionally.

The satellite approach of this study allowed the first assessment of the Chl-a conditions of hundreds of reservoirs and the effect of rainfall in the days before high cyanobacteria events in the main water utility of the country. The reservoirs in the south of the basin were identified as those with the highest risk of export of cyanobacterial biomass in five of the six events evaluated. These areas are characterized by constant irrigation, which favors high concentrations of Chl-a. Furthermore, their proximity to the AACC water utility and low slopes increase the risk of biomass transport. In contrast, the reservoirs in the northeast were identified with the lowest export risk, aligning with the environmental protection of the basin with the objective of water quality conservation for purification.

The methodological strategy described in this work has key potentials: identifying areas where blooms are more significant and classifying the reservoirs according to variables related to the biomass transport potential. This simple and economical methodology allows for advancing in the understanding of the connections between land use, rainfall patterns and intensity, the physical characteristics of the territory and the occurrence of bloom events. The availability of this information allows one to guide restoration and mitigation measures by defining priorities and implementing local territorial intervention strategies. Based on our results, it is necessary to integrate new variables to advance understanding of the complexity of the river basin toward an early warning system of cyanobacterial events in water intakes. These may include examining the influence of soil types and conditions, the impact of climate variability on dynamic groundwater, and

understanding how watercourses function as accumulators and biomass transport agents, among other factors.

3.7 **Supplementary material**

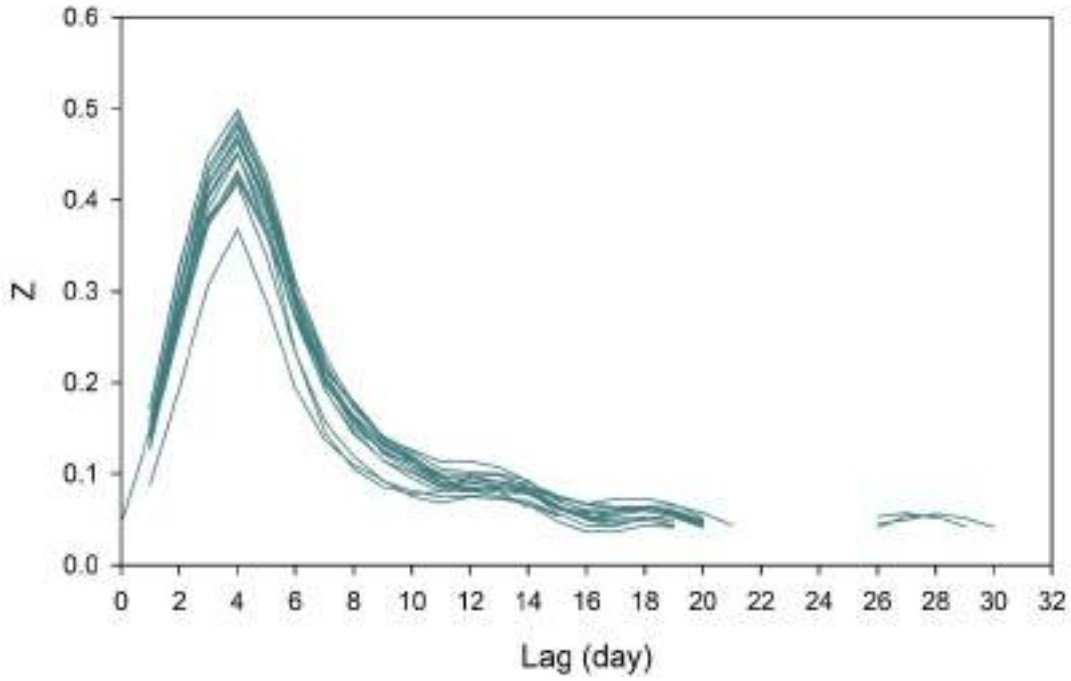

Fig. S3.1 Cross-correlation analysis, the lines correspond to meteorological stations, their continuity depends on the significance of the correlations (p-valor<0.05). Z: magnitude of the correlation (y axis), lag: delay time in days (x axis)

4. Capítulo 4

Spatio-temporal evaluation of the trophic state of water reservoirs located in the main basin for drinking water in Uruguay: influence of meteorological, morphological and land use variables.

4.1 **Abstract**

The intensification of agricultural activities increases the export of nutrients to inland water bodies, promoting eutrophication and phytoplankton blooms. The main water intake for potabilization in Uruguay (AACC) is in the Santa Lucía River Basin (SLRB), where 325 small agricultural reservoirs (median size 0.3 ha) drain directly into the AACC

and are considered potential sources of cyanobacteria inoculum. This study used a complementary approach by evaluating the spatiotemporal dynamics of phytoplankton chlorophyll-a (Chla) and transparency (Tr) in the 325 reservoirs and their relationship with meteorological variables (air temperature and precipitation), water body surface area, and intensity of land use of each micro basin. Free Sentinel-2 satellite images processed between 2016 and 2022 were used to monitor 25 dates. Surface reflectance of the reservoirs was extracted, followed by statistical clustering and machine learning analyses. High Chla concentrations (>20 µg L^{-1}) were observed in 61% of the study cases, with the highest concentrations in the southern and western areas. Chla and Tr were correlated with precipitation and temperature, forming clusters in their spatial distribution according to spatial autocorrelation analysis. The main regulating factors of Chla were the reservoir size, air temperature, and land use intensity. This study proposes a novel approach to identify the climatic and morphological factors influencing the trophic status of multiple reservoirs. The basins with intensive land use and used for drinking water production require risk assessment of harmful phytoplankton biomass export and the focus of *in situ* monitoring efforts in a climate change context to help mitigate eutrophication processes.

Keywords

Spatial patterns, remote sensing, phytoplankton blooms, chlorophyll *a*, cyanobacteria

4.2 **Introduction**

In regions with intensive agricultural activity, numerous water reservoirs are constructed for purposes such as irrigation, livestock consumption, and agroindustrial uses. These reservoirs primarily capture rainwater from groundwater and surface runoff from heavily used land plots, which can carry substantial nutrient loads. The combination of nutrient input, high water residence time, and elevated temperatures creates optimal conditions for the excessive growth of phytoplankton biomass (Beaver et al. 2014, 2012; Schindler 1977), typically dominated by cyanobacteria (Huisman et al. 2018; Burford and O'Donohue 2006), which can produce toxins harmful to aquatic and terrestrial life (Chorus and Welker 2021). When these reservoirs are located in basins where water is used for drinking purposes, they pose a significant health risk as they can continuously export potentially harmful phytoplankton biomass (Grill et al. 2019; Remmal et al. 2017)

or release large quantities after intense rainfall events (Aubriot et al. 2020; Grabowska and Mazur-Marzec 2011).

Traditional methods for continuous monitoring of numerous water reservoirs are very costly, primarily due to the labor-intensive process of collecting *in situ* samples and conducting subsequent laboratory analyses (Lins et al. 2017). To overcome this limitation, tools have been developed to evaluate water quality by interpreting Remote Sensing Reflectance (Rrs) remotely sensed by satellite sensors that provide free images (Page et al. 2018; Toming et al. 2016; Yacobi et al. 2011; Brando and Dekker 2003; Schalles et al. 1998).

The Rrs of inland water bodies results from various interactions between the optical properties of water and optically active constituents (OACs) such as phytoplankton pigments, suspended solids, and colored dissolved organic carbon (CDOM). OACs exhibit maximum energy absorption near the blue (~490 nm) and diminish towards the infrared, except for Chlorophyll-a (Chla), which has a second absorption peak in the red zone (~665 nm), facilitating its quantification (Ogashawara et al. 2017; Gitelson et al. 1992). However, the overlap in energy absorption introduces errors in the satellite estimation of OACs, which can be minimized by pre-classifying spectral signatures to differentiate the trophic status roughly first, and then applying specific OAC estimation indicators more precisely (Werther et al. 2021; Neil et al. 2019; Uudeberg et al. 2020).

Various band ratio indicators are used to estimate OACs, which must be calibrated with *in situ* information from target environments (Yang et al. 2017). Chla, an indicator of total biomass, has been successfully evaluated through the ratio between Rrs in the red (~665 nm) and the red-edge (~700 nm) bands (Mishra and Mishra 2012). Similarly, the ratio between Rrs (~665 nm) and Rrs green (~560 nm) has accurately estimated the Chla concentration (Oliveira et al. 2016; Ioannou et al. 2014), even in small and hyperturbid water reservoirs (<1 ha; transparency 4-55 cm) (Zabaleta et al. 2023). Additionally, transparency (Tr) has been estimated through a variety of satellite-based approaches (Zhang et al. 2021; Ouma et al. 2020; Topp et al. 2020), notably using near-infrared bands (>700 nm) (Zabaleta et al. 2023).

Processing and analyzing satellite images provide georeferenced information on the trophic state of numerous water bodies, creating large databases and evaluating spatial distribution patterns through geostatistical analyses across many lakes (Coffer et al. 2021;

Torbick et al. 2013). These approaches help identify high occurrence zones of blooms (Zabaleta et al. 2021) with a high risk of cyanobacteria biomass export (Zabaleta et al. 2024 under review) and evaluate seasonal and annual variations (Tate 2019). They also allow for determining the processes that regulate trophic status, mainly associated with meteorological, structural, and land use variables in the reservoir micro basins (Weber et al. 2020). For this, various statistical approaches, including machine learning analyses, are used (Zhang et al. 2021; Liu et al. 2017). Therefore, high-frequency satellite monitoring and subsequent spatial analysis provide inputs for developing alert systems, focusing on *in situ* monitoring efforts (Yunus et al. 2015), and preventing population contact with cyanobacteria blooms in the public water supply network.

In Uruguay, the Santa Lucía River Basin (SLRB) is the country's main source of drinking water. The water intake is located in Aguas Corrientes (AACC) and supplies more than 60% of the national population. For more than a decade, symptoms of eutrophication have been reported in the Santa Lucía River (Gorgoglione et al. 2020; Aubriot et al. 2017; Chalar et al. 2011). The study by Somma et al. (2022) suggests that small water reservoirs in intensive agricultural production areas are potential sources of cyanobacteria inoculum towards AACC.

The reservoirs are located on private properties, making them difficult to access and are numerous, limiting the possibility of regular *in situ* monitoring to know their trophic state and identify and quantify the factors regulating phytoplankton growth. These aspects are especially relevant in the current climate change context; according to the IPCC (2023), the region is experiencing increases in high temperatures directly related to human activities and extreme events. Projections indicate an intensification of these trends. Climate change has been identified as a promoter of cyanobacteria blooms, even in lotic environments where this phenomenon is usually rare (Kleinteich et al. 2024). Therefore, evaluating the influence of temperature and precipitation on phytoplankton growth and eutrophication processes in productive reservoirs supports decision making in the management of inland water bodies considering possible future scenarios.

In recent years, tools for monitoring reservoirs in the SLRB have been developed. A model for satellite estimation of Chla and Tr was successfully calibrated and used to monitor small reservoirs upstream of AACC and evaluate their spatial distribution (Zabaleta et al. 2023). In this context, this study aims to evaluate the spatial and temporal dynamics of Chla and Tr in 325 reservoirs in the SLRB that drain into the drinking water

intake of AACC, classify them according to their optics and evaluate their relationship to precipitation and temperature, morphological variables (size of micro basin of each reservoir, size of reservoirs), and land use intensity. Our goal was to deepen the understanding of the factors influencing eutrophication and phytoplankton biomass development, provide inputs for management in a climate change context and contribute to mitigating eutrophication processes.

4.3 **Methodology**

The methodological strategy consists of four stages. The first stage aimed to extract Rrs information from water reservoirs (>0.25 ha, n=325) using 25 MSI/Sentinel-2 images obtained with seasonal frequency during the period from 2016 to 2022. In the second stage, Rrs data were used to estimate Chla and Tr using band indicators. Distribution patterns were detected by spatial autocorrelation analysis and hotspot detection using the generated data. The third stage aimed to evaluate the spatial distribution of Spearman's rank correlation magnitude obtained from the analysis between Chla and Tr with temperature and cumulative precipitation in the reservoir drainage area. Finally, the fourth stage explored the main relationships between trophic state, size of reservoirs and microbasins, meteorological variables, and land use through machine learning analysis. To do so, the classification of spectral signatures of the reservoirs (Fig. 4.1) was used as the response variable.

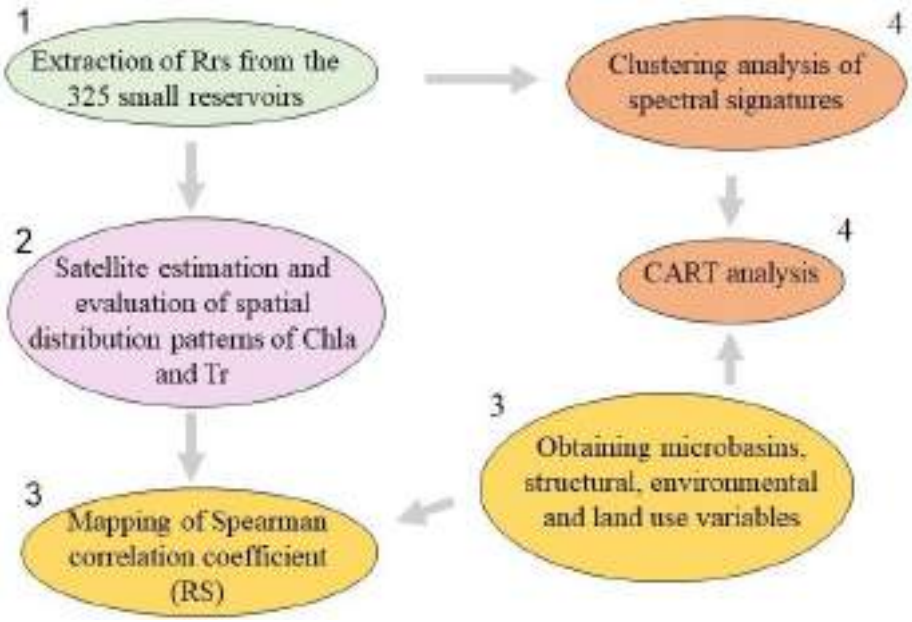

Fig. 4.1 Methodological strategy. The five stages of the research are differentiated by colors and numbers

4.3.1 Study Area

The study area encompasses the SLRB, which drains into Aguas Corrientes (AACC), excluding the sub-basins of the Paso Severino and Canelón Grande dams, as the water reservoirs located upstream do not drain directly into the intake for water treatment in AACC. Large cyanobacterial blooms have not been recorded in these dams, except for periods following their filling (Somma et al. 2022). The study basin covers a total area of 6355 km², primarily composed of the sub-basins of the Santa Lucía (81.4%), La Virgen (10.5%), Canelón Grande (6.9%), and the Santa Lucía Chico rivers (1.2%) (Fig. 4.2). Various productive activities occur in the SLRB, differentiated by zones. The South is characterized by horticulture, fruit growing, viticulture, and pig and poultry farming. The western area is dominated by dairy farming and dryland crops, while the northern and eastern regions of the basin are characterized by extensive livestock farming, forestry, and mining activities (Achkar et al. 2012) (Fig. 4.2).

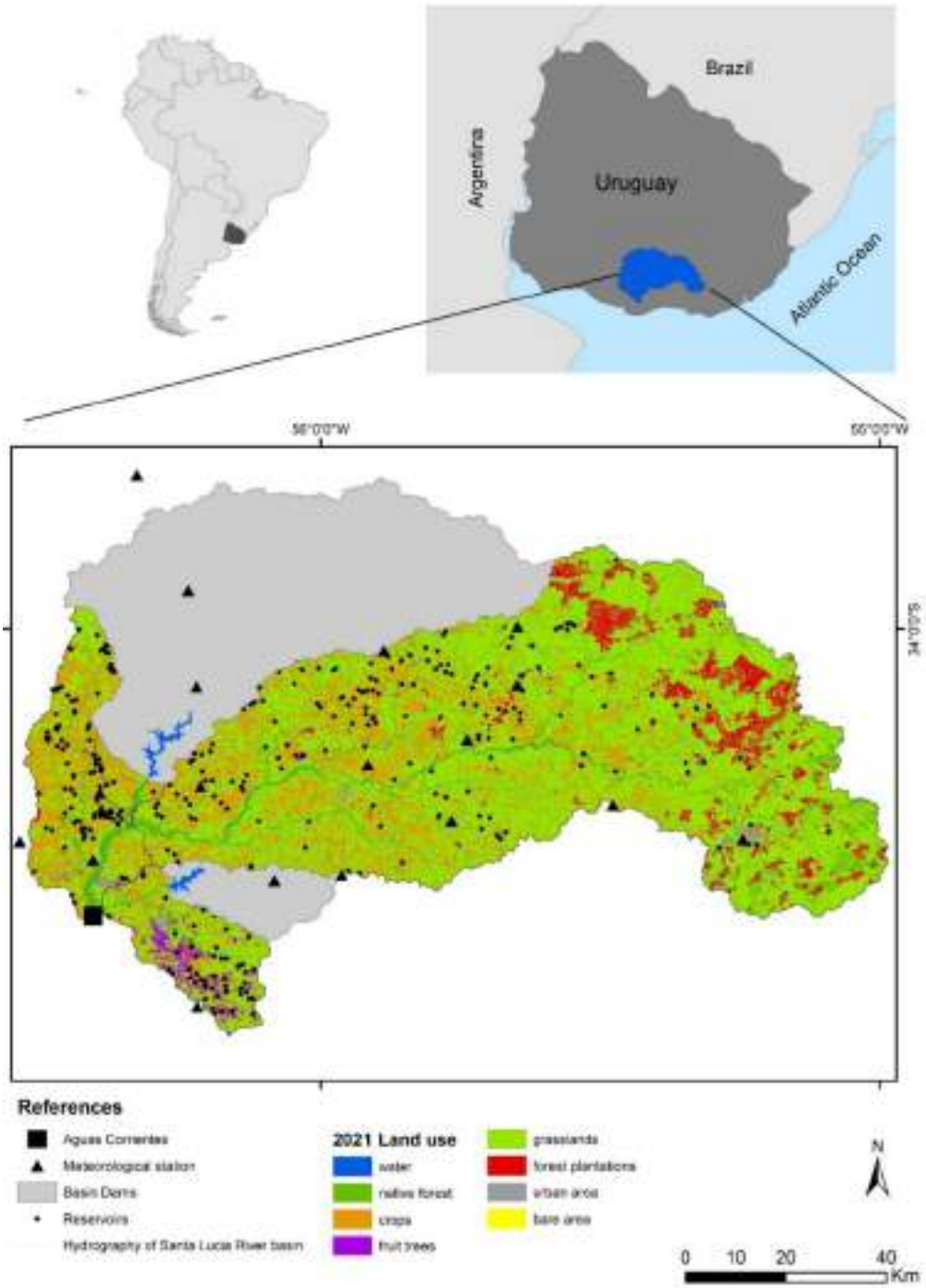

Fig. 4.2 Study Area. Land use in the Santa Lucía River basin reported for the year 2021 by the National Directorate of Territorial Planning. Weather stations located within and near the basin (<10 km). The basins of the Paso Severino and Canelón Grande dams, which were excluded from the study area, are outlined in gray. The reservoirs distributed within the study area and the Aguas Corrientes water treatment plant are shown in black.

4.3.2 Processing and Analysis of Satellite Images

To evaluate the spatial and temporal dynamics of the trophic state of productive reservoirs in the SLRB region (Fig. 4.1), we analyzed the Rrs of the water along with satellite-estimated concentrations of Chla and Tr. We utilized seasonal images with less than 10% cloud cover from the MSI sensor on Sentinel-2, covering the period from 2016 to 2022, which were downloaded from the Copernicus Data Space https://dataspace.copernicus.eu/. The images, at L1C level, were atmospherically corrected using the ACOLITE software (v20181210.0), a widely recognized tool for remote sensing of water quality in turbid and small water bodies (Zabaleta et al. 2023; Ansper 2018).

Spectral signatures were analyzed to classify the reservoirs based on their optical properties and identify outliers. We extracted average Rrs values from MSI/Sentinel-2 bands centered at 492 nm, 560 nm, 665 nm, 705 nm, 833 nm, 865 nm, and 1614 nm using polygons that outline the water surface of each reservoir (n = 325). The clustering analysis was then performed using the "elbow" method to determine the optimal number of clusters for the clustering of k-means. We also identified spectral signatures not exclusive to water surfaces, which were associated with wet land pixels, macrophytes and emergent vegetation at the land-water interface (Qing et al. 2020). Clustering analyses, widely used in global water bodies, revealed the main optical characteristics reflecting the trophic state of the environments (Neil et al. 2019; Spyrakos et al. 2018). Image processing and Rrs extraction were performed using the Sentinel Application Platform (SNAP) of the European Space Agency.

Chla and Tr concentrations were estimated using models from Zabaleta et al. (2023):

$$\text{Chla } (\mu g\ L^{-1}) = 10\ ^\wedge\ (1.6218 + 6.0575 * VR)$$

where

$$VR = (Rrs\ 560\ nm - Rrs\ 665\ nm) / (Rrs\ 560\ nm + Rrs\ 665\ nm)$$

and

$$Tr\ (cm) = 10\ ^\wedge\ (1.68706 - 6.03732 * Rrs\ 833\ nm).$$

For each cluster generated by the k-means analysis, we calculated the median and standard deviation of Chla and Tr.

4.3.3 Data Analysis

To understand the spatial distribution of Chla and Tr, we considered the warm season (Nov-Apr), cold season (May-Oct), and the entire period. For these temporal segments, the median Tr was estimated, while Chla was transformed into the percentage of occurrences exceeding 20 $\mu g\ L^{-1}$. According to Zabaleta et al. (2023), this concentration is the minimum at which Chla dominates the reflectance ratio between the red (665 nm) and green (560 nm) bands. This concentration exceeds alert levels 1 for drinking water and is slightly below alert level 2 for recreational waters (Chorus & Welker 2021). Using the obtained information, the presence of spatial distribution patterns was explored through Spatial Autocorrelation (Global Moran's I) (Moran 1948) and hotspot analysis (Getis & Ord 2010), which have been used to report the spatial distribution of the trophic state of numerous continental water bodies (Coffer et al. 2021).

To explore the correlations between Chla and Tr with meteorological variables (precipitation, air temperature), micro basins of the reservoirs were delineated using the ALOS PALSAR digital elevation model (resolution 12.5 m) downloaded for free from the server https://search.asf.alaska.edu/# . Cumulative daily precipitation data from meteorological stations located within or near (< 10 km) the studied basin during the period 2016-2022 (Fig. 4.2) were obtained from the National Institute of Meteorology (INUMET, in Spanish).

For all meteorological stations, we calculated the average accumulated precipitation over the seven (pp7D), fifteen (pp15D), and thirty days (pp30D) preceding the image acquisition dates. To obtain precipitation data for each reservoir's micro-basin, we employed the Inverse Distance Weight (IDW) interpolation method and extracted averages for polygons corresponding to the reservoirs' micro-basins. Furthermore, the average temperatures in the 30 days prior to the images (Tmed) were sourced from daily temperature averages registered for the National Institute of Agricultural Research in Las Brujas, located 30 km southwest of AACC, accessible via http://www.inia.uy/gras/Clima/Banco-datos-agroclimatico. To evaluate the effects of meteorological variables on the spatial and temporal distribution of Chla and Tr, we replicated the methodology outlined by Liu et al. (2024). We calculate the Spearman correlation coefficient (RS) between precipitation and temperature with Chla and Tr for each reservoir individually. Spatial autocorrelation analysis was used to assess the spatial

distribution of RS, and hotspot analysis was conducted where significant results were found.

To explore the influence of meteorological variables, morphological variables of reservoirs (such as the surface area of the water body and its microbasin), and land use intensity on Chla variation, we used land use information extracted for each micro-basin from the 2021 classification by the National Directorate of Territorial Planning. This information enabled us to estimate the Land Use Intensity Index (IAE) developed by Díaz et al. (2018) for the country. We then performed a classification and regression tree analysis (CART), a versatile method that does not assume a specific probability distribution and is adept at detecting non-linear relationships between variables, managing large datasets, and identifying key predictors (Caldwell et al. 2021). This analysis is extensively used to report the impact of environmental variables on water quality (Zhang et al. 2021; Liu et al. 2017). For the CART analysis, the previously identified spectral signature clusters were treated as the response variable, while precipitation, temperature, reservoir size, microbasin size, and land use intensity index served as explanatory variables without standardization. The CART model was executed using the 'rpart' package (Breiman et al. 1984) in R software version 4.0.0 (R Core Team 2020).

4.4 **Results**

We monitored a total of 325 reservoirs (average 0.98 ha, range 0.25 - 25 ha) by satellite, the microbasins ranged from 1.3 to 13,529 hectares, with the largest area corresponding to the microbasin of a reservoir used for drinking water storage. Excluding this reservoir, the largest micro-basin was 1,791 hectares, with an average of 80.1 hectares. The total water catchment area for the productive reservoirs was 25,960 hectares, representing 4.1% of the total study area. Among the monitored reservoirs, 46 are ponds located in the southern part of the basin, created by excavation and mainly receiving water from precipitation and groundwater. The remaining 279 reservoirs, known as *'taipas',* were built by damming intermittent watercourses. The ratio of micro basin size to reservoir size was lower in ponds compared to *taipas,* affecting surface runoff. Land use intensity, as indicated by the IAE, was high in the west and low in the south and east (Appendix 1).

4.4.1 Satellite Monitoring

Satellite images were collected on 25 dates between 2016 and 2022, covering 325 reservoirs and resulting in 8,125 observations. Chla had a median concentration of 33 µg L^{-1} (± 144), with higher standard deviation during the warm period (average: 43 µg L^{-1} ± 367) compared to the cold period (average: 20 µg L^{-1} ± 132). High Chla concentrations (>20 µg L^{-1}) were more frequent in the warm period (71% ± 36) than in the cold period (50% ± 34). Tr had a median value of 16.5 cm (± 6.5), consistent across both warm (16 cm ± 7) and cold periods (17 cm ± 6).

Chla and Tr exhibited clustered distributions as indicated by the spatial autocorrelation analysis. High Chla concentrations (>20 µg L^{-1}) were more frequent in the southern region, with additional clusters in the western zone and, to a lesser extent, the extreme eastern of the basin. Lower Chla concentrations clustered centrally. As far as Tr is concerned, minimal values were observed in the western zone, with elevated values in the south and east (Fig. 4.3).

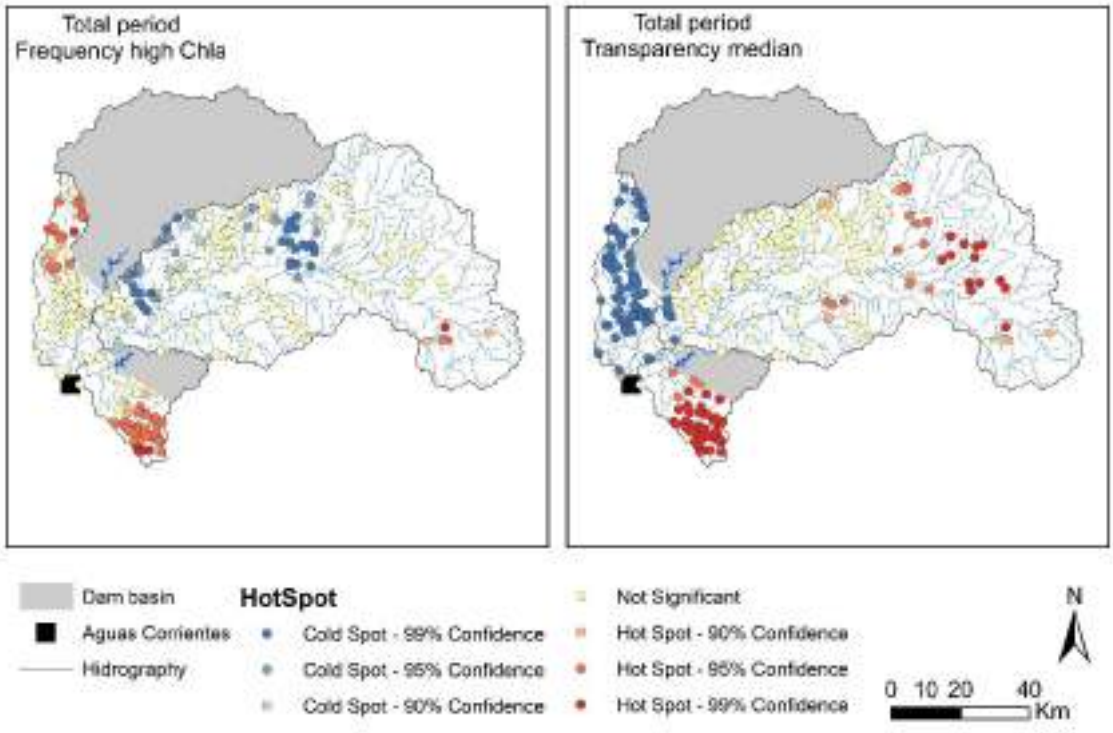

Fig. 4.3 Total spatial distribution of the frequency of high Chla values (>20 µg L^{-1}) and Tr according to the median, obtained from hotspot analysis (Getis-Ord Gi)

Seasonal variations in the spatial distribution of Chla and Tr were evident. During the cold period, reservoirs with a high frequency of Chla concentrations (>20 µg L^{-1}) clustered in the south, followed by the western zone, where their number increased during the warm period, while environments with low Chla concentrations (<20 µg L^{-1}) primarily clustered mainly in the center of the basin. Conversely, Tr was distributed in a large cluster with minimal values in the western zone, while the clearest reservoirs were concentrated in the south and east of the basin, where their numbers increased during the cold season (Fig. 4.4).

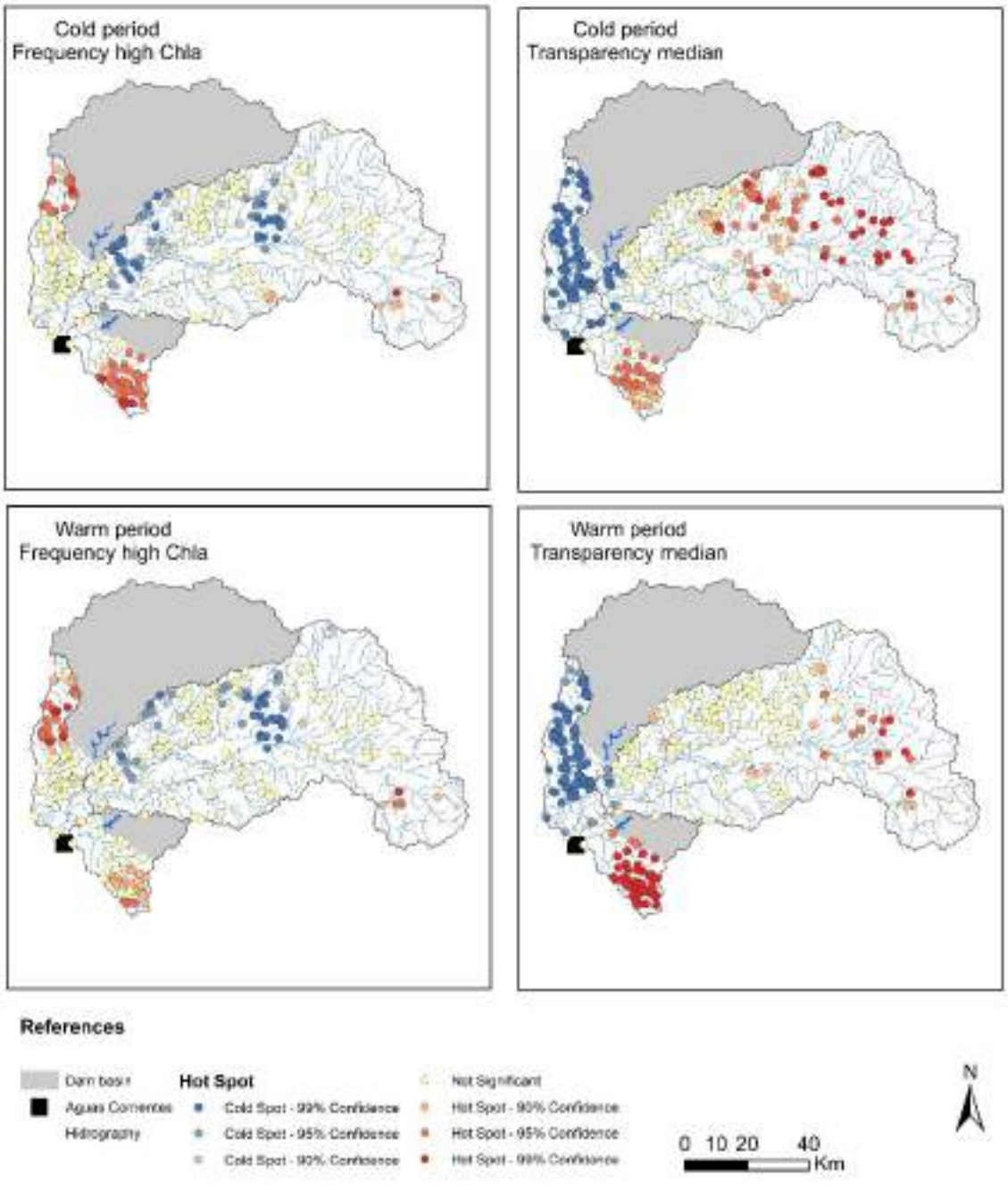

Fig. 4.4 Seasonal spatial distribution of the frequency of high Chla values (>20 μg L^{-1}) and Tr according to the median, obtained from the hotspot analysis (Getis-Ord Gi)

4.4.2 Spatial Distribution of Spearman Correlation Magnitude

On the 25 monitored dates, temperature and accumulated precipitation records (pp7D, pp15D, and pp30D) were obtained, with medians of 17°C (10-26°C), 5 mm (0-36 mm), 36 mm (0-149 mm), and 78 mm (18-339 mm), respectively.

Significant correlations between Chla and Tr with precipitation and temperature were detected in numerous reservoirs. However, the Spearman correlation magnitude was generally low (RS < [0.5]). Chla showed the highest correlation with average temperature (Tmed), with 52 reservoirs exhibiting RS > 0.5. On the contrary, negative relationships with precipitation were predominant, with higher pp30D and pp15D correlating with lower Chla, and 12 and 7 reservoirs showing RS < -0.5, respectively. pp7D showed the lowest correlation coefficients. Tr had the highest relationships with Tmed; 20 reservoirs had RS < -0.5, followed by pp7D (17 reservoirs with RS < -0.5), and were positively associated with pp15D and pp30D to a lesser extent (9 and 6 reservoirs with RS > 0.5, respectively).

Spatial clustering patterns were detected in the distribution of the RS coefficient obtained from the correlation analysis of Chla with Tmed, pp15D and pp30D, according to the Spatial Autocorrelation analysis. In the southern zone, a cluster of reservoirs showed a negative correlation between Chla and both pp15D and pp30D. In contrast, the reservoirs in the central part of the basin exhibited high and positive RS values between Chla and pp15D, which increased in number for the correlation between Chla and pp30D. High correlations between Chla and Tmed clustered in the south and south-central basin, while a cluster of reservoirs with minimal correlations was identified in the west (Fig. 4.5).

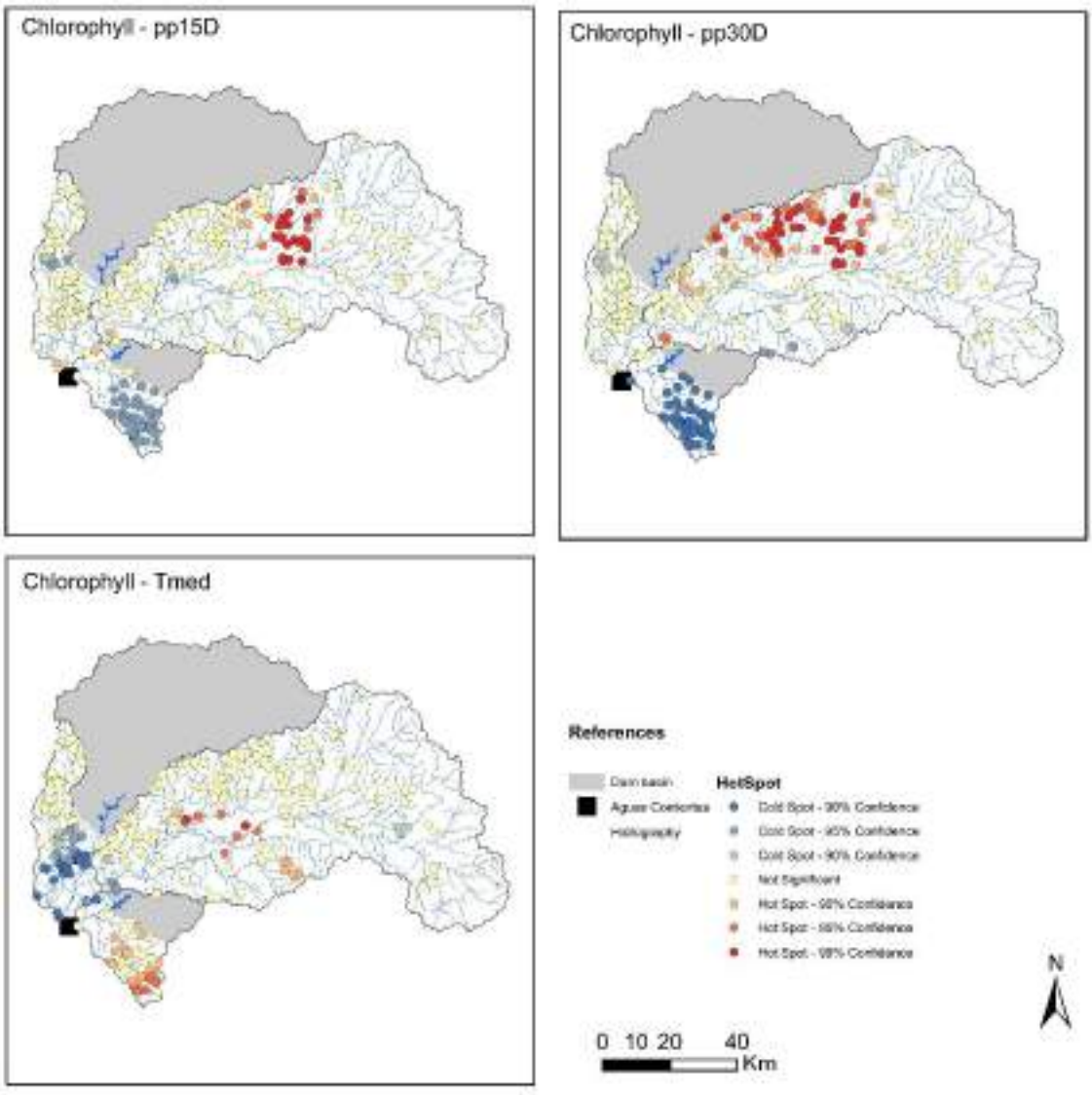

Fig. 4.5 Spatial distribution obtained from the hotspot analysis based on the Spearman correlation coefficient for each reservoir from the Spearman correlation analysis between Chla and pp15D, pp30D, and Tmed

Correlations between Tr and accumulated precipitation were detected, forming clusters of reservoirs with similar correlation magnitudes according to the spatial autocorrelation results. In the south, a cluster of reservoirs showed negative RS values for all precipitation timeframes. Conversely, in the west, reservoirs with maximum RS values, primarily with pp7D, were clustered. In the center, clusters of elevated RS values were detected with pp15D and pp30D, while in the east, minimal RS values with pp7D and pp30D were found (Fig. 4.6).

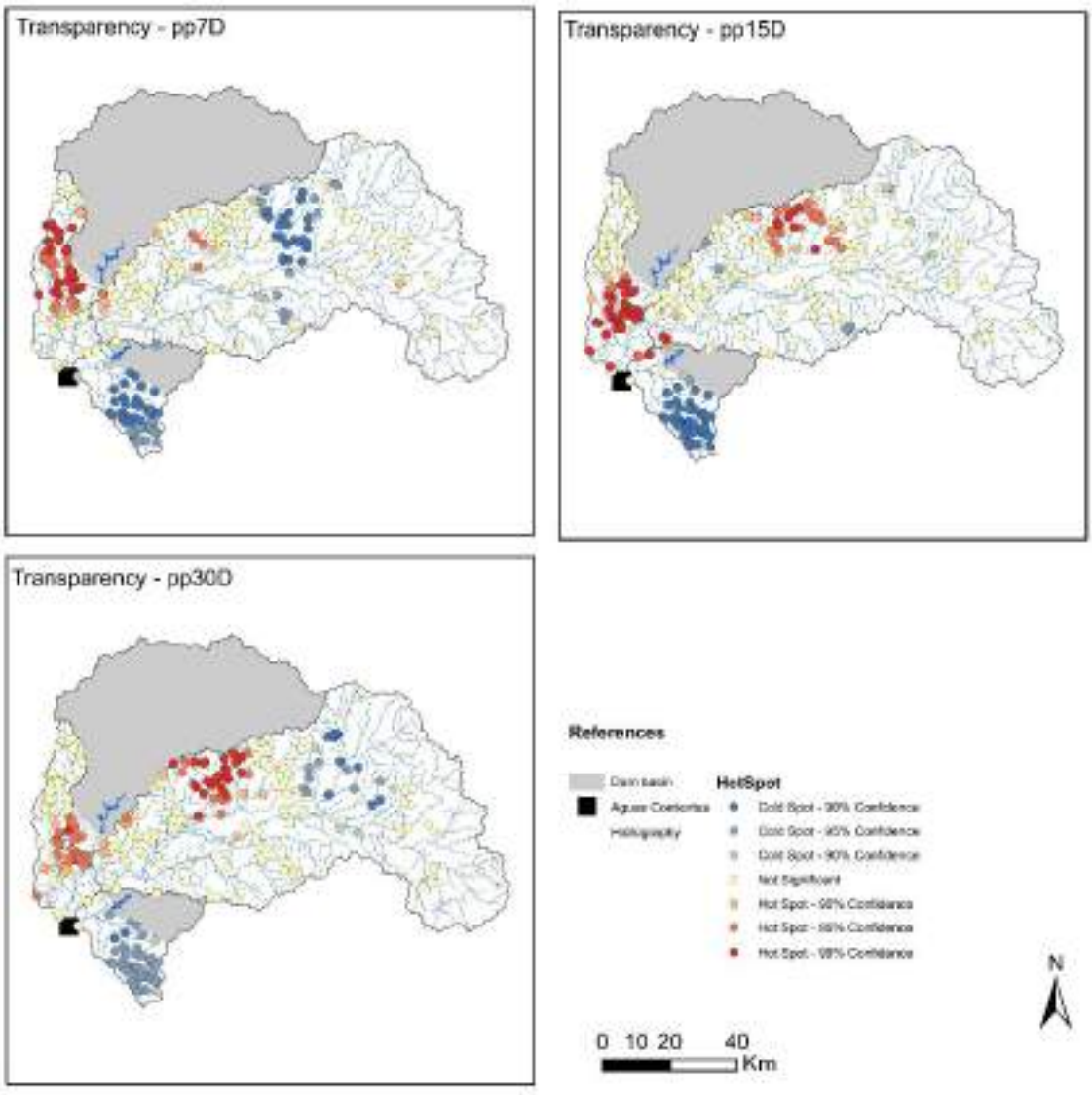

Fig. 4.6 Spatial distribution obtained from the hotspot analysis based on the Spearman correlation coefficient for each reservoir from the Spearman correlation analysis between Tr and pp7D, pp15D, and pp30D

4.4.3 Spectral Signatures

The spectral signatures of the 325 reservoirs were divided into three groups based on the clustering analysis of the Rrs on 25 dates between 2016 and 2022 (n=8125). Cluster 1 (A1) consists of 3257 spectral signatures and is characterized by high Rrs across all bands and a positive slope from 492 nm to the near-infrared (>704 nm). Cluster 2 (A2) includes 4508 signatures, with lower Rrs compared to A1, showing a peak Rrs at 560 nm and a minimum Rrs at 665 nm. Cluster 3 (A3) contains 360 signatures and also exhibits a peak Rrs at 560 nm, with high Rrs across all bands, especially in the near-infrared. The spectral characteristics of A3 indicate the presence of pixels covered partially or entirely by wet

land and emergent vegetation. Therefore, the information from this cluster is excluded from further analyses. The detected spectral clusters show significant differences in Chla and Tr concentrations according to Kruskal-Wallis analysis, with all combinations yielding p-values < 0.05, as evidenced by the medians calculated for each cluster (Fig. 4.7).

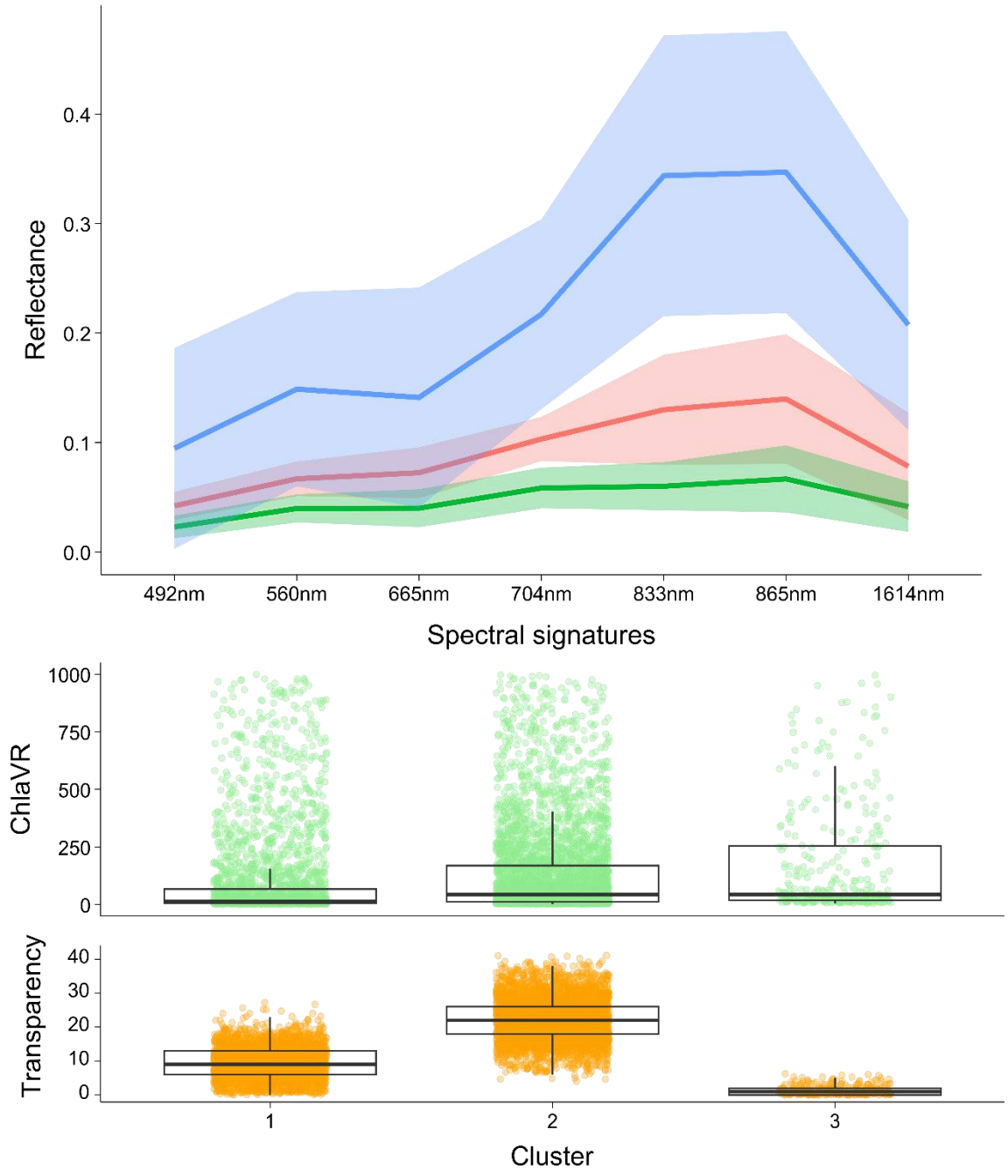

Fig. 4.7 Top: Spectral signatures according to the median of Sentinel-2 bands calculated for each cluster resulting from the k-means analysis (shaded areas represent standard deviation). Each line color represents a cluster; red, green, and blue correspond to clusters 1, 2, and 3, respectively. Bottom: Box plot of Chla and Tr concentrations for the groups obtained from the clustering analysis of the spectral signatures

For A1, the optimal number of clusters was determined to be six based on the "elbow" method. Spectral signatures were classified into six clusters using k-means, which are primarily distinguished by the Rrs ratio in the 560 nm and 665 nm bands; clusters with Chla medians > 20 µg L^{-1} exhibited a valley in Rrs (665 nm) relative to Rrs (560 nm), whereas clusters with Chla < 20 µg L^{-1} showed a progressive increase in Rrs from 492 nm to the near-infrared. Among the six clusters, there is a notable difference in the number of signatures (min. 193; max. 1158), a high average standard deviation in Chla (± 424), and a turbidity condition evidenced by a low average Tr (8 cm) (Fig. 4.8).

The previously classified signatures in A2 were also divided into six clusters. Compared to A1, A2 shows a reduced ratio between Rrs (560 nm) and Rrs (665 nm), lower Rrs magnitude across all bands, particularly in the near-infrared. The clusters identified in A2 are characterized by high Tr. Furthermore, the number of cases in these clusters was more evenly distributed compared to A1 (min. 463; max. 952) and presented a higher standard deviation in Chla concentration (± 773) (Fig. 4.8).

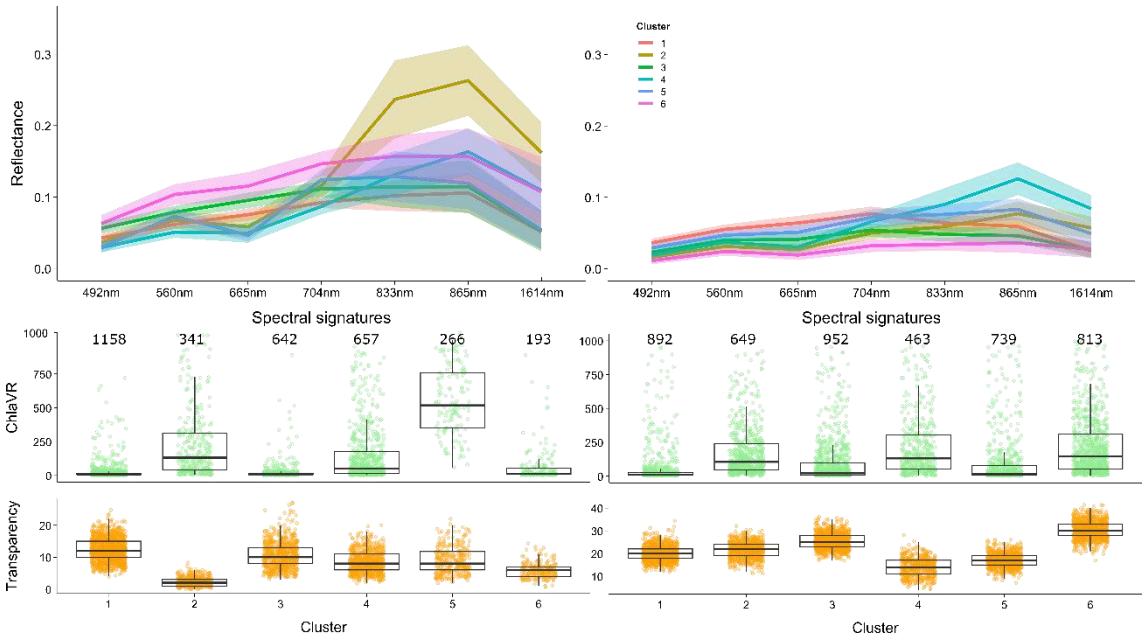

Fig. 4.8 Spectral signatures according to the median of Sentinel-2 bands calculated for clusters obtained from the k-means analysis of the previously classified spectral signatures into two clusters A1 (left) and A2 (right). Box plot of Chla and Tr concentrations for the clusters resulting from the clustering analysis of the spectral signatures

4.4.4 Classification Trees

Among the spectral signatures obtained for A1, clusters 1, 2, and 3 had low Chla concentrations (< 20 µg L^{-1}) and were assigned a value of 0 (C0), while clusters 4, 5, and 6 had high Chla concentrations (>20 µg L^{-1}) and were assigned a value of 1 (C1). The classification tree developed showed a 31% error rate in cross-validation. The most important predictor was IAE, which accounted for 29% of the cases; C0 signatures occurred mainly when IAE < 0.084. The second predictive variable was reservoir area; when it was > 0.6 ha, it divided 14% of the C0 cases. Lastly, when Tmed < 14 °C, it divided 18% of the data predominantly as C0, while Tmed > 14 °C grouped 39% of the cases, which were generally of type C1 (Fig. 4.9).

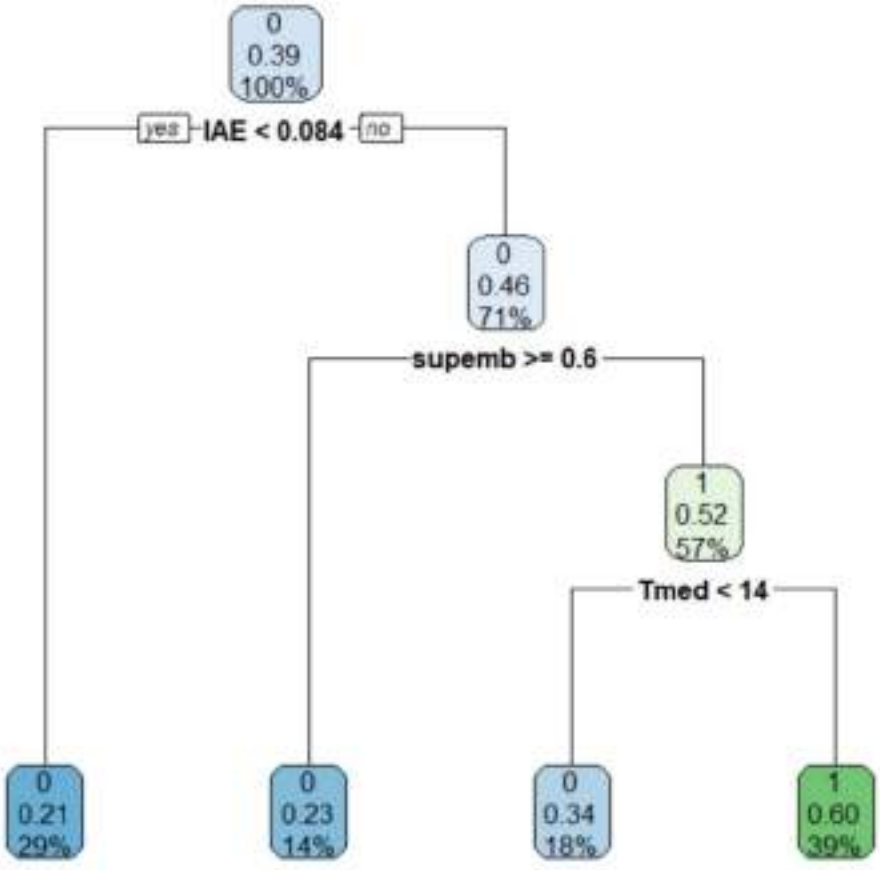

Fig. 4.9 Classification tree generated using the CART algorithm. Spectral signatures of A1 reclassified as 0 (low Chla and Tr) and 1 (high Chla and Tr) as the response variable, with meteorological, usage variables, size of the reservoirs and microbasin, as predictors. IAE: Land Use Intensity Index, supemb: reservoir area (ha), Tmed: air temperature median (°C)

In the spectral clusters obtained for A2, clusters 1, 2, and 3 had low Chla concentrations (< 26 µg L^{-1}) and were assigned a value of 0 (C0), while clusters 4, 5, and 6 had high Chla

concentrations (> 26 µg L^{-1}) and were assigned a value of 1 (C1). The classification tree showed a 33% error rate in cross-validation and identified the reservoir size as the most important predictive variable; when > 0.53 ha, it divided 36% of the C0 signatures. The second most important predictive variable was Tmed, which classified 36% of cases predominantly as C1 when > 16 °C. The third most relevant variable was pp15D; when > 22 mm, it favored the occurrence of C0 signatures (Fig. 4.10).

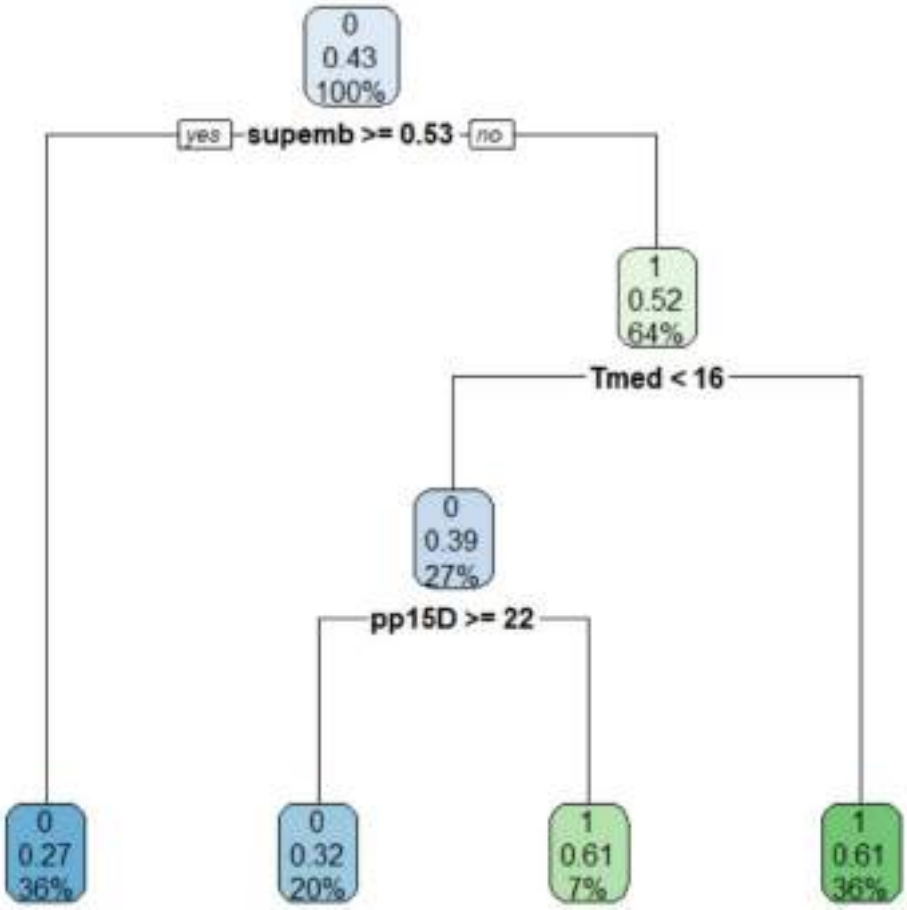

Fig. 4.10 Classification tree generated using the CART algorithm, considering the reclassified spectral signatures of A2 as 0 (low Chla and Tr) and 1 (high Chla and Tr) as response variables, with meteorological, structural, and usage variables as predictors. IAE: Land Use Intensity Index, supemb: reservoir area (ha), Tmed: air temperature median (°C), pp15D: Accumulated rainfall in the 15 days prior to the images used to monitor trophic state (mm)

4.5 **Discussion**

This study represents the first approach to identifying the climatic, land use intensity, and morphological factors of reservoirs and microbasins that affect the trophic state of the 325 small water reservoirs in SLRB and their spectral signatures. In the southern region,

higher precipitation favors a reduction in Chla, suggesting a washing and runoff effect of phytoplankton biomass downstream. In contrast, in reservoirs of the type *taipa* (central-north), precipitation is associated with the increase of the Chla, likely due to nutrient contributions from surface runoff from productive lands. This work contributes to the study of multiple water reservoirs for productive use reported as potential sources of cyanobacteria inoculum to the SLR and its transport to the water treatment plants in AACC (Zabaleta et al. 2024, under review; Somma et al. 2022).

Satellite monitoring of small and turbid reservoirs allowed the analysis of a total of 8125 spectral signatures, which were clustered into three sets mainly differentiated by Chla concentration. According to Gitelson et al. (1993), in turbid waters, a high Chla concentration determines the spectral response at wavelengths near red (~665 nm). This phenomenon resulted in a decrease in Rrs in the 665 nm band as the Chla concentration in the reservoirs increased (Fig. 4.7). The observed spectral signatures were expected for continental waters, consistent with Spyrakos et al. (2018), who compiled large international databases and obtained 3025 spectral signatures from various continental water bodies with a wide range of Chla, suspended solids, CDOM, and Tr. However, Spyrakos et al. (2018) did not report Rrs values as high as those found in the reservoirs located in the SLRB. On the other hand, Neil et al. (2019) reported spectral signatures similar in shape and magnitude to those recorded in A1, characterized mainly by high CDOM content and low Tr. The main difference in the water bodies monitored in our study is their exceptional small size and turbidity compared to previous investigations (Zabaleta et al. 2023; Coffer et al. 2021; Botha et al. 2020; Spyrakos et al. 2018).

Characteristic spectral signatures of pixels covered by wet land, macrophytes and/or emergent vegetation were identified, this is evidenced by some sets of spectral signatures with higher Rrs in all bands, mainly in the infrared (Qing et al. 2020). Interference in Rrs recording presents a challenge for satellite monitoring of small reservoirs, as it requires adjusting the water body size for each monitoring date. Various studies have developed techniques to specifically discriminate water-covered surfaces (Hu et al. 2021) and assess changes in their extent (Perin et al. 2021) through satellite imagery and field campaigns.

During the monitoring period, high Chla concentrations were predominantly observed in environments located in the southern part of the basin (Fig. 4.3). These areas feature deep ponds created through excavation, which provide water sources without inundating the soils of higher value of the SLRB (DIEA 2023). Although this area has the lowest

intensity of land use (Annex 4.1), various factors may contribute to the development of phytoplankton blooms in these ponds. The water input from precipitation and groundwater results in a prolonged water residence time. Additionally, these ponds are located within horticultural, viticulture, and fruit-growing establishments that use irrigation systems, which can continuously export nutrients, not just through precipitation events (Darré et al. 2019; Liu et al. 2019).

The ponds showed higher Tr compared to the *taipas* (Fig. 4.3), likely due to their greater depth and the fact that, unlike livestock watering sources, their sediment resuspension relies on vertical mixing and soil type. Beaver et al. (2017) found that in water bodies within intensively agricultural basins, light availability might limit primary productivity more than nutrient levels. Consequently, phytoplankton are not always directly correlated with their location in sub-basins of intensive agricultural use. In this context, the CART analysis with A2 data identified the size of the water body as the primary predictive variable (Fig. 4.10), supporting the findings of Weber et al. (2020), who reported the size of water bodies and the percentage of agriculture in their drainage area as the main variables regulating the concentration of cyanobacteria. On the contrary, pp7D are generally not significant for phytoplankton growing, as reported by Haakonsson et al. (2017), highlighting the complexity of factors influencing phytoplankton in ponds.

The reservoirs in the western part of the basin exhibited consistently high Chla concentrations throughout the study period, particularly during the warmer months (Fig. 4.4). This trend is in line with the higher land use intensity (Annex 4.1) due to the extensive area devoted to dryland crops, including both forage and cereal crops (Fig. 4.2), and the increased density of dairy cattle, which rises towards spring (Division of Livestock Control, https://web.snig.gub.uy/arcgisprtal/apps/opsdashboard/index.html#/f977f4c49b29466aa0ef13d09beb3fc6). Numerous studies in the SLRB indicate that mixed agricultural-dairy land uses are the main diffuse sources of nutrients to continental waters (Aubriot et al. 2017; Chalar et al. 2017; Goyenola et al. 2015). Zabaleta et al. (2023) specifically noted that reservoirs in dairy, dryland crop, and pig farming areas contribute high nitrogen and phosphorus levels, promoting the growth of cyanobacteria, consistent with international findings (Weber et al. 2020; Beaver et al. 2014). The CART analysis for A1 confirmed that the intensity of agricultural activities (IAE) is the primary predictive variable.

The correlation between Chla and temperature was unexpectedly weak, although Chla is a proxy for total phytoplankton biomass, as high temperatures usually promotes the growth of phytoplankton (Paerl et al. 2017) In our study, higher temperatures were associated with lower Chla in western reservoirs (Fig. 4.5). This may be explained by increased evaporation, which, combined with animal entry, creates turbidity that reduces light penetration. Conversely, in the southern area, rising temperatures were linked to higher Chla levels (Fig. 4.5). This finding is in line with the CART analysis result for A2, where deeper environments were predominant and temperature was the second most significant predictive variable (Fig. 4.10). The difference between southern and western reservoirs could be attributed to the depth disparity between ponds and *taipas*. In ponds, temperature does not affect turbidity as much as in *taipas* due to increased evaporation, shallower depth, and the resuspension of sediments generated by the ingress of livestock, significantly affecting the development of phytoplankton biomass.

In the eastern part of the basin, the strongest relationships between Chla and precipitation (pp15D, pp30D) were observed (Fig. 4.5). These reservoirs, located mainly in extensive livestock operations, feature the largest microbasins compared to other reservoirs. Precipitation can enhance Chla levels through increased nutrient export through surface runoff (Sinha et al. 2017; Goyenola et al. 2015). This effect contrasts with the results of the southern area and is consistent with Brasil et al. (2016), who found an increase in total phytoplankton biomass with a decrease in precipitation in lentic environments, particularly dominated by cyanobacteria. Havens et al. (2019) suggested that cyanobacterial biovolume increases with low flows, while Haakonsson et al. (2017) found no precipitation-cyanobacterial biovolume relationship. Thus, in the SLRB, the design of the water reservoir determines the impact of precipitation on phytoplankton; precipitation increases transparency in *taipas* but reduces it in ponds, thus limiting phytoplankton growth.

This study underscores the complexity of factors that influence the trophic state of various water bodies in productive basins. The identified associations reveal spatial patterns that respond to diverse productive activities and reservoir morphology and type. While our findings are for phytoplankton in general, they are consistent with Beaver et al. (2017), who reported that cyanobacterial blooms are distributed across ecoregions, with variability driven primarily by productive activities that define land-use intensity and reservoir characteristics. This study also explores key variables related to trophic state,

echoing Weber et al. (2020) on the predictive importance of water body size and land uses.

The results highlight a potential increase in eutrophication, aligning with global change projections indicating rising land use intensity and temperature (IPCC 2023; Gazzano et al. 2019). These trends, identified as drivers of cyanobacterial blooms even in low-risk environments (Kleinteich et al. 2024), pose health risks to water bodies and increase biomass export to treatment facilities such as AACC. Likewise, given the trend toward prolonged and recurrent water scarcity, an increase in the number of reservoirs supporting agricultural production is anticipated.

4.6 **Conclusions**

This study has identified various climatic, morphological, and land use factors that affect the phytoplankton biomass of water reservoirs used for productive purposes in the SLRB. It has also advanced our understanding of spatial patterns in the Chla distribution. High Chla concentrations are predominantly found in the southern and western regions, whereas lower concentrations are observed in the eastern part of the basin.

The influence of structural, environmental, and land use variables on the trophic state of reservoirs is not uniform. The relationship between trophic state and its regulating factors varies with spatial distribution. Specifically, ponds in the southern region are more sensitive to changes in accumulated precipitation and high temperatures. In contrast, in the turbid environments of the western region, land use intensity is the primary driver of phytoplankton growth.

4.7 **Supplementary material**

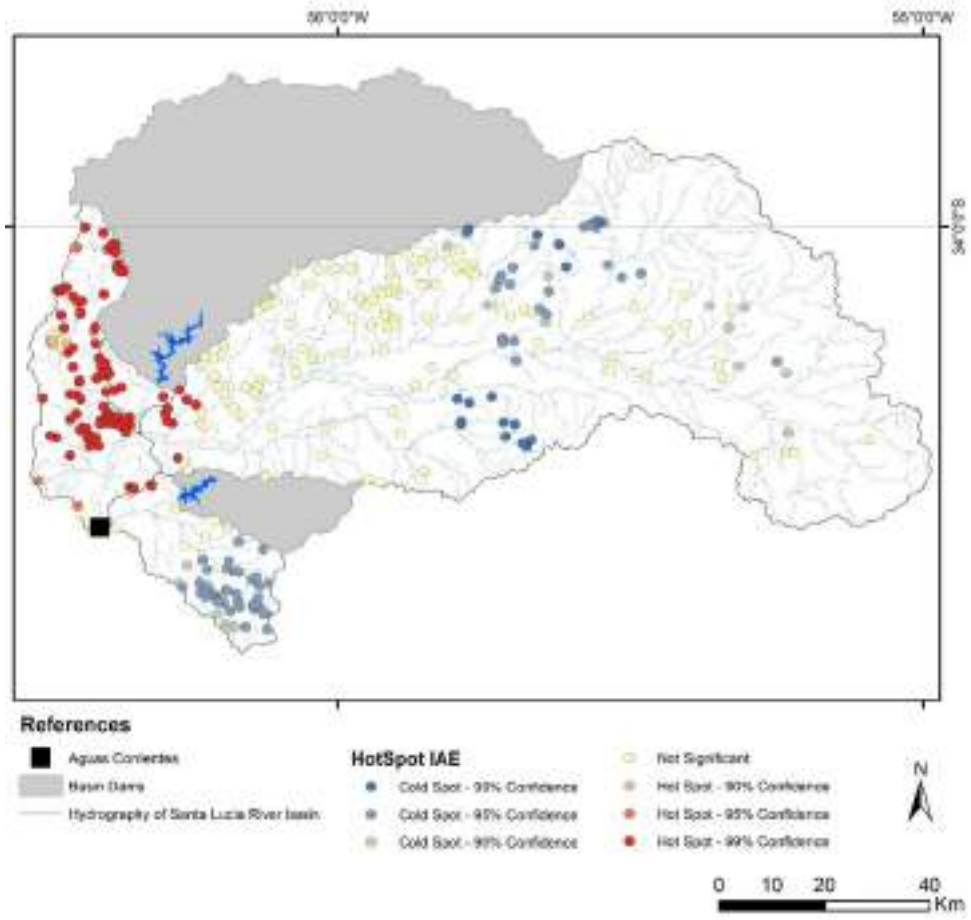

Annex 4.1 Spatial distribution obtained from the hotspot analysis based on IAE.

5. Capítulo 5

5.1 Discusión general

Esta tesis representa la primera experiencia a nivel nacional en que se diseña una estrategia para conocer el comportamiento óptico y el estado trófico de reservorios pequeños y medianos (0.25 - 30 ha). En particular se eligió como área de estudio a la SLRB debido a su importancia estratégica, ambiental y sanitaria, ya que drena directamente hacia AACC; la principal planta potabilizadora del país. La teledetección se utiliza a nivel internacional para complementar planes de monitoreo *in situ*, lo cual permite aumentar la escala espacial, temporal, disminuir los costos de monitoreo y elaborar series temporales (Seegers et al., 2021). En Uruguay, se destacan las investigaciones realizadas con teledetección en el Río de la Plata (Maciel et al., 2023; Zabaleta et al., 2023b;), en los embalses hidroeléctricos de Salto Grande (Drodz et al., 2014) y del Río Negro (Barreneche et al., 2023), y lagos urbanos profundos (Zabaleta et

al., 2021). Además, el Ministerio de Ambiente cuenta con una aproximación cualitativa al color del agua asociada a procesos de eutrofización y floraciones de fitoplancton https://observatorioan.users.earthengine.app/view/visualizador-floraciones-dinacea que se encuentra disponible para los principales cuerpos de agua del país. Dicha herramienta fue lograda mediante modelos entrenados a partir de detección visual de floraciones de fitoplancton en imágenes satelitales y bandas espectrales. Sin embargo, hasta el momento no se contaba con modelos de estimación satelital de la Chla y Tr, ajustados a las condiciones ópticas y con información *in situ* de los reservorios pequeños y medianos de la SLRB.

En Uruguay, se consolidó el uso de herramientas de teledetección en la década de 1990, a partir de ese entonces, han aumentado las capacidades conceptuales, operativas y técnicas para el procesamiento de imágenes satelitales que acompañan la evolución tecnológica de los sensores ópticos a bordo de plataformas satelitales. Esta tesis representa un avance en el proceso de evolución en la implementación de técnicas de teledetección en calidad del agua, ya que valida su aplicación en numerosos cuerpos de agua pequeños y turbios, que, hasta el momento se desconocía su estado trófico y su dinámica espaciotemporal.

Se logró ajustar un modelo que permite estimar con precisión la concentración de Chla en el rango 3 - 4439 µg L^{-1}, a partir de imágenes MSI/Sentinel-2. La relación de Rrs entre las bandas verde (560 nm) y roja (665 nm) presentó el mejor ajuste para estimar Chla. Cuando la relación Rrs (560 nm) - Rrs (665 nm) es positiva la Chla es < 20 µg L^{-1}, mientras que cuando es negativa la Chla es > 20 µg L^{-1} (Cap. 2). Este comportamiento dicotómico es prometedor como un indicador de sencilla interpretación que puede ser integrado a un sistema de monitoreo continuo y de alerta temprana (Chorus y Walker, 2021). Asimismo, la división en concentraciones elevadas o bajas de Chla podría usarse para evaluar la calidad del agua y su variación espacio temporal, así como Liu et al., (2024) utilizaron el color del agua.

El uso de bandas del espectro visible para estimar la Chla ofrece la posibilidad de utilizar imágenes satelitales que no cuentan con la banda del *borde rojo* y que conforman extensas bases de datos históricas como es el caso de la serie Landsat, aunque debido a su menor resolución espacial (30 m) podría aplicarse únicamente a los reservorios de mayor tamaño (Hu et al., 2022; Kayastha et al., 2022; Hu et al., 2021).

Las 8125 firmas espectrales obtenidas del monitoreo satelital realizado para los 325 reservorios en el período 2016-2022 se clasificaron en tres grupos, definidos principalmente por la relación Rrs (560 nm) - Rrs (665 nm) (Cap. 4). Los conjuntos de firmas espectrales son similares a las firmas espectrales de ambientes turbios y con elevada Chla clasificadas por Neil et al., (2019) a partir de una extensa base de datos de diversos ecosistemas acuáticos lénticos. También se asemejan a las reportadas por Spyrakos et al., (2018) donde los ambientes turbios se distinguen por el aumento progresivo de la Rrs hacía los infrarrojos cercanos y la actividad fotosintética determina un mínimo de Rrs ~ 665 nm. Cabe destacar la falta de una evaluación de la posible influencia del CDOM en las estimaciones satelitales de Chla (Maciel et al., 2023), lo cual representa una línea para la continuidad de esta investigación. Además, el CDOM podría explicar la falta de desarrollo de fitoplancton en ambientes con elevada Tr, ya que su concentración elevada podría actuar como un filtro de la radiación solar y determinar una menor captación lumínica destinada a la productividad primaria (Spyrakos et al., 2018). En comparación con los antecedentes mencionados, los reservorios de la SLRB son más pequeños y presentan una mayor magnitud de Rrs provocada por la alta turbidez. Los comportamientos espectrales identificados son un avance en la clasificación óptica de los reservorios y representan una aproximación a su estado trófico, de la cual se desprenden numerosas potencialidades, entre ellas la posibilidad de generar categorías ópticas que permitan determinar el estado trófico mediante un indicador de simple interpretación (Eleved et al., 2017).

La mayoría de los 325 reservorios son hipereutróficos, según los muestreos realizados in situ y mediante imágenes satelitales. El fenómeno se intensifica en los de menor tamaño y es esperable según lo reportado por Brainwood et al., (2004), quienes registraron mayores concentraciones de nutrientes y de Chla en los ambientes más pequeños ubicados en cuencas de uso agropecuario intensivo. Las zonas sur y oeste fueron identificadas como las de mayor riesgo de transporte de biomasa hacía AACC, principalmente debido a los conjuntos de reservorios con concentraciones elevadas de Chla (Cap. 3). Si bien entre 2016 y 2022 solamente en quince días las cianobacterias superaron la mitad del primer nivel de alerta (1000 cel/ml) en AACC, su ocurrencia puede generar grandes impactos sobre la calidad del agua de abastecimiento público y aumentar los costos de potabilización (Dunlap et al., 2019). La zona oeste se caracteriza por presentar la mayor carga ganadera lechera de la SLRB y por las altas superficies destinadas a cultivos de

secano, dichos usos han sido reportados como las principales fuentes difusas de nutrientes en la SLRB (Chalar et al., 2017; Goyenola et al., 2015). Mientras que en la zona sur los conjuntos de reservorios con elevada Chla corresponden a estanques utilizados para riego en establecimientos frutícolas, hortícolas y vitivinícolas, que se caracterizan por su alta Tr. Esta alta Tr puede deberse a que la mezcla vertical depende únicamente del viento, a diferencia de los ambientes donde ingresa ganado que generan una constante resuspensión de sedimentos.

Las concentraciones elevadas de Chla no ocurrieron siempre en las zonas de mayor intensidad de uso agrícola, pero sí se identificaron patrones de distribución espacial de la Chla. Principalmente se destacan los reservorios del sur, donde se detectó un punto caliente que se sostiene estacionalmente e interanualmente, y, sin embargo, presentó menor intensidad de uso del suelo (Cap. 4). Estos resultados coinciden con lo propuesto por Beaver et al., (2014) quienes sugieren que la luz podría limitar la Chla aún en ambientes con alta concentración de nutrientes. Por otro lado, se destacan los reservorios más grandes como potenciales fuentes de inóculo, que, por su cantidad limitada, resulta más accesible planificar su manejo y realizar el seguimiento de la calidad del agua mediante el uso de indicadores satelitales o instrumentos de medición instalados in situ como ser boyas, sensores ópticos, reportes ciudadanos, entre otros.

El noreste de la cuenca presentó el menor riesgo de exportación de biomasa (Cap. 3), esto podría deberse a la menor disponibilidad de nutrientes en los reservorios producida por los suelos de menor productividad y la ganadería extensiva; reconocida por su bajo aporte de nutrientes a los cuerpos de agua (Chalar et al., 2017). En comparación con los cultivos de secano y las pasturas forrajeras, los pastizales son poco fertilizados, disminuyen el escurrimiento superficial y con ello el aporte de materiales particulados provenientes de la pérdida de suelo (Barreto et al., 2017: Lescano et al., 2017). La ganadería extensiva no requiere de períodos sin cobertura vegetal, como en el caso de cultivos, tanto bajo práctica de siembra directa, como de siembra convencional, lo que favorece los procesos de erosión de suelos y con ello el aporte de nutrientes (García et al., 2018). Además, en muchos casos coexiste con la conservación de las zonas riparias y humedales, lo cual disminuye la carga de nutrientes en el agua de escorrentía superficial (Calvo et al., 2024). Asimismo, en esta zona los reservorios son utilizados como abrevadero de ganado que, si bien aporta nutrientes mantiene constantemente una condición turbia que disminuye el ingreso de luz a la columna de agua y la productividad primaria.

Los resultados obtenidos son consistentes con la propuesta de construir una represa de agua para potabilización en la subcuenca del Arroyo Casupá (Presidencia, 2016). Dicha represa se ubicaría al noreste de la SLRB, donde si bien predominan usos del suelo de menor intensidad que en la cuenca de la represa de Paso Severino, se han identificado tendencias crecientes de forestación según el Plan de Cuenca del Río Santa Lucía (2023). Dicho plan define medidas de restauración, como la exclusión de ganado para evitar que abreve directamente en el cuerpo de agua y lo enriquezca con nutrientes, para ello, se deben utilizar tomas indirectas con bombeo. También promueve la conservación de las zonas riparias con la finalidad de reducir la carga de nutrientes en el agua de escorrentía superficial. Se destaca que en la zona noreste los reservorios no son tan abundantes, lo cual simplifica la implementación de prácticas para reducir el desarrollo de floraciones de cianobacterias y su potencial transporte hacía una represa ubicada aguas abajo.

El estado trófico se relaciona con el diseño de construcción de los reservorios y con su ubicación, esto se evidenció en los patrones de distribución espacial detectados mediante la magnitud de correlación de la Chla y la Tr con las precipitaciones y la temperatura. En particular, la Chla se correlacionó con la Tmed de forma negativa en el oeste (*taipas*) y positiva en el sur (estanques), la principal diferencia entre ambas zonas es el diseño de los reservorios (Cap. 4). El diseño somero de las *taipas* podría generar que las elevadas Tmed aumenten la turbidez e inhiban el desarrollo de fitoplancton, lo cual es consistente con lo reportado por Beaver et al., (2017). En los estanques, el mayor tiempo de residencia y el aumento de temperatura podrían favorecer el crecimiento del fitoplancton, consistentemente con algunos antecedentes bibliográficos (Paerl et al., 2016; Reynolds, 2006).

En algunos reservorios el estado trófico es regulado por variables climáticas, mientras que en otros ambientes con características similares no se relacionan entre sí (Cap. 4), lo cual es esperable según Liu et al., (2024), quienes llegaron a dicha conclusión tras detectar diferencias entre el color del agua y las variables climáticas de numerosos cuerpos de agua pequeños. En esta tesis se alcanzaron resultados similares; las precipitaciones se correlacionaron de forma inversa con la Chla de acuerdo a su ubicación. En el sur la relación fue negativa, mientras que en el centro y este de la cuenca las correlaciones fueron positivas, donde los predios de ganadería extensiva presentan microcuencas grandes y las precipitaciones podrían favorecer la exportación de nutrientes en pulsos mediante el escurrimiento superficial (Díaz et al., 2021; Sinha et al., 2017; Goyenola et

al., 2015). Mientras que, en los estanques las precipitaciones se encuentran inversamente relacionadas con la Chla lo cual también es apoyado por antecedentes bibliográficos (Havens et al., 2017; Brasil et al., 2016). El contraste en las relaciones identificadas evidencia las diferencias en los vínculos con las variables ambientales que presentan distintos tipos de cuerpos de agua y los desafíos que implica evaluarlos en profundidad.

Las principales variables predictivas del desarrollo de fitoplancton son el tamaño de los reservorios y la IAE (Índice de intensidad de uso del suelo, Díaz et al., 2018) (Cap. 4). Los resultados obtenidos del análisis CART son consistentes con lo reportado por Weber et al., (2020) quienes, tras monitorear satelitalmente numerosos cuerpos de agua, identificaron al tamaño del reservorio seguido en menor medida por el porcentaje de agricultura como las principales variables predictivas. Cabe destacar que la IAE formó un conjunto de microcuencas con baja intensidad de uso en la zona sur, sin embargo, fue un punto caliente recurrente de Chla en los análisis realizados. Este resultado podría evidenciar el impacto del riego sobre el aporte constante de nutrientes a los reservorios del sur (Darré et al., 2019). El manejo de los predios también podría determinar pulsos de nutrientes generados por fertilización, cosechas, rotaciones, quemas, así como también aportes de agroquímicos como pesticidas, fungicidas, herbicidas, etc., para futuros trabajos se debe integrar información de productividad vegetal mediante indicadores satelitales y consultas a los productores.

La degradación de los suelos genera la exportación de materiales particulados, con el consecuente aumento en la concentración de nutrientes y de sólidos en suspensión de los cuerpos de agua (Issaka y Ashraf, 2017). La variación en la calidad del suelo también ha sido identificada como una de las variables relacionadas con el color del agua de pequeños cuerpos de agua continentales (Liu et al., 2024). Sin embargo, de acuerdo a la revisión bibliográfica, en Uruguay aún no se ha realizado un mapeo del estado de conservación de los suelos que permita analizar la información a escala apropiada de las microcuencas de los reservorios e incluirla como otra variable explicativa del estado trófico. Además, no se cuenta con información sobre la fecha de construcción de los reservorios; o aspectos técnicos para conocer su profundidad y volumen. Asimismo, se destaca la carencia de información sobre el manejo u obras de mantenimiento para mitigar fenómenos como la erosión de los vertederos de máximas, eventos de desmoronamiento de la *taipa*, obstrucción de vertederos de mínimas, colmatación, entre otros (García et al., 2008), que

podrían brindar elementos para determinar el origen de inóculos de cianobacterias que alcanzan AACC.

5.2 Conclusiones finales

Esta tesis mostró que es posible conocer el estado trófico en numerosos reservorios de agua pequeños mediante imágenes satelitales gratuitas; se ajustaron con éxito modelos para la estimación satelital de la Chla y la Tr. Representa la primera experiencia a nivel nacional con estas características, mientras que, en el contexto de estudios similares a nivel internacional, se destaca por el pequeño tamaño de los ambientes y su elevada turbidez. Lo cual puede introducir sesgos relacionados a efectos ópticos de la interfaz tierra-agua, por lo tanto, en futuras investigaciones se deberían delimitar las superficies cubiertas de agua en cada fecha que se pretenda monitorear.

Se identificaron dos grandes conjuntos de reservorios que se diferencian por la concentración de Chla, la división se observó en los muestreos in situ y también en las firmas espectrales. Se detectaron patrones espaciales en su distribución, lo cual aporta información indispensable en planes de gestión ajustados a las condiciones territoriales de la SLRB, así como también en monitoreos que tengan la finalidad de focalizar esfuerzos de mitigación de los procesos de eutrofización para reducir el impacto sobre la calidad del agua de AACC. En general, los reservorios presentaron elevada concentración de Chla, con mayor recurrencia en las zonas sur y oeste que representan el mayor riesgo de exportación de biomasa debido a su cercanía con AACC.

El estado trófico de los reservorios varía de forma compleja y es regulado en distinta medida por numerosas variables, sin embargo, se logró detectar relaciones que varían de acuerdo a la ubicación y diseño de construcción de los reservorios. En particular, el tamaño de los cuerpos de agua, la intensidad en los usos del suelo de las microcuencas, la temperatura y las precipitaciones fueron las variables de mayor importancia para el desarrollo fitoplanctónico.

Los resultados obtenidos aportan una herramienta operativa y de bajo costo, que brinda insumos para el cumplimiento de las medidas orientadas a la protección de la calidad del agua en la principal cuenca de producción de agua potable del país; propuestas en el Plan de Acción para la Protección del Agua en la Cuenca del Santa Lucía (2020). Asimismo,

la información generada, en especial la identificación de patrones espaciales en las concentraciones de la Chla aporta al diseño de planes de gestión de los reservorios ajustados a las condiciones territoriales.

6. Bibliografía

Achkar M. (2002). Hacia la gestión sustentable del agua. Programa: Uruguay sustentable. Laboratorio de desarrollo sustentable y gestión ambiental del territorio. Departamento de Geografía. Facultad de Ciencias. Universidad de la República, 7 p.

Achkar, M., Díaz, I., Sosa, B., Da Costa, E., & Chiale, C. (2016). Producto 3 Inventario para la Cuenca del río Santa Lucía. Proyecto. Inventario Nacional de Humedales. Acuerdo DINAMA-LDSGA Instituto de Ecología y Ciencias Ambientales Facultad de Ciencias UdelaR.

Achkar, M., Domínguez, A., & Pesce, F. (2012). Cuenca del Río Santa Lucía-Uruguay. Aportes para la discusión ciudadana. Facultad de Ciencias-UdelaR, REDES-AT, Programa Uruguay Sustentable.

Aguilera A., Aubriot L., Echenique R., Salerno G., Brena B., Pírez M. y Bonilla S. (2017). Synergistic effects of nutrients and light favor Nostocales over non-heterocystous cyanobacteria. Hydrobiologia, 794:241-255.

Almuhtaram, H., Kibuye, F., Ajjampur, S., Glover, C., Hofmann, R., Gaget, V., Owen, C., Wert, E. & Zamyadi, A. (2021). State of knowledge on early warning tools for cyanobacteria detection. Ecological Indicators, 133, 108442.

Amorín, C. & Larghero, S. (2017). Informe de situación de las medidas que se están implementando para el aseguramiento de la potabilización del agua del sistema de abastecimiento de Montevideo y Laguna del Sauce. URSEA, Montevideo, Uruguay.

Ansper, A. (2018). Sentinel-2/msi applications for european union water framework directive reporting purposes (Doctoral dissertation, Faculty of Science and Technology, University of Tartu).

APHA (2005) Standard methods for the examination of wáter and wastewater, American Public Health Association, APHA/AWWA/WPCF, Washington.

Aubriot, L., & Bonilla, S. (2018). Regulation of phosphate uptake reveals cyanobacterial bloom resilience to shifting N: P ratios. Freshwater biology, 63(3), 318-329.

Aubriot, L., Delbene, L., Haakonsson, S., Somma, A., Hirsch, F., & Bonilla, S. (2017). Evolución de la eutrofización en el Río Santa Lucía: influencia de la intensificación productiva y perspectivas. Innotec, (14): 07-16. https://doi.org/10.26461/14.04https://doi.org/10.26461/14.04

Aubriot, L., Zabaleta, B., Bordet, F., Sienra, D., Risso, J., Achkar, M., & Somma, A. (2020). Assessing the origin of a massive cyanobacterial bloom in the Río de la Plata (2019): Towards an early warning system. Water Research, 115944.

https://doi.org/10.1016/j.watres.2020.115944https://doi.org/10.1016/j.watres.2020.115944

Augusto-Silva, P. B., Ogashawara, I., Barbosa, C. C., De Carvalho, L. A., Jorge, D. S., Fornari, C. I., & Stech, J. L. (2014). Analysis of MERIS reflectance algorithms for estimating chlorophyll-a concentration in a Brazilian reservoir. Remote Sensing, 6(12), 11689-11707.

Avdan, Z., Kaplan, G., Goncu, S., & Avdan, U. (2019). Monitoring the water quality of small water bodies using high-resolution remote sensing data. ISPRS International Journal of Geo-Information, 8(12), 553.

Baldwin, D. S., Wilson, J., Gigney, H., & Boulding, A. (2010). Influence of extreme drawdown on water quality downstream of a large water storage reservoir. River research and Applications, 26(2), 194-206.

Barreneche, J. M., Guigou, B., Gallego, F., Barbieri, A., Smith, B., Fernández, M., ... & Pahlevan, N. (2023). Monitoring Uruguay's freshwaters from space: An assessment of different satellite image processing schemes for chlorophyll-a estimation. Remote Sensing Applications: Society and Environment, 29, 100891.

Barreto, P., Dogliotti, S., & Perdomo, C. (2017). Surface water quality of intensive farming areas within the Santa Lucia River basin of Uruguay. Air, Soil and Water Research, 10, 1178622117715446.

Beaver, J., Manis, E., Loftin, K., Graham, J., Pollard, A., & Mitchell, M. (2014). Land use patterns, ecoregion, and microcystin relationships in US lakes and reservoirs: a preliminary evaluation. Harmful Algae, 36, 57-62. https://doi.org/10.1016/j.hal.2014.03.005https://doi.org/10.1016/j.hal.2014.03.005

Beaver, J., Scotese, K., Minerovic, A., Buccier, K., Tausz, C. & Clapham, W. (2012). Land use patterns, ecoregion and phytoplankton relationships in productive Ohio reservoirs. Inland Waters, 2(2), 101-108. https://doi.org/10.5268/IW-2.2.481https://doi.org/10.5268/IW-2.2.481

Beck, R., Zhan, S., Liu, H., Tong, S., Yang, B., Xu, M., ... & Su, H. (2016). Comparison of satellite reflectance algorithms for estimating chlorophyll-a in a temperate reservoir using coincident hyperspectral aircraft imagery and dense coincident surface observations. Remote Sensing of Environment, 178, 15-30.

Berbery, E. H., & Barros, V. R. (2002). The hydrologic cycle of the La Plata basin in South America. Journal of Hydrometeorology, 3(6), 630-645.Bresciani, M., Giardino, C., Stroppiana, D., Dessena, M. A., Buscarinu, P., Cabras, L., Schenk, K., Heege, T., Bernet, H., Bazdanis, G. & Tzimas, A. (2019). Monitoring water quality in two dammed reservoirs from multispectral satellite data. European Journal of Remote Sensing, 52(sup4), 113-122.

Bonilla, S., Aguilera, A., Aubriot, L., Huszar, V., Almanza, V., Haakonsson, S., ... & Antoniades, D. (2023). Nutrients and not temperature are the key drivers for cyanobacterial biomass in the Americas. Harmful Algae, 121, 102367. https://doi.org/10.1016/j.hal.2022.102367

Bonilla, S., Conde, D., Aubriot, L., Rodríguez-Gallego, L., Piccini, C., Meerhoff, E., ... & Britos, A. (2006). Procesos estructuradores de las comunidades biológicas en lagunas costeras de Uruguay. Bases para la conservación y el manejo de la costa uruguaya, 611-630.

Bonilla, S., Haakonsson, S., Somma, A., Gravier, A., Britos, A., Vidal, L., ... & de la Escalera, G. M. (2015). Cianobacterias y cianotoxinas en ecosistemas límnicos de Uruguay. Innotec, (10 ene-dic), 9-22.

Bordet, F., Fontanarrosa, M. S., & O'farrell, I. (2017). Influence of light and mixing regime on bloom-forming phytoplankton in a subtropical reservoir. River Research and Applications, 33(8), 1315-1326.

Botha, E., Anstee, J., Sagar, S., Lehmann, E. & Medeiros, T. (2020). Classification of Australian waterbodies across a wide range of optical water types. Remote Sensing, 12(18), 3018. https://doi.org/10.3390/rs12183018https://doi.org/10.3390/rs12183018

Bowling, L., Merrick, C., Swann, J., Green, D., Smith, G., & Neilan, B. (2013). Effects of hydrology and river management on the distribution, abundance and persistence of cyanobacterial blooms in the Murray River, Australia. Harmful algae, 30, 27-36.

Brainwood, M. A., Burgin, S., & Maheshwari, B. (2004). Temporal variations in water quality of farm dams: impacts of land use and water sources. Agricultural Water Management, 70(2), 151-175.

Brando, V., & Dekker, A. (2003). Satellite hyperspectral remote sensing for estimating estuarine and coastal water quality. IEEE transactions on geoscience and remote sensing, 41(6), 1378-1387. https://doi.org/10.1109/TGRS.2003.812907https://doi.org/10.1109/TGRS.2003.812907

Brasil, J., Attayde, J., Vasconcelos, F., Dantas, D., & Huszar, V. (2016). Drought-induced water-level reduction favors cyanobacteria blooms in tropical shallow lakes. Hydrobiologia, 770, 145-164. https://doi.org/10.1007/s10750-015-2578-5

Breiman, L., Friedman, J., Olshen, R., & Stone, C. (1984). Classification and regression trees–crc press. Boca Raton, Florida.

Brena, B. M., Font, E., Pírez Schirmer, M., Badagian, N., Cardozo, E., Pérez Parada, A., & Bonilla, S. (2021). Microcystin ELISA in water and animal serum for an integrated environmental monitoring strategy. International Journal of Environmental Analytical Chemistry, 103(8), 1711–1723. https://doi.org/10.1080/03067319.2021.1881073https://doi.org/10.1080/03067319.2021.1881073

Bresciani, M., Giardino, C., Stroppiana, D., Dessena, M. A., Buscarinu, P., Cabras, L., Schenk, K., Heege, T., Bernet, H., Bazdanis, G. & Tzimas, A. (2019). Monitoring water quality in two dammed reservoirs from multispectral satellite data. European Journal of Remote Sensing, 52(sup4), 113-122.

Burford, M., & O'Donohue, M. (2006). A comparison of phytoplankton community assemblages in artificially and naturally mixed subtropical water reservoirs. Freshwater Biology, 51(5), 973-982. https://doi.org/10.1111/j.1365-2427.2006.01536.xhttps://doi.org/10.1111/j.1365-2427.2006.01536.x

Burford, M., Carey, C., Hamilton, D., Huisman, J., Paerl, H., Wood, S., & Wulff, A. (2020). Perspective: Advancing the research agenda for improving understanding of cyanobacteria in a future of global change. Harmful Algae, 91, 101601.

Caldwell, T., Chandra, S., Albright, T., Harpold, A., Dilts, T., Greenberg, J., ... & Dettinger, M. (2021). Drivers and projections of ice phenology in mountain lakes in the western United States. Limnology and Oceanography, 66(3), 995-1008. https://doi.org/10.1002/lno.11656

Calvo, C., Rodríguez-Gallego, L., de León, G., Cabrera-Lamanna, L., Castagna, A., Costa, S., ... & Meerhoff, M. (2024). Potential of different buffer zones as nature-based solutions to mitigate agricultural runoff nutrients in the subtropics. Ecological Engineering, 207, 107354.

Carmichael, W. (2001). Health effects of toxin-producing cyanobacteria:"The CyanoHABs". Human and ecological risk assessment: An International Journal, 7(5), 1393-1407.

Carpenter, S. R., Stanley, E. H., & Vander Zanden, M. J. (2011). State of the world's freshwater ecosystems: physical, chemical, and biological changes. Annual review of Environment and Resources, 36(1), 75-99.

Carpenter, S., Caraco, N., Correll, D., Howarth, R., Sharpley, A., & Smith, V. (1998). Nonpoint pollution of surface waters with phosphorus and nitrogen. Ecological applications, 8(3), 559-568.

Castagna, A., & García, F. (2020). Análisis de los cambios en el uso de la tierra en el país entre 2000 y 2017 a partir de una serie temporal de relevamientos remotos. Estudios de Economía Agraria y Ambiental, (20-01).

Caussi M. (2018). Estudio del estado trófico de la Laguna del Sauce mediante estimación de profundidad de Secchi y clorofila utilizando imágenes de Landsat 8. Tesis de grado, Universidad Católica del Uruguay.

Chalar, G., Arocena, R., Pacheco, J., & Fabián, D. (2011). Trophic assessment of streams in Uruguay: a trophic State Index for Benthic Invertebrates (TSI-BI). Ecological Indicators, 11(2), 362-369. https://doi.org/10.1016/j.ecolind.2010.06.004

Chalar, G., Garcia-Pesenti, P., Silva-Pablo, M., Perdomo, C., Olivero, V., & Arocena, R. (2017). Weighting the impacts to stream water quality in small basins devoted to forage crops, dairy and beef cow production. Limnologica, 65, 76-84. https://doi.org/10.1016/j.limno.2017.06.002https://doi.org/10.1016/j.limno.2017.06.002

Chapin III, F., Matson, P., & Vitousek, P. (2011). Principles of terrestrial ecosystem ecology. Springer Science & Business Media.

Chorus, I., & Welker, M. (2021). Toxic cyanobacteria in water: a guide to their public health consequences, monitoring and management (p. 858). Taylor & Francis.

Chuvieco E. (2002). Teledetección ambiental. La observación de la Tierra desde el Espacio.

Clark, J., Schaeffer, B., Darling, J., Urquhart, E., Johnston, J., Ignatius, A., Myer, M., Loftin, K., Werdell, J. & Stumpf, R. (2017). Satellite monitoring of cyanobacterial harmful algal

bloom frequency in recreational waters and drinking water sources. Ecological indicators, 80, 84-95.

Coffer, M., Schaeffer, B., Salls, W., Urquhart, E., Loftin, K., Stumpf, R., ... & Darling, J. (2021). Satellite remote sensing to assess cyanobacterial bloom frequency across the United States at multiple spatial scales. Ecological Indicators, 128, 107822. https://doi.org/10.1016/j.ecolind.2021.107822

Conde, D., Arocena, R. & Rodríguez-Gallego, L. (2002). Recursos acuáticos superficiales de Uruguay: ambientes algunas problemáticas y desafíos para la gestión (I y II). Ambios, 3(10), 5-9.

Conley, D., Paerl, H., Howarth, R., Boesch, D., Seitzinger, S., Havens, K., ... & Likens, G. (2009). Controlling eutrophication: nitrogen and phosphorus. Science, 323(5917), 1014-1015.

Cook, K. V., Beyer, J. E., Xiao, X., & Hambright, K. D. (2023). Ground-based remote sensing provides alternative to satellites for monitoring cyanobacteria in small lakes. Water Research, 242, 120076.

Copado-Rivera, A. G., Bello-Pineda, J., Aké-Castillo, J. A., & Arceo, P. (2020). Spatial modeling to detect potential incidence zones of harmful algae blooms in Veracruz, Mexico. Estuarine, Coastal and Shelf Science, 243, 106908.

Cremella, B., Huot, Y., & Bonilla, S. (2018). Interpretation of total phytoplankton and cyanobacteria fluorescence from cross-calibrated fluorometers, including sensitivity to turbidity and colored dissolved organic matter. Limnology and Oceanography: Methods, 16(12), 881-894.

Crisci, C., Goyenola, G., Terra, R., Lagomarsino, J. J., Pacheco, J. P., Díaz, I., ... & Mazzeo, N. (2017). Dinámica ecosistémica y calidad de agua: estrategias de monitoreo para la gestión de servicios asociados a Laguna del Sauce (Maldonado, Uruguay). Innotec, (13 ene-jun), 46-57.

Cunha, D., do Carmo Calijuri, M., & Lamparelli, M. (2013). A trophic state index for tropical/subtropical reservoirs (TSItsr). Ecological Engineering, 60, 126-134.

Darré, E., Cadenazzi, M., Mazzilli, S., Rosas, J. & Picasso, V. (2019). Environmental impacts on water resources from summer crops in rainfed and irrigated systems. Journal of environmental management, 232, 514-522. https://doi.org/10.1016/j.jenvman.2018.11.090https://doi.org/10.1016/j.jenvman.2018.11.090

Díaz, I. (2013). Modelación de los aportes de nitrógeno y fósforo en cuencas hidrográficas del departamento de Canelones (Uruguay). Tesis de maestría, Universidad de la República (Uruguay), Facultad de Ciencias.

Díaz, I., Ceroni Acosta, M. B., López Orrego, G., & Achkar, M. (2018). Análisis espacio-temporal de la intensificación agraria y su incidencia en la productividad primaria neta: propuesta metodológica para Uruguay 2000-2011. Revista Electrónica de Medio Ambiente, 2018, 19 (1), 24-40.

Díaz, I., Levrini, P., Achkar, M., Crisci, C., Fernández Nion, C., Goyenola, G. and Mazzeo, N. (2021). Empirical modeling of stream nutrients for countries without robust water quality monitoring systems. Environments 8(11), 129.

DIEA (2023). Serie "Precio de la tierra" Compraventas Año 2022. https://www.gub.uy/ministerio-ganaderia-agricultura-pesca/sites/ministerio-ganaderia-agricultura-pesca/files/2023-05/DIEA-COMPRAVENTAS-A%C3%91O-2022_Definitivo.pdf

Dodds, W., Bouska, W., Eitzmann, J., Pilger, T., Pitts, K., Riley, A., ... & Thornbrugh, D. (2009). Eutrophication of US freshwaters: analysis of potential economic damages.

Donat, M., Lowry, A., Alexander, L., O'Gorman, P. & Maher, N. (2016). More extreme precipitation in the world's dry and wet regions. Nature Climate Change 6, 508. https://doi.org/10.1038/nclimate2941https://doi.org/10.1038/nclimate2941.

Dörnhöfer K., Klinger P., Heege T. y Oppelt N. (2018). Multi-sensor satellite and in situ monitoring of phytoplankton development in a eutrophic-mesotrophic lake. Science of The Total Environment, 612:1200-1214.

Drozd, A. A., Ibáñez, G., Bordet, F., & Torrusio, S. E. (2014). Remote Sensing of chlorophyll in Salto Grande waters using hyperspectral resolution spectrometer, SPOT-4 (HRVIR) and Landsat-7 ETM+ data. In Congreso Internacional de Hidrología de Llanuras (Vol. 1, pp. 1-10).

Drozd, A., de Tezanos Pinto, P., Fernandez, V., Bazzalo, M., Bordet, F., & Ibañez, G. (2019). Hyperspectral remote sensing monitoring of cyanobacteria blooms in a large South American reservoir: high-and medium-spatial resolution satellite algorithm simulation. Marine and Freshwater Research, 71(5), 593-605.

Dunlap, C., Sklenar, K. & Blake, L. (2015). A costly endeavor: addressing algae problems in a water supply. Journal-American Water Works Association, 107(5), E255-E262.

Dzialowski, A.R., Smith, V.H., Wang, S.-H., Martin, M.C. and Jr, F.d. 2011. Effects of non-algal turbidity on cyanobacterial biomass in seven turbid Kansas reservoirs. Lake Reservoir Manag. 27(1), 6-14. https://doi.org/10.1080/07438141.2011.551027https://doi.org/10.1080/07438141.2011.551027.

Eleveld, M. A., Ruescas, A. B., Hommersom, A., Moore, T. S., Peters, S. W., & Brockmann, C. (2017). An optical classification tool for global lake waters. Remote Sensing, 9(5), 420.

Ernst, O., & Siri-Prieto, G. (2011). La agricultura en Uruguay: Su trayectoria y consecuencias. In Proceedings of the II Simposio Nacional de Agricultura, Paysandú, Uruguay (pp. 29-30).

Fletcher, K. (2012). Sentinel-2: ESA's optical high-resolution misión for GMES Operational Services (European Spatial Agency SP-1322/2) ISBN 978-92-9221-419-7.

Gallegos C. y Neale P. (2015). Long-term variations in primary production in a eutrophic sub-estuary: contribution of short-term events. Estuarine, Coastal and Shelf Science, 162: 22-34.

García Petillo, M., Cánepa, P., & Ronzoni, C. (2008). Manual para el diseño y la construcción de tajamares de aguada. Proyecto producción responsable.

García, P., Badano, N., Menéndez, A., Bert, F., García, G., Podesta, G., Rovere, S., Verdin, A., Rajagoplan, B. & Arora, P (2018). Influencia de los cambios en el uso del suelo y la precipitación sobre la dinámica hídrica de una cuenca de llanura extensa. Caso de estudio: Cuenca del Río Salado, Buenos Aires, Argentina. Ribagua, 5(2), p. 92-106. https://doi.org/10.1080/23863781.2018.1495990.

García, C., Catalini, C. & García, C. (2019). Empleo de nuevas metodologías en el monitoreo y zonificación de los cuerpos de agua en Argentina. Calidad del Agua en las Américas, 54.

Gazzano, I., Achkar, M., & Díaz, I. (2019). Agricultural Transformations in the Southern Cone of Latin America: Agricultural Intensification and Decrease of the Aboveground Net Primary Production, Uruguay's Case. Sustainability, 11(24), 7011. https://doi.org/10.3390/su11247011https://doi.org/10.3390/su11247011

Getis, A., & Ord, J. (2010). The analysis of spatial association by use of distance statistics. Perspectives on spatial data analysis. Springer, Berlin, pp 127–145. https://doi.org/10.1007/978-3-642-01976-0_10https://doi.org/10.1007/978-3-642-01976-0_10

Giardino, C., Brando, V., Gege, P., Pinnel, N., Hochberg, E., Knaeps, E., Reusen, I., Doerffer, R., Bresciani, M., Braga, F., Foerster, S., Champollion, N. & Dekker, A. (2019). Imaging spectrometry of inland and coastal waters: state of the art, achievements and perspectives. Surveys in Geophysics, 40, 401-429.

Gitelson A., Nikanorov A., Sabo G. y Szilagyi F. (1986). Etude de la qualite des eaux de surface parteledetection. IAHS Publications, 157:111-121.

Gitelson, A. (1992). The peak near 700 nm on radiance spectra of algae and water: relationships of its magnitude and position with chlorophyll concentration. International Journal of Remote Sensing, 13(17), 3367-3373. https://doi.org/10.1080/01431169208904125https://doi.org/10.1080/01431169208904125

Gitelson, A., Garbuzov, G., Szilagyi, F., Mittenzwey, K., Karnieli, A., & Kaiser, A. (1993). Quantitative remote sensing methods for real-time monitoring of inland waters quality. International Journal of Remote Sensing, 14(7), 1269-1295. https://doi.org/10.1080/01431169308953956https://doi.org/10.1080/01431169308953956

Gons H. (1999). Optical teledetection of chlorophyll a in turbid inland waters. Environmental Science & Technology, 33 (7):1127-1132.

González-Madina, L., Levrini, P., de Tezanos Pinto, P., Burwood, M., Crisci, C., Cardozo, A., Lagomarsino, J., Pacheco, J., Fosalba, C., Méndez, G., Garrido, L. & Mazzeo, N. (2022). Blooms of toxic Raphidiopsis raciborskii in Laguna del Sauce (Uruguay): environmental drivers and impacts. Hydrobiologia, 1-18.

Gordon H., Clark D., Mueller J. y Hovis W. (1980). Phytoplankton pigments from the Nimbus-7 Coastal Zone Color Scanner: comparisons with surface measurements. Science, 210 (4465):63-6.

Gorgoglione, A., Gregorio, J., Rios, A., Alonso, J., Chreties, C., & Fossati, M. (2020). Influence of land use/land cover on surface-water quality of Santa Lucìa river, Uruguay. Sustainability, 12(11), 4692. https://doi.org/10.3390/su12114692

Goyenola, G., Meerhoff, M., Teixeira-de Mello, F., González-Bergonzoni, I., Graeber, D., Fosalba, C., ... & Kronvang, B. (2015). Monitoring strategies of stream phosphorus under contrasting climate-driven flow regimes. Hydrology and Earth System Sciences, 19(10), 4099-4111. https://doi.org/10.5194/hess-19-4099-2015https://doi.org/10.5194/hess-19-4099-2015

Grabowska, M., & Mazur-Marzec, H. (2011). The effect of cyanobacterial blooms in the Siemianówka Dam Reservoir on the phytoplankton structure in the Narew River. Oceanological and Hydrobiological Studies, 40, 19-26. https://doi.org/10.2478/s13545-011-0003-xhttps://doi.org/10.2478/s13545-011-0003-x

Grill, G., Lehner, B., Thieme, M., Geenen, B., Tickner, D., Antonelli, F., Babu, S., Borelli, P., Cheng, L., Crochetiere, H., Macedo, E., Filgueiras, R., Goichot, M., Higgins, J., Hogan, Z., Lip, B., McClain, E., Meng, J., Mulligan, M., Nilsson, C., Olden, J., Opperman, J., Petry, P., Liermann, R., Saens, L., Salinas-Rodriguez, S., Schelle, P., Schmitt, R., Snider, J., Tan, F., Tockner, K., Valdujo, P., van Soesbergen, A. & Zarfl, C. (2019). Mapping the world's free-flowing rivers. Nature, 569(7755), 215-221. https://doi.org/10.1038/s41586-019-1111-9https://doi.org/10.1038/s41586-019-1111-9

Ha, N., Thao, N., Koike, K., & Nhuan, M. (2017). Selecting the best band ratio to estimate chlorophyll-a concentration in a tropical freshwater lake using sentinel 2A images from a case study of Lake Ba Be (Northern Vietnam). ISPRS International Journal of Geo-Information, 6(9), 290.

Haakonsson, S., Rodríguez-Gallego, L., Somma, A., & Bonilla, S. (2017). Temperature and precipitation shape the distribution of harmful cyanobacteria in subtropical lotic and lentic ecosystems. Science of the Total Environment, 609, 1132-1139. https://doi.org/10.1016/j.scitotenv.2017.07.067https://doi.org/10.1016/j.scitotenv.2017.07.067

Hansen, C. H., Williams, G. P., Adjei, Z., Barlow, A., Nelson, E. J., & Miller, A. W. (2015). Reservoir water quality monitoring using remote sensing with seasonal models: case study of five central-Utah reservoirs. Lake and Reservoir Management, 31(3), 225-240.

Havens, K., Ji, G., Beaver, J., Fulton III, R. & Teacher, C. (2019). Dynamics of cyanobacteria blooms are linked to the hydrology of shallow Florida lakes and provide insight into possible impacts of climate change. Hydrobiologia, 829(1), 43-59. https://doi.org/10.1007/s10750-017-3425-7https://doi.org/10.1007/s10750-017-3425-7

Ho, J., Michalak, A. & Pahlevan, N. (2019). Widespread global increase in intense lake phytoplankton blooms since the 1980s. Nature, 574(7780), 667-670.

Hu, M., Ma, R., Cao, Z., Xiong, J., & Xue, K. (2021). Remote estimation of trophic state index for inland waters using Landsat-8 OLI imagery. Remote Sensing, 13(10), 1988. https://doi.org/10.3390/rs13101988

Huisman, J., Codd, G., Paerl, H., Ibelings, B., Verspagen, J., & Visser, P. (2018). Cyanobacterial blooms. Nature Reviews Microbiology, 16(8), 471–483. https://doi.org/10.1038/s41579-018-0040-1https://doi.org/10.1038/s41579-018-0040-1

Ioannou, I., Gilerson, A., Ondrusek, M., Foster, R., El-Habashi, A., Bastani, K., & Ahmed, S. (2014). Algorithms for the remote estimation of chlorophyll-a in the Chesapeake Bay. In Ocean Sensing and Monitoring VI (Vol. 9111, p. 911118). International Society for Optics and Photonics. https://doi.org/10.1117/12.2053753https://doi.org/10.1117/12.2053753

IPCC, 2021: Climate Change 2021: The Physical Science Basis. Contribution of Working Group I to the Sixth Assessment Report of the Intergovernmental Panel on Climate Change [Masson-Delmotte, V., Zhai, A., Pirani, S., Connors, C., Péan, S., Berger, N., Caud, Y., Chen, L., Goldfarb, M., Gomis, M., Huang, K., Leitzell, E., Lonnoy, J., Matthews, T., Maycock, T. Waterfield, O. Yelekçi, R. Yu, & B. Zhou (eds.)]. Cambridge University Press, Cambridge, United Kingdom and New York, NY, USA, 2391 pp.

IPCC, 2023: Sections. In: Climate Change 2023: Synthesis Report. Contribution of Working Groups I, II and III to the Sixth Assessment Report of the Intergovernmental Panel on Climate Change [Core Writing Team, H. Lee and J. Romero (eds.)]. IPCC, Geneva, Switzerland, pp. 35-115, https://doi.org/10.59327/IPCC/AR6-9789291691647

Issaka, S., & Ashraf, M. A. (2017). Impact of soil erosion and degradation on water quality: a review. Geology, Ecology, and Landscapes, 1(1), 1-11.

Kayastha, P., Dzialowski, A. R., Stoodley, S. H., Wagner, K. L., & Mansaray, A. S. (2022). Effect of Time Window on Satellite and Ground-Based Data for Estimating Chlorophyll-a in Reservoirs. Remote Sensing, 14(4), 846.

Kibuye, F., Almuhtaram, H., Zamyadi, A., Gaget, V., Owen, C., Hofmann, R. & Wert, E. (2021). Utility practices and perspectives on monitoring and source control of cyanobacterial blooms. AWWA Water Science, 3(6), e1264.

Kleinteich, J., Frassl, M. A., Schulz, M., & Fischer, H. (2024). Climate change triggered planktonic cyanobacterial blooms in a regulated temperate river. Scientific Reports, 14(1), 16298. https://doi.org/10.1038/s41598-024-66586-whttps://doi.org/10.1038/s41598-024-66586-w

Knoll, L.B., Hagenbuch, E.J., Stevens, M.H., Vanni, M.J., Renwick, W.H., Denlinger, J.C., Hale, R.S. and González, M.J. 2015. Predicting eutrophication status in reservoirs at large spatial scales using landscape and morphometric variables. Inland Waters 5(3), 203-214. https://doi.org/10.5268/iw-5.3.812.

Koolhaas, (2003). Embalses agrícolas. Diseño y construcción. Ed. Hemisferio Sur.

Kouzminov, A., Ruck, J. & Wood, S. (2007). New Zealand risk management approach for toxic cyanobacteria in drinking water. Australian and New Zealand Journal of Public Health, 31(3), 275-281.

Kruk, C., Martínez, A., de la Escalera, G., Trinchin, R., Manta, G., Segura, A., … (2019). Floración excepcional de cianobacterias tóxicas en la costa de Uruguay, verano 2019. Innotec (18), 36–68.

Kutser, T., Paavel, B., Verpoorter, C., Ligi, M., Soomets, T., Toming, K., & Casal, G. (2016). Remote sensing of black lakes and using 810 nm reflectance peak for retrieving water quality parameters of optically complex waters. Remote Sensing, 8(6), 497.

Kutser, T., Koponen, S., Kallio, K. Y., Fincke, T., & Paavel, B. (2017). Bio-optical modeling of colored dissolved organic matter. In Bio-optical modeling and remote sensing of inland waters (pp. 101-128). Elsevier.

Leflaive J. & Ten-Hage, L. (2007). Algal and cyanobacterial secondary metabolites in freshwaters: a comparison of allelopathic compounds and toxins. Freshwater Biology, 52(2), 199-214.

Lescano, C., Ruibal, M., Barreto, P., Piñeiro, V., Lozoya, J. P., Perdomo, C., & Rodríguez-Gallego, L. (2017). Rol de los pastizales naturales en la retención de nutrientes provenientes de la agricultura. INNOTEC, (13 ene-jun), 78–91. https://doi.org/10.26461/13.08https://doi.org/10.26461/13.08

Lins, R., Martinez, J., Motta Marques, D., Cirilo, J., & Fragoso, C. (2017). Assessment of chlorophyll-a remote sensing algorithms in a productive tropical estuarine-lagoon system. Remote Sensing, 9(6), 516. https://doi.org/10.3390/rs9060516https://doi.org/10.3390/rs9060516

Liu, H., Li, Q., Shi, T., Hu, S., Wu, G., Zhou, Q., (2017). Application of sentinel 2 MSI images to retrieve suspended particulate matter concentrations in Poyang Lake. Rem. Sens. 9 (7), 761. https://doi.org/10.3390/rs9070761https://doi.org/10.3390/rs9070761

Liu, S., Kim, S., Glamore, W., Tamburic, B., & Johnson, F. (2024). Remote sensing of water colour in small southeastern Australian waterbodies. Journal of Environmental Management, 352, 120096. https://doi.org/10.1016/j.jenvman.2024.120096https://doi.org/10.1016/j.jenvman.2024.120096

Liu, X., Zhang, G., Sun, G., Wu, Y. and Chen, Y. (2019). Assessment of lake water quality and eutrophication risk in an agricultural irrigation area: A case study of the chagan lake in northeast China. Water 11(11), 2380. https://doi.org/10.3390/w11112380https://doi.org/10.3390/w11112380

Maciel, F. P., Haakonsson, S., Ponce de León, L., Bonilla, S., & Pedocchi, F. (2023). Challenges for chlorophyll-a remote sensing in a highly variable turbidity estuary, an implementation with sentinel-2. Geocarto International, 38(1), 2160017.

Martigani, F. (2017). Fluctuaciones en la disponibilidad de nutrientes como factor promotor de floraciones de cianobacterias tóxicas. Tesis de Maestría, PEDECIBA. Facultad de Ciencias, Universidad de la República.

Matthews, M. W., & Bernard, S. (2013). Characterizing the absorption properties for remote sensing of three small optically-diverse South African reservoirs. Remote Sensing, 5(9), 4370-4404.

Mazzeo, N., Ciganda, A. L., Nion, C. F., Peñas, F. J., González-Ferreras, A. M., Crisci, C., ... & Díaz, I. (2024). Inter and transdisciplinarity strategies for evaluating and improving water quality monitoring systems: Uruguay as a study case. Environmental Science & Policy, 154, 103699.

McCullough, I. M., Loftin, C. S., & Sader, S. A. (2012). Combining lake and watershed characteristics with Landsat TM data for remote estimation of regional lake clarity. Remote Sensing of Environment, 123, 109-115.

MGAP (Ministerio de Ganadería, Agricultura y Pesca). (1976). Unidades de suelos CONEAT. MGAP-DGRNAR-CONEAT.Montevideo.

Michalak, A., Anderson, E., Beletsky, D., Boland, S., Bosch, N., Bridgeman, T., ... & DePinto, J. (2013). Record-setting algal bloom in Lake Erie caused by agricultural and meteorological trends consistent with expected future conditions. Proceedings of the National Academy of Sciences, 110(16), 6448-6452.

Mishra, S., & Mishra, D. (2012). Normalized difference chlorophyll index: a novel model for remote estimation of chlorophylla concentration in turbid productive waters. Remote Sensing of Environment, 117, 394-406. https://doi.org/10.1016/j.rse.2011.10.016https://doi.org/10.1016/j.rse.2011.10.016

Moran, P. (1948). The interpretation of statistical maps. Journal of the Royal Statistical Society. Series B (Methodological), 10(2), 243-251.

Moreno A. (2007). Sistemas y análisis de la información geográfica. RA-MA Madrid. 940 p.

MVOTMA (2017). Plan Nacional de Aguas. Ministerio de Vivienda, Ordenamiento Territorial y Medio Ambiente.

Navalgund, R., Jayaraman, V., & Roy, P. (2007). Remote sensing applications: An overview. Current Science (00113891), 93(12).

Nechad, B., Ruddick, K. G., & Park, Y. (2010). Calibration and validation of a generic multisensor algorithm for mapping of total suspended matter in turbid waters. Remote Sensing of Environment, 114(4), 854-866.

Nechad, B., Ruddick, K., Schroeder, T., Oubelkheir, K., Blondeau-Patissier, D., Cherukuru, N., ... & Brockmann, C. (2015). CoastColour Round Robin data sets: a database to evaluate the performance of algorithms for the retrieval of water quality parameters in coastal waters. Earth system science data, 7(2), 319-348.

Neil, C., Spyrakos, E., Hunter, P., & Tyler, A. (2019). A global approach for chlorophyll-a retrieval across optically complex inland waters based on optical water types. Remote Sensing of Environment, 229, 159-178. https://doi.org/10.1016/j.rse.2019.04.027https://doi.org/10.1016/j.rse.2019.04.027

Nusch, E. A. (1980). Comparison of different methods for chlorophyll and phaeopigment determination. Arch Hydrobiol Beih Ergebn Limnol, 14, 14-36.

O'Neil, J., Davis, T., Burford, M. & Gobler, C. (2012). The rise of harmful cyanobacteria blooms: the potential roles of eutrophication and climate change. Harmful algae, 14, 313-334.

Ogashawara I., Mishra D. & Gitelson A. (2017). Remote sensing of inland waters: background and current state-of-the-art. In Bio-optical modeling and remote sensing of inland waters. Elsevier, pp. 1-24. https://doi.org/10.1016/B978-0-12-804644-9.00001-Xhttps://doi.org/10.1016/B978-0-12-804644-9.00001-X

Olano, (2024). Floraciones de fitoplancton en embalses agropecuarios de la cuenca del Río Santa Lucía: promotores de su crecimiento y alternativas para su detección. Tesis de Maestría, Facultad de Ciencias, Universidad de la República.

Oliveira, E., Fernandes, A., Kampel, M., Cordeiro, R., Brandini, N., Vinzon, S., ... & Paranhos, R. (2016). Assessment of remotely sensed chlorophyll-a concentration in Guanabara Bay, Brazil. Journal of Applied Remote Sensing, 10(2), 026003. https://doi.org/10.1117/1.JRS.10.026003https://doi.org/10.1117/1.JRS.10.026003

O'Neil, J M, Davis, T W, Burford, M A, Gobler, C J, 2012. The rise of harmful cyanobacteria blooms: the potential roles of eutrophication and climate change. Harmful Algae 14, 313–334.

Ouma, Y., Noor, K., & Herbert, K. (2020). Modelling reservoir chlorophyll-a, TSS, and turbidity using Sentinel-2A MSI and Landsat-8 OLI satellite sensors with empirical multivariate regression. Journal of Sensors, 2020. https://doi.org/10.1155/2020/8858408https://doi.org/10.1155/2020/8858408

Paerl, H. (2017). Controlling harmful cyanobacterial blooms in a climatically more extreme world: management options and research needs. Journal of Plankton Research, 39(5), 763-771. https://doi.org/10.1093/plankt/fbx042https://doi.org/10.1093/plankt/fbx042

Page, B., Kumar, A., Mishra, D., (2018). A novel cross-satellite based assessment of the spatio-temporal development of a cyanobacterial harmful algal bloom. Int. J. Appl. Earth Obs. Geoinf. 66, 69–81. https://doi.org/10.1016/j.jag.2017.11.003https://doi.org/10.1016/j.jag.2017.11.003

Papenfus, M., Schaeffer, B., Pollard, A. I., & Loftin, K. (2020). Exploring the potential value of satellite remote sensing to monitor chlorophyll-a for US lakes and reservoirs. Environmental Monitoring and Assessment, 192(12), 1-22.

Pearson, L., Dittmann, E., Mazmouz, R., Ongley, S., D'Agostino, P., & Neilan, B. (2016). The genetics, biosynthesis and regulation of toxic specialized metabolites of cyanobacteria. Harmful Algae, 54, 98-111.

Perin, V., Tulbure, M., Gaines, M., Reba, M., & Yaeger, M. (2021). On-farm reservoir monitoring using Landsat inundation datasets. Agricultural Water Management, 246, 106694. https://doi.org/10.1016/j.agwat.2020.106694https://doi.org/10.1016/j.agwat.2020.106694

Pierson, D. C., & Strömbeck, N. (2001). Estimation of radiance reflectance and the concentrations of optically active substances in Lake Mälaren, Sweden, based on direct and inverse solutions of a simple model. Science of the total environment, 268(1-3), 171-188.

Presidencia (2013) Plan de acción para la protección del agua en la cuenca del Santa Lucía. Consulta web realizada el 16/08/2024 https://www.gub.uy/ministerio-ambiente/politicas-y-gestion/plan-accion-para-proteccion-del-agua-cuenca-del-santa-lucia

Powers, S.M., Tank, J.L. & Robertson, D.M. Control of nitrogen and phosphorus transport by reservoirs in agricultural landscapes. Biogeochemistry 124, 417–439 (2015). https://doi.org/10.1007/s10533-015-0106-3

Presidencia (2016). Consulta web realizada el 05/08/2024 en el sitio https://www.gub.uy/presidencia/comunicacion/noticias/ose-construira-represa-arroyo-casupa-100-millones-dolares

Qing, S., Runa, A., Shun, B., Zhao, W., Bao, Y., & Hao, Y. (2020). Distinguishing and mapping of aquatic vegetations and yellow algae bloom with Landsat satellite data in a complex shallow Lake, China during 1986–2018. Ecological Indicators, 112, 106073. https://doi.org/10.1016/j.ecolind.2020.106073https://doi.org/10.1016/j.ecolind.2020.106073

R Core Team (2020). R: A Language and Environment for Statistical Computing. R Foundation for Statistical Computing, Vienna, Austria. Available at: https://www. R-project.org/

Reichwaldt, E. S., & Ghadouani, A. (2012). Effects of rainfall patterns on toxic cyanobacterial blooms in a changing climate: Between simplistic scenarios and complex dynamics. Water Research, 46(5), 1372-1393. https://doi.org/10.1016/j.watres.2011.11.052https://doi.org/10.1016/j.watres.2011.11.052.

Remmal, Y., Hudon, C., Hamilton, P. B., Rondeau, M., & Gagnon, P. (2017). Forecasting the magnitude and composition of phytoplankton blooms in a eutrophic lowland river (Rivière Yamaska, Que., Canada). Canadian Journal of Fisheries and Aquatic Sciences, 74(8), 1298-1311. https://doi.org/10.1139/cjfas-2016-0305https://doi.org/10.1139/cjfas-2016-0305

Reynolds, C.S. (2006) The ecology of phytoplankton, Cambridge University Press, Cambridge. https://doi.org/10.1017/CBO9780511542145https://doi.org/10.1017/CBO9780511542145

Ritchie, J. C., Zimba, P. V., & Everitt, J. H. (2003). Remote sensing techniques to assess water quality. Photogrammetric engineering & remote sensing, 69(6), 695-704.

Santos, C., González, M. & Sanguinetti, M. (2021). El agua como subsidio ambiental del agronegocio en Uruguay. Economía ecológica latinoamericana.

Schalles J., Sheil A., Tycast J., Alberts J. & Yacobi Y. (1998). Detection of chlorophyll, seston, and dissolved organic matter in the estuarine mixing zone of Georgia coastal plain rivers. In 5th International Conference on Remote Sensing for Marine and Coastal Environments, 2:315-324.

Schindler, D. (1977). Evolution of phosphorus limitation in lakes: natural mechanisms compensate for deficiencies of nitrogen and carbon in eutrophied lakes. Science, 195(4275), 260-262.

Schön, F., Zabaleta, B., & Achkar, M. (2022). Causas de eventos de inundación en la ciudad de San José de Mayo, Uruguay. Revista de Geografía Norte Grande, (82), 209-230.

Seegers, B. N., Werdell, P. J., Vandermeulen, R. A., Salls, W., Stumpf, R. P., Schaeffer, B. A., ... & Loftin, K. A. (2021). Satellites for long-term monitoring of inland US lakes: The MERIS time series and application for chlorophyll-a. Remote Sensing of Environment, 266, 112685.

Shi, K., Li, Y., Li, L., Lu, H., Song, K., Liu, Z., ... & Li, Z. (2013). Remote chlorophyll-a estimates for inland waters based on a cluster-based classification. Science of the Total Environment, 444, 1-15.

Shin, J. K., Park, Y., Kim, N. Y., & Hwang, S. J. (2022). Downstream transport of geosmin based on harmful cyanobacterial outbreak upstream in a reservoir cascade. International Journal of Environmental Research and Public Health, 19(15), 9294.

Sinha, E., Michalak, A. & Balaji, V. (2017). Eutrophication will increase during the 21st century as a result of precipitation changes. Science 357(6349), 405-408. https://doi.org/10.1126/science.aan2409https://doi.org/10.1126/science.aan2409

Smayda T. (1997). What is a Bloom? A Commentary. The Ecology and Oceanography of Harmful Algal Bloom. Limnology and Oceanography, 42 (5, part 2):1132-1136.

Somma, A., Bonilla, S., & Aubriot, L. (2022). Nuisance phytoplankton transport is enhanced by high flow in the main river for drinking water in Uruguay. Environmental Science and Pollution Research, 29(4), 5634-5647. https://doi.org/10.1007/s11356-021-14683-yhttps://doi.org/10.1007/s11356-021-14683-y

Soria, X., Delegido, J., Urrego, E. P., Pereira-Sandoval, M., Vicente, E., Ruíz-Verdú, A., ... & Moreno, J. (2017, October). Validación de algoritmos para la estimación de la clorofila-a con Sentinel-2 en la Albufera de València. In Proceedings of the XVII Congreso de la Asociación Española de Teledetección (pp. 289-292).

Spyrakos, E., O'donnell, R., Hunter, P. D., Miller, C., Scott, M., Simis, S. G., ... & Tyler, A. N. (2018). Optical types of inland and coastal waters. Limnology and Oceanography, 63(2), 846-870.

Stocker, T., Qin, D., Plattner, G., Tignor, M., Allen, S., Boschung, J. & Midgley, P. (2013). Climate change 2013: the physical science basis. Contribution of workinggroup I to the fifth assessment report of the intergovernmental panel on climate change, 1535.

Strong A. (1974). Remote sensing of algal blooms by aircraft and satellite in Lake Erie and Utah Lake. Remote sensing of Environment, 3 (2):99-107.

Svirčev, Z., Lalić, D., Bojadžija Savić, G., Tokodi, N., Drobac Backović, D., Chen, L., ... & Codd, G. A. (2019). Global geographical and historical overview of cyanotoxin distribution and cyanobacterial poisonings. Archives of toxicology, 93, 2429-2481.

Tamm, M., Ligi, M., Panksep, K., Teeveer, K., Freiberg, R., Laas, P., ... & Nõges, T. (2019). Boosting the monitoring of phytoplankton in optically complex coastal waters by combining pigment-based chemotaxonomy and in situ radiometry. Ecological Indicators, 97, 329-340.

Tate, R. (2019). Landsat collections reveal long-term algal bloom hot spots of Utah Lake. Brigham Young University.

Toming, K., Kutser, T., Laas, A., Sepp, M., Paavel, B., Noges, T., (2016). First experiences in mapping lake water quality parameters with Sentinel-2 MSI imagery. Rem. Sens. 8 (8), 640. https://doi.org/10.3390/rs8080640https://doi.org/10.3390/rs8080640

Topp, S., Pavelsky, T., Jensen, D., Simard, M., & Ross, M. (2020). Research trends in the use of remote sensing for inland water quality science: Moving towards multidisciplinary applications. Water, 12(1), 169. https://doi.org/10.3390/w12010169https://doi.org/10.3390/w12010169

Torbick, N., Hession, S., Hagen, S., Wiangwang, N., Becker, B., & Qi, J. (2013). Mapping inland lake water quality across the Lower Peninsula of Michigan using Landsat TM imagery. International journal of remote sensing, 34(21), 7607-7624. https://doi.org/10.1080/01431161.2013.822602https://doi.org/10.1080/01431161.2013.822602

Uudeberg, K., Aavaste, A., Kõks, K., Ansper, A., Uusõue, M., Kangro, K., ... & Reinart, A. (2020). Optical Water Type Guided Approach to Estimate Optical Water Quality Parameters. Remote Sensing, 12(6), 931. https://doi.org/10.3390/rs12060931https://doi.org/10.3390/rs12060931

Valderrama J. (1981). The simultaneous analysis of total nitrogen and total phosphorus in natural waters. Marine Chemistry, 10:109-122.

Vidal, L. & Britos, A. (2012). Uruguay: occurrence, toxicity and regulation of Cyanobacteria. Current approaches to Cyanotoxin risk assessment, risk management and regulations in different countries. Dessau-Roßlau: Federal Environment Agency (Umweltbundesamt), 130-136.

Vincent R., Qin X., McKay R., Miner J., Czajkowski K., Savino J. y Bridgeman T. (2004). Phycocyanin detection from LANDSAT TM data for mapping cyanobacterial blooms in Lake Erie. Remote Sensing of Environment, 89 (3):381-392.

Wang, L., Bie, W., Li, H., Liao, T., Ding, X., Wu, G., & Fei, T. (2022). Small Water Body Detection and Water Quality Variations with Changing Human Activity Intensity in Wuhan. Remote Sensing, 14(1), 200.

Watanabe F., Alcântara E. y Stech J. (2018). High performance of chlorophyll-a prediction algorithms based on simulated OLCI Sentinel-3A bands in cyanobacteria-dominated inland waters. Advances in Space Research, 62 (2):265-273.

Watanabe, F., Alcantara, E., Rodrigues, T., Rotta, L., Bernardo, N. & Imai, N. (2017). Remote sensing of the chlorophyll-a based on OLI/Landsat-8 and MSI/Sentinel-2A (Barra Bonita reservoir, Brazil). Anais da Academia Brasileira de Ciências, 90, 1987-2000.

Weber, S., Mishra, D., Wilde, S.., & Kramer, E. (2020). Risks for cyanobacterial harmful algal blooms due to land management and climate interactions. Science of the Total Environment, 703, 134608. https://doi.org/10.1016/j.scitotenv.2019.134608https://doi.org/10.1016/j.scitotenv.2019.134608

Werther, M., Spyrakos, E., Simis, S., Odermatt, D., Stelzer, K., Krawczyk, H., ... & Tyler, A. (2021). Meta-classification of remote sensing reflectance to estimate trophic status of inland and nearshore waters. ISPRS Journal of Photogrammetry and Remote Sensing, 176, 109-126. https://doi.org/10.1016/j.isprsjprs.2021.04.003https://doi.org/10.1016/j.isprsjprs.2021.04.003

Williamson, N., Kobayashi, T., Outhet, D., & Bowling, L. C. (2018). Survival of cyanobacteria in rivers after their release into water from large headwater reservoirs. Harmful algae, 75, 1-15.

Yacobi Y., Moses W., Kaganovsky S., Sulimani B., Leavitt B. y Gitelson A. (2011). NIR-red reflectance-based algorithms for chlorophyll-a estimation in mesotrophic inland and coastal waters: Lake Kinneret case study. Water Research, 45 (7):2428-2436. https://doi.org/10.1016/j.watres.2011.02.002https://doi.org/10.1016/j.watres.2011.02.002

Yang, Z., Reiter, M., & Munyei, N. (2017). Estimation of chlorophyll-a concentrations in diverse water bodies using ratio-based NIR/Red indices. Remote Sensing Applications: Society and Environment, 6, 52-58. https://doi.org/10.1016/j.rsase.2017.04.004https://doi.org/10.1016/j.rsase.2017.04.004

Yunus A., Dou J. y Sravanthi N. (2015). Remote sensing of chlorophyll-a as a measure of red tide in Tokyo Bay using hotspot analysis. Remote Sensing Applications: Society and Environment, 2, 11-25. https://doi.org/10.1016/j.rsase.2015.09.002https://doi.org/10.1016/j.rsase.2015.09.002

Zabaleta, B., Achkar, M., & Aubriot, L. (2021). Hotspot analysis of spatial distribution of algae blooms in small and medium water bodies. Environmental Monitoring and Assessment, 193, 1-25. https://doi.org/10.1007/s10661-021-08944-zhttps://doi.org/10.1007/s10661-021-08944-z

Zabaleta, B., Achkar, M., & Aubriot, L. (2024). Zoning the risk of transporting cyanobacterial blooms to the main water utility in Uruguay. In review in Inland Waters. https://doi.org/10.21203/rs.3.rs-3687826/v1https://doi.org/10.21203/rs.3.rs-3687826/v1

Zabaleta, B., Aubriot, L., Olano, H., & Achkar, M. (2023). Satellite assessment of eutrophication hot spots and algal blooms in small and medium-sized productive reservoirs in Uruguay's main drinking water basin. Environmental Science and Pollution Research, 30(15), 43604-43618. https://doi.org/10.1007/s11356-023-25334-9https://doi.org/10.1007/s11356-023-25334-9

Zabaleta, B., Haakonsson, S., Achkar, M., & Aubriot, L. (2023b). High-frequency zones of phytoplankton blooms in the Río de la Plata Estuary associated with El Niño-Southern Oscillation. Estuarine, Coastal and Shelf Science, 286, 108342.

Zhang J. y Jørgensen S. (2005). Modelling of point and nonpoint nutrient loadings from a watershed. Environmental Modelling & Software, 20:561-574.

Zhang, Y., Zhang, Y., Shi, K., Zhou, Y., & Li, N. (2021). Remote sensing estimation of water clarity for various lakes in China. Water Research, 192, 116844. https://doi.org/10.1016/j.watres.2021.116844